Chapter 3
Gas and Oil Properties and Correlations

3.1 Introduction

Chap. 3 covers the properties of oil and gas systems, their nomenclature and units, and correlations used for their prediction. Sec. 3.2 covers the fundamental engineering quantities used to describe phase behavior, including molecular quantities, critical and reduced properties, component fractions, mixing rules, volumetric properties, transport properties, and interfacial tension (IFT).

Sec. 3.3 discusses the properties of gas mixtures, including correlations for Z factor, pseudocritical properties and wellstream gravity, gas viscosity, dewpoint pressure, and total formation volume factor (FVF). Sec. 3.4 covers oil properties, including correlations for bubblepoint pressure, compressibility, FVF, density, and viscosity. Sec. 3.5 gives correlations for IFT and diffusion coefficients. Sec. 3.6 reviews the estimation of K values for low-pressure applications, such as surface separator design, and convergence-pressure methods used for reservoir calculations.

3.2 Review of Properties, Nomenclature, and Units

3.2.1 Molecular Quantities. All matter is composed of elements that cannot be decomposed by ordinary chemical reactions. Carbon (C), hydrogen (H), sulfur (S), nitrogen (N), and oxygen (O) are examples of the elements found in naturally occurring petroleum systems.

The physical unit of the element is the atom. Two or more elements may combine to form a chemical compound. Carbon dioxide (CO_2), methane (CH_4), and hydrogen sulfide (H_2S) are examples of compounds found in naturally occurring petroleum systems. When two atoms of the same element combine, they form diatomic compounds, such as nitrogen (N_2) and oxygen (O_2). The physical unit of the compound is the molecule.

Mass is the basic quantity for measuring the amount of a substance. Because chemical compounds always combine in a definite proportion (i.e., as a simple ratio of whole numbers), the mass of the atoms of different elements can be conveniently compared by relating them with a standard. The current standard is carbon-12, where the element carbon has been assigned a relative atomic mass of 12.011.

The relative atomic mass of all other elements have been determined relative to the carbon-12 standard. The smallest element is hydrogen, which has a relative atomic mass of 1.0079. The relative atomic mass of one element contains the same number of atoms as the relative atomic mass of any other element. This is true regardless of the units used to measure mass.

According to the SI standard, the definition of the mole reads "the mole is the amount of substance of a system which contains as many elementary entities as there are atoms in 0.012 kilograms of carbon-12." The SI symbol for mole is mol, which is numerically identical to the traditional g mol.

The SPE SI standard[1] uses kmol as the unit for a mole where kmol designates "an amount of substance which contains as many kilograms (groups of molecules) as there are atoms in 12.0 kg (incorrectly written as 0.012 kg in the original SPE publication) of carbon-12 multiplied by the relative molecular mass of the substance involved."

A practical way to interpret kmol is "kg mol" where kmol is numerically equivalent to 1,000 g mol (i.e., 1,000 mol). Otherwise, the following conversions apply.

$$\begin{aligned} 1 \text{ kmol} &= 1{,}000 \text{ mol} \\ &= 1{,}000 \text{ g mol} \\ &= 2.2046 \text{ lbm mol} \end{aligned}$$

$$\begin{aligned} 1 \text{ lbm mol} &= 0.45359 \text{ kmol} \\ &= 453.59 \text{ mol} \\ &= 453.59 \text{ g mol} \end{aligned}$$

$$\begin{aligned} 1 \text{ mol} &= 1 \text{ g mol} \\ &= 0.001 \text{ kmol} \\ &= 0.0022046 \text{ lbm mol} \end{aligned}$$

The term molecular weight has been replaced in the SI system by molar mass. Molar mass, M, is defined as the mass per mole ($M = m/n$) of a given substance where the unit mole must be consistent with the unit of mass. The numerical value of molecular weight is independent of the units used for mass and moles, as long as the units are consistent. For example, the molar mass of methane is 16.04, which for various units can be written

$$\begin{aligned} M &= 16.04 \text{ kg/kmol} \\ &= 16.04 \text{ lbm/lbm mol} \\ &= 16.04 \text{ g/g mol} \\ &= 16.04 \text{ g/mol} \end{aligned}$$

3.2.2 Critical and Reduced Properties. Most equations of state (EOS's) do not use pressure and temperature explicitly to define the state of a system, but instead they generalize according to corresponding-states theory by use of two or more reduced properties, which are dimensionless.[2]

$$T_r = T/T_c, \quad \ldots\ldots\ldots\ldots\ldots\ldots\ldots\ldots\ldots\ldots\ldots\ldots\ldots\ldots (3.1a)$$

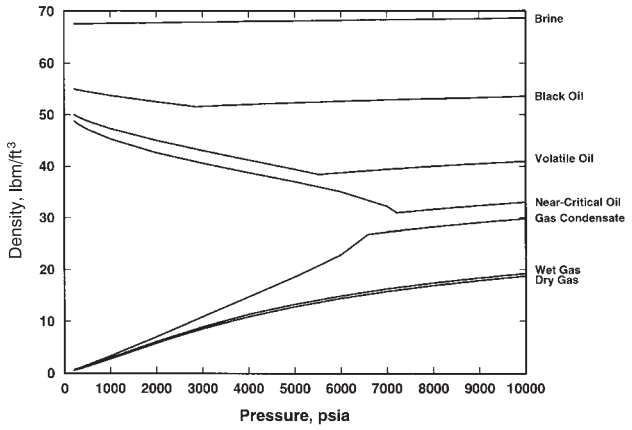

Fig. 3.1—Reservoir densities as functions of pressure and temperature.

$$p_r = p/p_c, \quad \ldots\ldots\ldots\ldots\ldots\ldots\ldots\ldots\ldots\ldots \quad (3.1b)$$

$$V_r = V/V_c, \quad \ldots\ldots\ldots\ldots\ldots\ldots\ldots\ldots\ldots\ldots \quad (3.1c)$$

$$\text{and } \rho_r = \rho/\rho_c, \quad \ldots\ldots\ldots\ldots\ldots\ldots\ldots\ldots\ldots\ldots \quad (3.1d)$$

where $\rho_r = 1/V_r$. Absolute units must be used when calculating reduced pressure and temperature. p_c, T_c, V_c, and ρ_c are the true critical properties of a pure component, or some average for a mixture. In most petroleum engineering applications, the range of reduced pressure is from 0.02 to 30 for gases and 0.03 to 40 for oils; reduced temperature ranges from <1 to 2.5 for gases and from 0.4 to 1.1 for oils. Reduced density can vary from 0 at low pressures to about 3.5 at high pressures.

Average mixture, or pseudocritical, properties are calculated from simple mixing rules or mixture specific gravity.[3,4] Denoting a mixture pseudocritical property by θ_{pc}, the pseudoreduced property is defined $\theta_{pr} = \theta/\theta_{pc}$. Pseudocritical properties are not approximations of the true critical properties, but are chosen instead so that mixture properties will be estimated correctly with corresponding-states correlations.

3.2.3 Component Fractions and Mixing Rules. Petroleum reservoir mixtures contain hundreds of well-defined and "undefined" components. These components are quantified on the basis of mole, weight, and volume fractions. For a mixture having N components, $i = 1,\ldots,N$, the overall mole fractions are given by

$$z_i = \frac{n_i}{\sum_{j=1}^{N} n_j} = \frac{m_i/M_i}{\sum_{j=1}^{N} m_j/M_j}, \quad \ldots\ldots\ldots\ldots\ldots\ldots \quad (3.2)$$

where n = moles, m = mass, M = molecular weight, and the sum of z_i is 1.0. In general, oil composition is denoted by x_i and gas composition by y_i.

Weight or mass fractions, w_i, are given by

$$w_i = \frac{m_i}{\sum_{j=1}^{N} m_j} = \frac{n_i M_i}{\sum_{j=1}^{N} n_j M_j}, \quad \ldots\ldots\ldots\ldots\ldots\ldots \quad (3.3)$$

where the sum of $w_i = 1.0$. Although the composition of a mixture is usually expressed in terms of mole fraction, the measurement of composition is usually based on mass, which is converted to mole fraction with component molecular weights.

For oil mixtures at standard conditions (14.7 psia and 60°F), the total volume can be approximated by the sum of the volumes of individual components, assuming ideal-solution mixing. This results in the following relation for volume fractions x_{vi}, based on component densities at standard conditions ρ_i or specific gravities γ_i.

$$x_{vi} = \frac{m_i/\rho_i}{\sum_{j=1}^{N} m_j/\rho_j} = \frac{n_i M_i/\rho_i}{\sum_{j=1}^{N} n_j M_j/\rho_j} = \frac{x_i M_i/\rho_i}{\sum_{j=1}^{N} x_j M_j/\rho_j}$$

$$= \frac{x_i M_i/\gamma_i}{\sum_{j=1}^{N} x_j M_j/\gamma_j}, \quad \ldots\ldots\ldots\ldots\ldots\ldots\ldots\ldots \quad (3.4)$$

where the sum of x_{vi} is unity.

Having defined component fractions, we can introduce some common mixing rules for averaging the properties of mixtures. Kay's[5] mixing rule, the simplest and most widely used, is given by a mole-fraction average,

$$\bar{\theta} = \sum_{i=1}^{N} z_i \theta_i. \quad \ldots\ldots\ldots\ldots\ldots\ldots\ldots\ldots\ldots\ldots \quad (3.5)$$

This mixing rule is usually adequate for molecular weight, pseudocritical temperature, and acentric factor.[6] We can write a generalized linear mixing rule as

$$\bar{\theta} = \frac{\sum_{i=1}^{N} \phi_i \theta_i}{\sum_{i=1}^{N} \phi_i}, \quad \ldots\ldots\ldots\ldots\ldots\ldots\ldots\ldots\ldots\ldots \quad (3.6)$$

where ϕ_i is usually one of the following weighting factors: $\phi_i = z_i$, mole fraction (Kay's rule); $\phi_i = w_i$, weight fraction; or $\phi_i = x_{vi}$, volume fraction. Depending on the quantity being averaged, other mixing rules and definitions of ϕ_i may be appropriate.[7,8] For example, the mixing rules used for constants in an EOS (Chap. 4) can be chosen on the basis of statistical thermodynamics.

3.2.4 Volumetric Properties. Density, ρ, is defined as the ratio of mass to volume,

$$\rho = m/V, \quad \ldots\ldots\ldots\ldots\ldots\ldots\ldots\ldots\ldots\ldots \quad (3.7)$$

expressed in such units as lbm/ft^3, kg/m^3, and g/cm^3. **Fig. 3.1** shows the magnitudes of density for reservoir mixtures. Molar density, ρ_M, gives the volume per mole:

$$\rho_M = n/V. \quad \ldots\ldots\ldots\ldots\ldots\ldots\ldots\ldots\ldots\ldots \quad (3.8)$$

Specific volume, $\hat{v}$, is defined as the ratio of volume to mass and is equal to the reciprocal of density.

$$\hat{v} = V/m = 1/\rho. \quad \ldots\ldots\ldots\ldots\ldots\ldots\ldots\ldots\ldots\ldots \quad (3.9)$$

Molar volume, v, defines the ratio of volume per mole,

$$v = V/n = M/\rho = 1/\rho_M, \quad \ldots\ldots\ldots\ldots\ldots\ldots\ldots\ldots \quad (3.10)$$

and is typically used in cubic EOS's. Molar density, ρ_M, is given by

$$\rho_M = 1/v = \rho/M, \quad \ldots\ldots\ldots\ldots\ldots\ldots\ldots\ldots\ldots\ldots \quad (3.11)$$

and is used in the formulas of some EOS's.

According to the SI standard, relative density replaces specific gravity as the term used to define the ratio of the density of a mixture to the density of a reference material. The conditions of pressure and temperature must be specified for both materials, and the densities of both materials are generally measured at standard conditions (standard conditions are usually 14.7 psia and 60°F).

$$\gamma = \frac{\rho(p_{sc}, T_{sc})}{\rho_{\text{ref}}(p_{sc}, T_{sc})}, \quad \ldots\ldots\ldots\ldots\ldots\ldots\ldots\ldots\ldots\ldots \quad (3.12a)$$

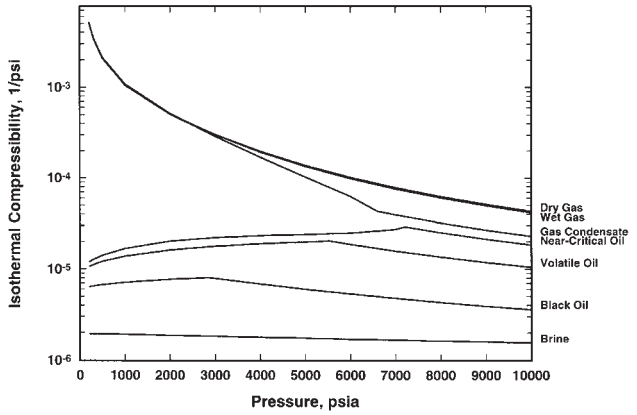

Fig. 3.2—Reservoir compressibilities as functions of pressure.

$$\gamma_o = \frac{(\rho_o)_{sc}}{(\rho_w)_{sc}}, \quad \ldots\ldots\ldots\ldots\ldots\ldots\ldots\ldots\ldots\ldots \quad (3.12b)$$

$$\text{and } \gamma_g = \frac{(\rho_g)_{sc}}{(\rho_{\text{air}})_{sc}}. \quad \ldots\ldots\ldots\ldots\ldots\ldots\ldots\ldots\ldots\ldots \quad (3.12c)$$

Air is used as the reference material for gases, and water is used as the reference material for liquids. Specific gravity is dimensionless, although it is customary and useful to specify the material used as a reference (air = 1 or water = 1). In older references, liquid specific gravities are sometimes followed by the temperatures of both the liquid and water, respectively; for example, $\gamma_o = 0.823_{60/60}$, where the temperature units here are understood to be in degrees Fahrenheit.

The oil gravity, γ_{API}, in degrees API is used to classify crude oils on the basis of the following relation,

$$\gamma_{\text{API}} = \frac{141.5}{\gamma_o} - 131.5 \quad \ldots\ldots\ldots\ldots\ldots\ldots\ldots\ldots\ldots\ldots \quad (3.13a)$$

$$\text{and } \gamma_o = \frac{141.5}{\gamma_{\text{API}} + 131.5}, \quad \ldots\ldots\ldots\ldots\ldots\ldots\ldots\ldots\ldots\ldots \quad (3.13b)$$

where γ_o = oil specific gravity (water = 1). Officially, the SPE does not recognize γ_{API} in its SI standard, but because oil gravity (in degrees API) is so widely used (and understood) and because it is found in many property correlations, its continued use is justified for qualitative description of stock-tank oils.

Isothermal compressibility, c, of a fixed mass of material is defined as

$$c = -\frac{1}{V}\left(\frac{\partial V}{\partial p}\right)_T = -\frac{1}{\hat{v}}\left(\frac{\partial \hat{v}}{\partial p}\right)_T = -\frac{1}{v}\left(\frac{\partial v}{\partial p}\right)_T, \quad \ldots\ldots \quad (3.14)$$

where the units are psi^{-1} or kPa^{-1}. In terms of density, ρ, and FVF, B, isothermal compressibility is given by

$$c = \frac{1}{\rho}\left(\frac{\partial \rho}{\partial p}\right)_T = \frac{1}{B}\left(\frac{\partial B}{\partial p}\right)_T, \quad \ldots\ldots\ldots\ldots\ldots\ldots \quad (3.15)$$

where B is defined in the next section. **Fig. 3.2** shows the variation in compressibility with pressure for typical reservoir mixtures. A discontinuity in oil compressibility occurs at the bubblepoint because gas comes out of solution. When two or more phases are present, a total compressibility is useful.[8,9]

3.2.5 Black-Oil Pressure/Volume/Temperature (PVT) Properties. The FVF, B; solution gas/oil ratio, R_s; and solution oil/gas ratio, r_s, are volumetric ratios used to simplify engineering calculations. Specifically, they allow for the introduction of surface volumes of gas, oil, and water into material-balance equations. These are not standard engineering quantities, and they must be defined precisely. These properties constitute the black-oil or "beta" PVT formula used in petroleum engineering. Chap. 7 gives a detailed discussion of black-oil properties.

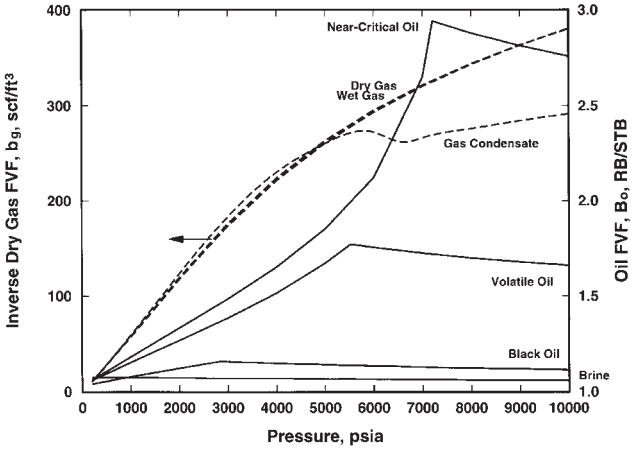

Fig. 3.3—Reservoir FVF's as functions of pressure.

FVF, or simply volume factor, is used to convert a volume at elevated pressure and temperature to surface volume, and vice versa. More specifically, FVF is defined as the volume of a mixture at specified pressure and temperature divided by the volume of a product phase measured at standard conditions,

$$B = \frac{V_{\text{mixture}}\,(p, T)}{V_{\text{product}}\,(p_{sc}, T_{sc})}. \quad \ldots\ldots\ldots\ldots\ldots\ldots\ldots \quad (3.16)$$

The units of B are bbl/STB for oil and water, and ft^3/scf or bbl/Mscf for gas. The surface product phase may consist of all or only part of the original mixture.

Primarily, four volume factors are used in petroleum engineering. They are oil FVF, B_o; water FVF, B_w; gas FVF, B_g; and total FVF of a gas/oil system, B_t, where

$$B_o = \frac{V_o}{(V_o)_{sc}} = \frac{V_o}{V_{\bar{o}}}, \quad \ldots\ldots\ldots\ldots\ldots\ldots\ldots\ldots\ldots\ldots \quad (3.17a)$$

$$B_w = \frac{V_w}{(V_w)_{sc}} = \frac{V_w}{V_{\bar{w}}}, \quad \ldots\ldots\ldots\ldots\ldots\ldots\ldots\ldots\ldots\ldots \quad (3.17b)$$

$$B_g = \frac{V_g}{(V_g)_{sc}} = \frac{V_g}{V_{\bar{g}}}, \quad \ldots\ldots\ldots\ldots\ldots\ldots\ldots\ldots\ldots\ldots \quad (3.17c)$$

$$\text{and } B_t = \frac{V_t}{(V_o)_{sc}} = \frac{V_o + V_g}{(V_o)_{sc}} = \frac{V_o + V_g}{V_{\bar{o}}}; \quad \ldots\ldots\ldots\ldots \quad (3.17d)$$

and the total FVF of a gas/water system is

$$B_{tw} = \frac{V_t}{(V_w)_{sc}} = \frac{V_g + V_w}{V_{\bar{w}}}. \quad \ldots\ldots\ldots\ldots\ldots\ldots\ldots \quad (3.17e)$$

In Eq. 3.17, V_o = oil volume at p and T; V_g = gas volume at p and T; V_w = water/brine volume at p and T; $V_{\bar{o}} = (V_o)_{sc}$ = stock-tank-oil volume at standard conditions; $V_{\bar{w}} = (V_w)_{sc}$ = stock-tank-water volume at standard conditions; and $V_{\bar{g}} = (V_g)_{sc}$ = surface-gas volume at standard conditions.

Because gas FVF is inversely proportional to pressure, a reciprocal gas volume factor, b_g (equal to $1/B_g$), is sometimes used, where the units of b_g may be scf/ft^3 or Mscf/bbl. **Fig. 3.3** shows FVF's of typical reservoir systems. Inverse oil FVF, b_o (equal to $1/B_o$) is also used in reservoir simulation.

Wet gas and gas-condensate reservoir fluids produce liquids at the surface, and for these gases the surface product (separator gas) consists of only part of the original reservoir gas mixture. Two gas FVF's are used for these systems: the "dry" FVF, B_{gd}, and the "wet" FVF, B_{gw} (or just B_g). B_{gd} gives the ratio of reservoir gas volume to the actual surface separator gas. B_{gw} gives the ratio of reservoir gas volume to a hypothetical "wet" surface-gas volume (the actual separator-gas volume plus the stock-tank condensate converted to an equivalent surface-gas volume). Chap. 7 describes when B_{gd} and B_{gw} are used. The standard definition of $B_g = (p_{sc}/T_{sc})(ZT/p)$ (see Eq. 3.38) represents the wet-gas FVF.

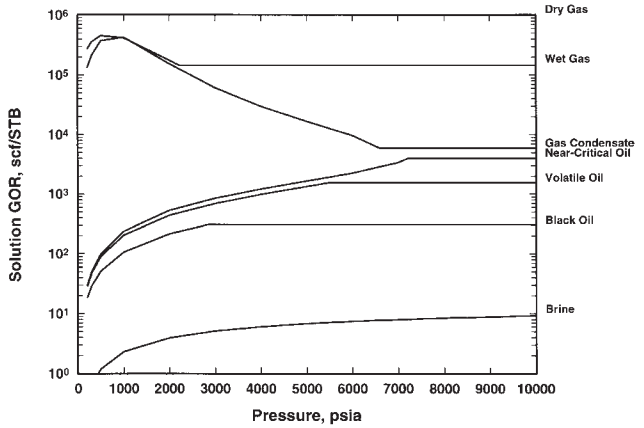

Fig. 3.4—Solution gas/oil ratios for brine, R_{sw}, and reservoir oils, R_s, and inverse solution oil/gas ratio for reservoir gases, $1/r_s$, as functions of pressure.

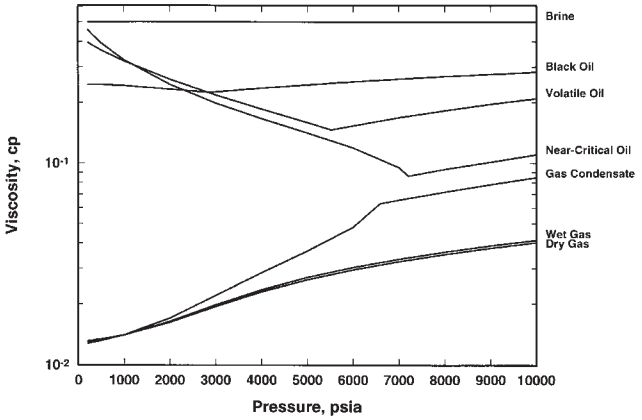

Fig. 3.5—Reservoir viscosities as functions of pressure.

When a reservoir mixture produces both surface gas and oil, the GOR, R_{go}, defines the ratio of standard gas volume to a reference oil volume (stock-tank- or separator-oil volume),

$$R_{go} = \frac{(V_g)_{sc}}{(V_o)_{sc}} = \frac{V_{\bar{g}}}{V_{\bar{o}}} \quad \ldots\ldots\ldots\ldots\ldots\ldots\ldots\ldots (3.18a)$$

$$\text{and } R_{sp} = \frac{(V_g)_{sc}}{(V_o)_{sp}} = \frac{V_{\bar{g}}}{(V_o)_{sp}} \quad \ldots\ldots\ldots\ldots\ldots\ldots\ldots (3.18b)$$

in units of scf/STB and scf/bbl, respectively. The separator conditions should be reported when separator GOR is used.

Solution gas/oil ratio, R_s, is the volume of gas (at standard conditions) liberated from a single-phase oil at elevated pressure and temperature divided by the resulting stock-tank-oil volume, with units scf/STB. R_s is constant at pressures greater than the bubblepoint and decreases as gas is liberated at pressures below the bubblepoint.

The producing GOR, R_p, defines the instantaneous ratio of the total surface-gas volume produced divided by the total stock-tank-oil volume. At pressures greater than bubblepoint, R_p is constant and equal to R_s at bubblepoint. At pressures less than the bubblepoint, R_p may be equal to, less than, or greater than the R_s of the flowing reservoir oil. Typically, R_p will increase 10 to 20 times the initial R_s because of increasing gas mobility and decreasing oil mobility during pressure depletion.

The surface volume ratio for gas condensates is usually expressed as an oil/gas ratio (OGR), r_{og}.

$$r_{og} = \frac{(V_o)_{sc}}{(V_g)_{sc}} = \frac{V_{\bar{o}}}{V_{\bar{g}}} = \frac{1}{R_{go}}. \quad \ldots\ldots\ldots\ldots\ldots\ldots (3.19)$$

The unit for r_{og} is STB/scf or, more commonly, "barrels per million" (STB/MMscf). To avoid misinterpretation, it should be clearly specified whether the OGR includes natural gas liquids (NGL's) in addition to stock-tank condensate. In most petroleum engineering calculations, NGL's are not included in the OGR.

The ratio of surface oil to surface gas produced from a single-phase reservoir gas is referred to as the solution oil/gas ratio, r_s. At pressures above the dewpoint, the producing OGR, r_p is constant and equal to r_s at the dewpoint. At pressures below the dewpoint, r_p is typically equal to or just slightly greater than r_s; the contribution of flowing reservoir oil to surface-oil production is negligible in most gas-condensate reservoirs.

In the definitions of R_p and r_p, the total producing surface-gas volume equals the surface gas from the reservoir gas plus the solution gas from the reservoir oil; likewise, the total producing surface oil equals the stock-tank oil from the reservoir oil plus the condensate from the reservoir gas. **Fig. 3.4** shows the behavior of R_p, R_s, and $1/r_s$ as a function of pressure.

3.2.6 Viscosity. Two types of viscosity are used in engineering calculations: dynamic viscosity, μ, and kinematic viscosity, ν. The definition of μ for Newtonian flow (which most petroleum mixtures follow) is

$$\mu = \frac{\tau g_c}{\mathrm{d}u/\mathrm{d}y}, \quad \ldots\ldots\ldots\ldots\ldots\ldots\ldots\ldots (3.20)$$

where τ = shear stress per unit area in the shear plane parallel to the direction of flow, $\mathrm{d}u/\mathrm{d}y$ = velocity gradient perpendicular to the plane of shear, and g_c = a units conversion from mass to force. The two viscosities are related by density, where $\mu = \nu\rho$.

Most petroleum engineering applications use dynamic viscosity, which is the property reported in commercial laboratory studies. The unit of dynamic viscosity is centipoise (cp), or in SI units, mPa·s, where 1 cp = 1 mPa·s. Kinematic viscosity is usually reported in centistoke (cSt), which is obtained by dividing μ in cp by ρ in g/cm^3; the SI unit for ν is mm^2/s, which is numerically equivalent to centistoke. **Fig. 3.5** shows oil, gas, and water viscosities for typical reservoir systems.

3.2.7 Diffusion Coefficients. In the absence of bulk flow, components in a single-phase mixture are transported according to gradients in concentration (i.e., chemical potential). Fick's[10] law for 1D molecular diffusion in a binary system is given by

$$u_i = -D_{ij}(\mathrm{d}C_i/\mathrm{d}x), \quad \ldots\ldots\ldots\ldots\ldots\ldots\ldots (3.21)$$

where u_i = molar velocity of Component i; D_{ij} = binary diffusion coefficient; and C_i = molar concentration of Component $i = y_i\rho_M$, where y_i = mole fraction; and x = distance.

Eq. 3.21 clearly shows that mass transfer by molecular diffusion can be significant for three reasons: (1) large diffusion coefficients, (2) large concentration differences, and (3) short distances. A combination of moderate diffusion coefficients, concentration gradients, and distance may also result in significant diffusive flow. Molecular diffusion is particularly important in naturally fractured reservoirs[11,12] because of relatively short distances (e.g., small matrix block sizes).

Low-pressure binary diffusion coefficients for gases, D^o_{ij}, are independent of composition and can be calculated accurately from fundamental gas theory (Chapman and Enskog[6]), which are basically the same relations used to estimate low-pressure gas viscosity. No well-accepted method is available to correct D^o_{ij} for mixtures at high pressure, but two types of corresponding-states correlations have been proposed: $D_{ij} = D^o_{ij}\,\mathrm{f}(T_r, p_r)$ and $D_{ij} = D^o_{ij}\,\mathrm{f}(\rho_r)$.

At low pressures, diffusion coefficients are several orders of magnitude smaller in liquids than in gases. At reservoir conditions, the difference between gas and liquid diffusion coefficients may be less than one order of magnitude.

3.2.8 IFT. Interfacial forces act between equilibrium gas, oil, and water phases coexisting in the pores of a reservoir rock. These forces

are generally quantified in terms of IFT, σ; units of σ are dynes/cm (or equivalently, mN/m). The magnitude of IFT varies from ≈ 50 dynes/cm for crude-oil/gas systems at standard conditions to < 0.1 dyne/cm for high-pressure gas/oil mixtures. Gas/oil capillary pressure, P_c, is usually considered proportional to IFT according to the Young-Laplace equation $P_c = 2\sigma/r$, where $\bar{r}$ is an average pore radius.[13-15] Recovery mechanisms that are influenced by capillary pressure (e.g., gas injection in naturally fractured reservoirs) will necessarily be sensitive to IFT.

3.3 Gas Mixtures

This section gives correlations for PVT properties of natural gases, including the following.

1. Review of gas volumetric properties.
2. *Z*-factor correlations.
3. Gas pseudocritical properties.
4. Wellstream gravity of wet gases and gas condensates.
5. Gas viscosity.
6. Dewpoint pressure.
7. Total volume factor.

3.3.1 Review of Gas Volumetric Properties. The properties of gas mixtures are well understood and have been accurately correlated for many years with graphical charts and EOS's based on extensive experimental data.[16-19] The behavior of gases at low pressures was originally quantified on the basis of experimental work by Charles and Boyle, which resulted in the ideal-gas law,[3]

$$pV = nRT, \quad \ldots\ldots\ldots\ldots\ldots\ldots\ldots\ldots\ldots\ldots \quad (3.22)$$

where R is the universal gas constant given in Appendix A for various units (Table A-2). In customary units,

$$R = 10.73146 \frac{\text{psia} \times \text{ft}^3}{^\circ\text{R} \times \text{lbm mol}}, \quad \ldots\ldots\ldots\ldots\ldots\ldots \quad (3.23)$$

while for other units, R can be calculated from the relation

$$R = 10.73146 \left(\frac{p_{\text{unit}}}{\text{psia}}\right)\left(\frac{^\circ\text{R}}{T_{\text{unit}}}\right)\left(\frac{V_{\text{unit}}}{\text{ft}^3}\right)\left(\frac{\text{lbm}}{m_{\text{unit}}}\right). \quad \ldots\ldots\ldots \quad (3.24)$$

For example, the gas constant for SPE-preferred SI units is given by

$$\begin{aligned} R &= 10.73146 \times \left(6.894757 \frac{\text{kPa}}{\text{psia}}\right) \times \left(1.8 \frac{^\circ\text{R}}{\text{K}}\right) \\ &\quad \times \left(0.02831685 \frac{\text{m}^3}{\text{ft}^3}\right) \times \left(2.204623 \frac{\text{lbm}}{\text{kg}}\right) \\ &= 8.3143 \frac{\text{kPa} \cdot \text{m}^3}{\text{K} \cdot \text{kmol}}. \quad \ldots\ldots\ldots\ldots\ldots\ldots\ldots\ldots \quad (3.25) \end{aligned}$$

The gas constant can also be expressed in terms of energy units (e.g., $R = 8.3143$ J/mol·K); note that $\text{J} = \text{N} \cdot \text{m} = (\text{N/m}^2)\,\text{m}^3 = \text{Pa} \cdot \text{m}^3$. In this case, the conversion from one unit system to another is given by

$$R = 8.3143 \left(\frac{E_{\text{unit}}}{\text{J}}\right)\left(\frac{\text{K}}{T_{\text{unit}}}\right)\left(\frac{\text{g}}{m_{\text{unit}}}\right). \quad \ldots\ldots\ldots\ldots\ldots \quad (3.26)$$

An ideal gas is a hypothetical mixture with molecules that are negligible in size and have no intermolecular forces. Real gases mimic the behavior of an ideal gas at low pressures and high temperatures because the mixture volume is much larger than the volume of the molecules making up the mixture. That is, the mean free path between molecules that are moving randomly within the total volume is very large and intermolecular forces are thus very small.

Most gases at low pressure follow the ideal-gas law. Application of the ideal-gas law results in two useful engineering approximations. First, the standard molar volume representing the volume occupied by one mole of gas at standard conditions is independent of the gas composition.

$$\begin{aligned} \left(v_g\right)_{sc} &= v_{\bar{g}} = \frac{\left(V_g\right)_{sc}}{n} = \frac{RT_{sc}}{p_{sc}} \\ &= \frac{10.73146(60 + 459.67)}{14.7} \\ &= 379.4 \text{ scf/lbm mol} \\ &= 23.69 \text{ std m}^3\text{/kmol}. \quad \ldots\ldots\ldots\ldots\ldots\ldots \quad (3.27) \end{aligned}$$

Second, the specific gravity of a gas directly reflects the gas molecular weight at standard conditions,

$$\gamma_g = \frac{\left(\rho_g\right)_{sc}}{\left(\rho_{\text{air}}\right)_{sc}} = \frac{M_g}{M_{\text{air}}} = \frac{M_g}{28.97}$$

$$\text{and } M_g = 28.97\,\gamma_g. \quad \ldots\ldots\ldots\ldots\ldots\ldots\ldots\ldots \quad (3.28)$$

For gas mixtures at moderate to high pressure or at low temperature the ideal-gas law does not hold because the volume of the constituent molecules and their intermolecular forces strongly affect the volumetric behavior of the gas. Comparison of experimental data for real gases with the behavior predicted by the ideal-gas law shows significant deviations. The deviation from ideal behavior can be expressed as a factor, Z, defined as the ratio of the actual volume of one mole of a real-gas mixture to the volume of one mole of an ideal gas,

$$Z = \frac{\text{volume of 1 mole of real gas at } p \text{ and } T}{\text{volume of 1 mole of ideal gas at } p \text{ and } T}, \quad \ldots\ldots\ldots\ldots\ldots\ldots \quad (3.29)$$

where Z is a dimensionless quantity. Terms used for Z include deviation factor, compressibility factor, and Z factor. Z factor is used in this monograph, as will the SPE reserve symbol Z (instead of the recommended SPE symbol z) to avoid confusion with the symbol z used for feed composition.

From Eqs. 3.22 and 3.29, we can write the real-gas law including the Z factor as

$$pV = nZRT, \quad \ldots\ldots\ldots\ldots\ldots\ldots\ldots\ldots\ldots\ldots \quad (3.30)$$

which is the standard equation for describing the volumetric behavior of reservoir gases. Another form of the real-gas law written in terms of specific volume ($\hat{v} = 1/\rho$) is

$$p\hat{v} = ZRT/M \quad \ldots\ldots\ldots\ldots\ldots\ldots\ldots\ldots\ldots\ldots \quad (3.31)$$

or, in terms of molar volume ($v = M/\rho$),

$$pv = ZRT. \quad \ldots\ldots\ldots\ldots\ldots\ldots\ldots\ldots\ldots\ldots \quad (3.32)$$

Z factor, defined by Eq. 3.30,

$$Z = pV/nRT, \quad \ldots\ldots\ldots\ldots\ldots\ldots\ldots\ldots\ldots\ldots \quad (3.33)$$

is used for both phases in EOS applications (see Chap. 4). In this monograph we use both Z and Z_g for gases and Z_o for oils; Z without a subscript always implies the Z factor of a "gas-like" phase.

All volumetric properties of gases can be derived from the real-gas law. Gas density is given by

$$\rho_g = pM_g/ZRT \quad \ldots\ldots\ldots\ldots\ldots\ldots\ldots\ldots\ldots\ldots \quad (3.34)$$

or, in terms of gas specific gravity, by

$$\rho_g = 28.97 \frac{p\gamma_g}{ZRT}. \quad \ldots\ldots\ldots\ldots\ldots\ldots\ldots\ldots \quad (3.35)$$

For wet-gas and gas-condensate mixtures, wellstream gravity, γ_w, must be used instead of γ_g in Eq. 3.35.[3] Gas density may range from 0.05 lbm/ft^3 at standard conditions to 30 lbm/ft^3 for high-pressure gases.

Gas molar volume, v_g, is given by

$$v_g = ZRT/p, \quad \ldots\ldots\ldots\ldots\ldots\ldots\ldots\ldots\ldots\ldots \quad (3.36)$$

where typical values of v_g at reservoir conditions range from 1 to 1.5 ft^3/lbm mol compared with 379 ft^3/lbm mol for gases at standard conditions. In Eqs. 3.30 through 3.36, R = universal gas constant.

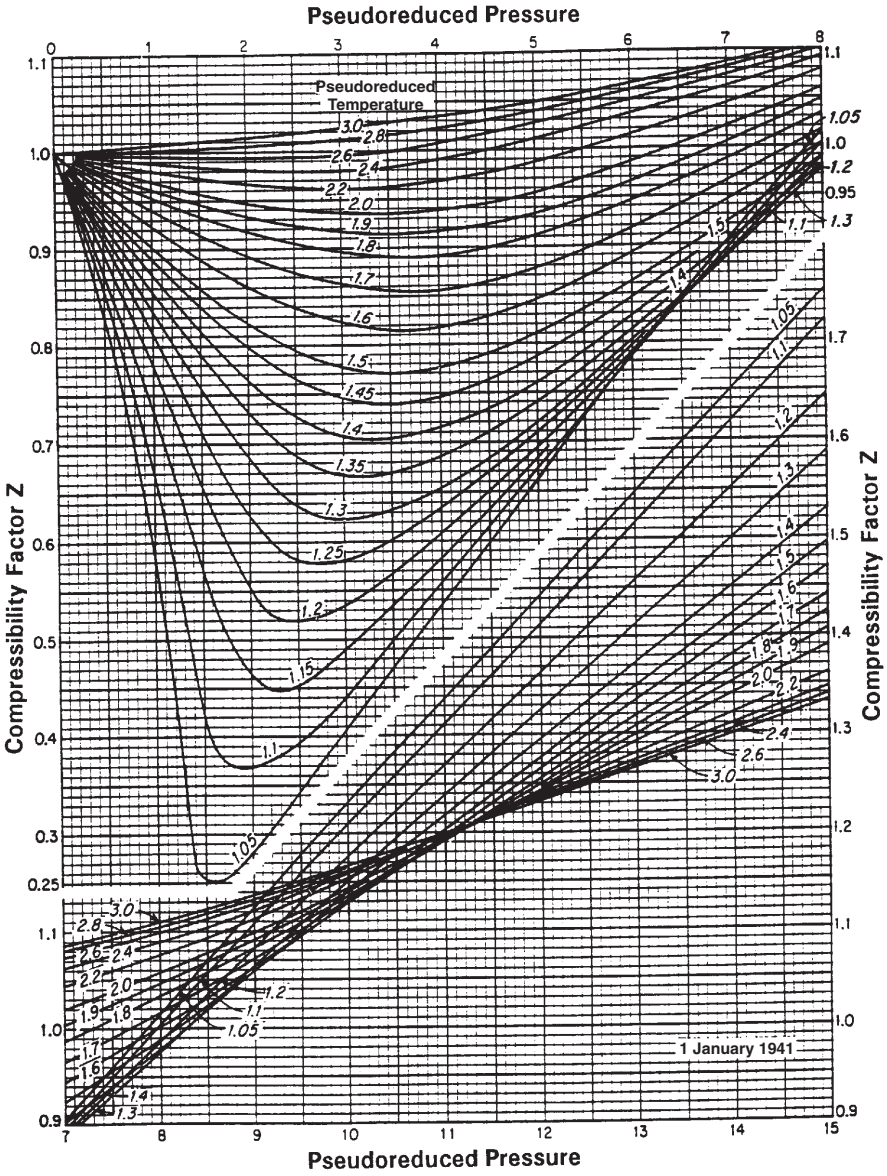

Fig. 3.6—Standing-Katz[4] *Z*-factor chart.

Gas compressibility, c_g, is given by

$$c_g = -\frac{1}{V_g}\left(\frac{\partial V_g}{\partial p}\right)$$

$$= \frac{1}{p} - \frac{1}{Z}\left(\frac{\partial Z}{\partial p}\right)_T \quad \ldots\ldots\ldots\ldots\ldots\ldots\ldots\ldots \quad (3.37)$$

For sweet natural gas (i.e., not containing H_2S) at pressures less than $\approx$1,000 psia, the second term in Eq. 3.37 is negligible and $c_g = 1/p$ is a reasonable approximation.

Gas volume factor, B_g, is defined as the ratio of gas volume at specified p and T to the ideal-gas volume at standard conditions,

$$B_g = \left(\frac{p_{sc}}{T_{sc}}\right)\frac{ZT}{p}. \quad \ldots\ldots\ldots\ldots\ldots\ldots\ldots\ldots\ldots \quad (3.38)$$

For customary units ($p_{sc} = 14.7$ psia and $T_{sc} = 520$°R), this is

$$B_g = 0.02827\ \frac{ZT}{p}, \quad \ldots\ldots\ldots\ldots\ldots\ldots\ldots\ldots \quad (3.39)$$

with temperature in °R and pressure in psia. This definition of B_g assumes that the gas volume at p and T remains as a gas at standard conditions. For wet gases and gas condensates, the surface gas will not contain all the original gas mixture because liquid is produced after separation. For these mixtures, the traditional definition of B_g may still be useful; however, we refer to this quantity as a hypothetical wet-gas volume factor, B_{gw}, which is calculated from Eq. 3.38.

Because B_g is inversely proportional to pressure, the inverse volume factor, $b_g = 1/B_g$, is commonly used. For field units,

$$b_g \text{ in scf/ft}^3 = 35.37\ \frac{p}{ZT} \quad \ldots\ldots\ldots\ldots\ldots\ldots \quad (3.40a)$$

and

$$b_g \text{ in Mscf/bbl} = 0.1985\ \frac{p}{ZT}. \quad \ldots\ldots\ldots\ldots\ldots \quad (3.40b)$$

If the reservoir gas yields condensate at the surface, the dry-gas volume factor, B_{gd}, is sometimes used.[20]

$$B_{gd} = \left(\frac{p_{sc}}{T_{sc}}\right)\left(\frac{ZT}{p}\right)\left(\frac{1}{F_{\bar{g}g}}\right), \quad \ldots\ldots\ldots\ldots\ldots\ldots \quad (3.41)$$

where $F_{\bar{g}g}$ = ratio of moles of surface gas, $n_{\bar{g}}$, to moles of wellstream mixture (i.e., reservoir gas, n_g); see Eqs. 7.10 and 7.11 of Chap. 7.

3.3.2 *Z*-Factor Correlations. Standing and Katz[4] present a generalized *Z*-factor chart (**Fig. 3.6**), which has become an industry standard for predicting the volumetric behavior of natural gases. Many empirical equations and EOS's have been fit to the original Standing-Katz chart. For example, Hall and Yarborough[21,22] present an

accurate representation of the Standing-Katz chart using a Carnahan-Starling hard-sphere EOS,

$$Z = \alpha p_{pr}/y, \quad \ldots\ldots\ldots\ldots\ldots\ldots\ldots\ldots\ldots\ldots \quad (3.42)$$

where $\alpha = 0.06125\,t \exp[-1.2(1-t)^2]$, where $t = 1/T_{pr}$.

The reduced-density parameter, y (the product of a van der Waals covolume and density), is obtained by solving

$$\begin{aligned} f(y) = 0 = &-\alpha p_{pr} + \frac{y + y^2 + y^3 - y^4}{(1-y)^3} \\ &- (14.76t - 9.76t^2 + 4.58t^3)y^2 \\ &+ (90.7t - 242.2t^2 + 42.4t^3)y^{2.18+2.82t}, \quad \ldots\ldots\ldots \quad (3.43) \end{aligned}$$

$$\begin{aligned} \text{with } \frac{df(y)}{dy} = &\frac{1 + 4y + 4y^2 - 4y^3 + y^4}{(1-y)^4} \\ &- (29.52t - 19.52t^2 + 9.16t^3)y \\ &+ (2.18 + 2.82t)(90.7t - 242.2t^2 + 42.4t^3) \\ &\times y^{1.18+2.82t}. \quad \ldots\ldots\ldots\ldots\ldots\ldots\ldots \quad (3.44) \end{aligned}$$

The derivative $\partial Z/\partial p$ used in the definition of c_g is given by

$$\left(\frac{\partial Z}{\partial p}\right)_T = \frac{\alpha}{p_{pc}}\left[\frac{1}{y} - \frac{\alpha p_{pr}/y^2}{df(y)/dy}\right]. \quad \ldots\ldots\ldots\ldots\ldots\ldots \quad (3.45)$$

An initial value of $y = 0.001$ can be used with a Newton-Raphson procedure, where convergence should be obtained in 3 to 10 iterations for $|f(y)| = 1 \times 10^{-8}$.

On the basis of Takacs'[23] comparison of eight correlations representing the Standing-Katz[4] chart, the Hall and Yarborough[21] and the Dranchuk and Abou-Kassem[24] equations give the most accurate representation for a broad range of temperatures and pressures. Both equations are valid for $1 \leqq T_r \leqq 3$ and $0.2 \leqq p_r \leqq 25$ to 30.

For many petroleum engineering applications, the Brill and Beggs[25] equation gives a satisfactory representation (± 1 to 2%) of the original Standing-Katz Z-factor chart for $1.2 < T_r < 2$. Also, this equation can be solved explicitly for Z. The main limitations are that reduced temperature must be >1.2 (≈ 80°F) and <2.0 (≈ 340°F) and reduced pressure should be <15 ($\approx 10{,}000$ psia).

The Standing and Katz Z-factor correlation may require special treatment for wet gas and gas-condensate fluids containing significant amounts of heptanes-plus material and for gas mixtures with significant amounts of nonhydrocarbons. An apparent discrepancy in the Standing-Katz Z-factor chart for $1.05 < T_r < 1.15$ has been "smoothed" in the Hall-Yarborough[21] correlations. The Hall and Yarborough (or Dranchuk and Abou-Kassem[24]) equation is recommended for most natural gases. With today's computing capabilities, choosing simple, less-reliable equations, such as the Brill and Beggs[25] equation, is normally unnecessary.

The Lee-Kesler,[26,27] AGA-8,[28] and DDMIX[29] correlations for Z factor were developed with multiconstant EOS's to give accurate volumetric predictions for both pure components and mixtures. They require more computation but are very accurate. These equations are particularly useful in custody-transfer calculations. They also are required for gases containing water and concentrations of nonhydrocarbons that exceed the limits of the Wichert and Aziz method.[30,31]

3.3.3 Gas Pseudocritical Properties. Z factor, viscosity, and other gas properties have been correlated accurately with corresponding-states principles, where the property is correlated as a function of reduced pressure and temperature.

$$Z = f(p_r, T_r)$$

$$\text{and } \mu_g/\mu_{gsc} = f(p_r, T_r), \quad \ldots\ldots\ldots\ldots\ldots\ldots \quad (3.46)$$

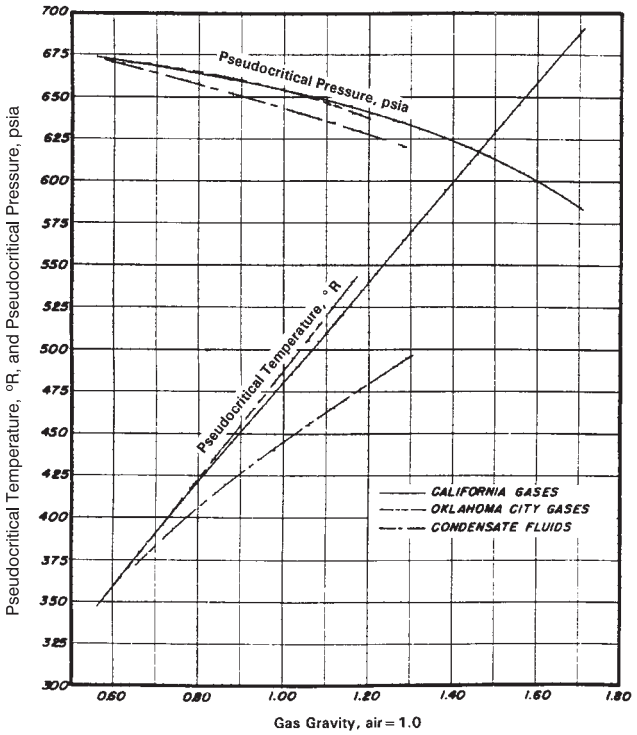

Fig. 3.7—Gas pseudocritical properties as functions of specific gravity.

where $p_r = p/p_c$ and $T_r = T/T_c$. Such corresponding-states relations should be valid for most pure compounds when component critical properties p_c and T_c are used. The same relations can be used for gas mixtures if the mixture pseudocritical properties p_{pc} and T_{pc} are used. Pseudocritical properties of gases can be estimated with gas composition and mixing rules or from correlations based on gas specific gravity.

Sutton[7] suggests the following correlations for hydrocarbon gas mixtures.

$$T_{pcHC} = 169.2 + 349.5\gamma_{gHC} - 74.0\gamma_{gHC}^2 \ldots\ldots\ldots (3.47a)$$

$$\text{and } p_{pcHC} = 756.8 - 131\gamma_{gHC} - 3.6\gamma_{gHC}^2. \ldots\ldots\ldots (3.47b)$$

He claims that Eqs. 3.47a and 3.47b are the most reliable correlations for calculating pseudocritical properties with the Standing-Katz Z-factor chart. He even claims that this method is superior to the use of composition and mixing rules.

Standing[3] gives two sets of correlations: one for dry hydrocarbon gases ($\gamma_{gHC} < 0.75$),

$$T_{pcHC} = 168 + 325\gamma_{gHC} - 12.5\gamma_{gHC}^2 \ldots\ldots\ldots\ldots (3.48a)$$

$$\text{and } p_{pcHC} = 667 + 15.0\gamma_{gHC} - 37.5\gamma_{gHC}^2, \ldots\ldots\ldots (3.48b)$$

and one for wet-gas mixtures ($\gamma_{gHC} \geqq 0.75$),

$$T_{pcHC} = 187 + 330\gamma_{gHC} - 71.5\gamma_{gHC}^2 \ldots\ldots\ldots\ldots (3.49a)$$

$$\text{and } p_{pcHC} = 706 - 51.7\gamma_{gHC} - 11.1\gamma_{gHC}^2. \ldots\ldots\ldots (3.49b)$$

The Standing correlations are used extensively in the industry; **Fig. 3.7** compares them with the Sutton correlations. The Sutton and the Standing wet-gas correlations for T_{pc} give basically the same results, whereas the three p_{pc} correlations are quite different at $\gamma_g > 0.85$.

Kay's[5] mixing rule is typically used when gas composition is available.

$$M = \sum_{i=1}^{N} y_i M_i, \quad \ldots\ldots\ldots\ldots\ldots\ldots\ldots\ldots\ldots (3.50a)$$

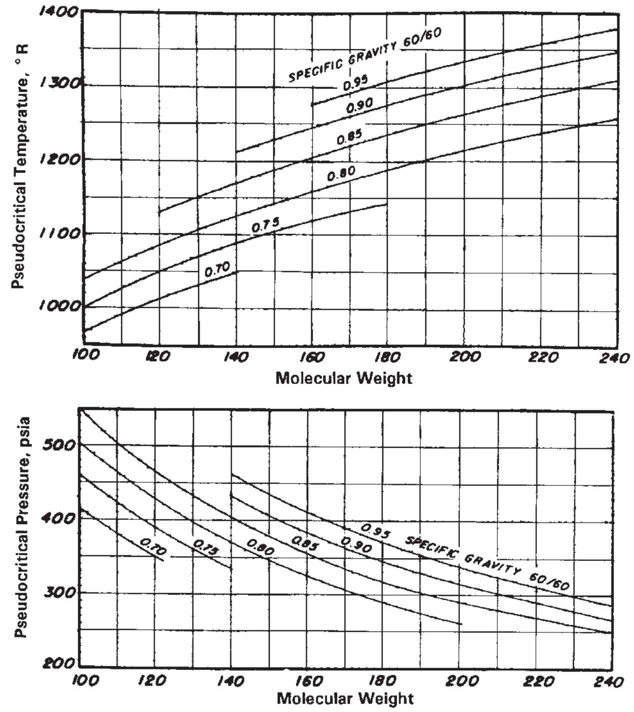

Fig. 3.8—Heptanes-plus (pseudo)critical properties recommended for reservoir gases (from Standing,[33] after Matthews *et al.*[32]).

$$T_{pc} = \sum_{i=1}^{N} y_i T_{ci}, \quad \text{(3.50b)}$$

and
$$p_{pc} = \sum_{i=1}^{N} y_i p_{ci}, \quad \text{(3.50c)}$$

where the pseudocritical properties of the C_{7+} fraction can be estimated from the Matthews *et al.*[32] correlations (**Fig. 3.8**),[3]

$$T_{cC_{7+}} = 608 + 364 \log\left(M_{C_{7+}} - 71.2\right) + \left(2{,}450 \log M_{C_{7+}} - 3{,}800\right)\log \gamma_{C_{7+}} \quad \text{(3.51a)}$$

and
$$p_{cC_{7+}} = 1{,}188 - 431 \log\left(M_{C_{7+}} - 61.1\right) + \left[2{,}319 - 852 \log\left(M_{C_{7+}} - 53.7\right)\right]\left(\gamma_{C_{7+}} - 0.8\right). \quad \text{(3.51b)}$$

Kay's mixing rule is usually adequate for lean natural gases that contain no nonhydrocarbons. Sutton suggests that pseudocriticals calculated with Kay's mixing rule are adequate up to $\gamma_g \approx 0.85$, but that errors in calculated *Z* factors increase linearly at higher specific gravities, reaching 10 to 15% for $\gamma_g > 1.5$. This bias may be a result of the C_{7+} critical-property correlations used by Sutton (not Eqs. 3.51a and 3.51b).

When significant quantities of CO_2 and H_2S nonhydrocarbons are present, Wichert and Aziz[33,31] suggest corrections to arrive at pseudocritical properties that will yield reliable *Z* factors from the Standing-Katz chart. The Wichert and Aziz corrections are given by

$$T_{pc} = T^*_{pc} - \epsilon, \quad \text{(3.52a)}$$

$$p_{pc} = \frac{p^*_{pc}\left(T^*_{pc} - \epsilon\right)}{T^*_{pc} + y_{H_2S}\left(1 - y_{H_2S}\right)\epsilon}, \quad \text{(3.52b)}$$

and
$$\epsilon = 120\left[\left(y_{CO_2} + y_{H_2S}\right)^{0.9} - \left(y_{CO_2} + y_{H_2S}\right)^{1.6}\right] + 15\left(y^{0.5}_{H_2S} - y^4_{H_2S}\right), \quad \text{(3.52c)}$$

where T^*_{pc} and p^*_{pc} are mixture pseudocriticals based on Kay's mixing rule. This method was developed from extensive data from natural gases containing nonhydrocarbons, with CO_2 molar concentration ranging from 0 to 55% and H_2S molar concentrations ranging from 0 to 74%.

If only gas gravity and nonhydrocarbon content are known, the hydrocarbon specific gravity is first calculated from

$$\gamma_{gHC} = \frac{\gamma_g - \left(y_{N_2}M_{N_2} + y_{CO_2}M_{CO_2} + y_{H_2S}M_{H_2S}\right)/M_{air}}{1 - y_{N_2} - y_{CO_2} - y_{H_2S}}. \quad \text{(3.53)}$$

Hydrocarbon pseudocriticals are then calculated from Eqs. 3.47a and 3.47b, and these values are adjusted for nonhydrocarbon content on the basis of Kay's[5] mixing rule.

$$p^*_{pc} = \left(1 - y_{N_2} - y_{CO_2} - y_{H_2S}\right)p_{pcHC} + y_{N_2}p_{cN_2} + y_{CO_2}p_{cCO_2} + y_{H_2S}p_{cH_2S} \quad \text{(3.54a)}$$

and
$$T^*_{pc} = (1 - y_{N_2} - y_{CO_2} - y_{H_2S})T_{pcHC} + y_{N_2}T_{cN_2} + y_{CO_2}T_{cCO_2} + y_{H_2S}T_{cH_2S}. \quad \text{(3.54b)}$$

T^*_c and p^*_c are used in the Wichert-Aziz equations with CO_2 and H_2S mole fractions to obtain mixture T_{pc} and p_{pc}.

The Sutton[7] correlations (Eqs. 3.47a and 3.47b) are recommended for hydrocarbon pseudocritical properties. If composition is available, Kay's mixing rule should be used with the Matthews *et al.*[32] pseudocriticals for C_{7+}. Gases containing significant amounts of CO_2 and H_2S nonhydrocarbons should always be corrected with the Wichert-Aziz equations. Finally, for gas-condensate fluids the wellstream specific gravity, γ_w (discussed in the next section), should replace γ_g in the equations above.

3.3.4 Wellstream Specific Gravity. Gas mixtures that produce condensate at surface conditions may exist as a single-phase gas in the reservoir and production tubing. This can be verified by determining the dewpoint pressure at the prevailing temperature. If wellstream properties are desired at conditions where the mixture is single-phase, surface-gas and -oil properties must be converted to a wellstream specific gravity, γ_w. This gravity should be used instead of γ_g to estimate pseudocritical properties.

Wellstream gravity r_p represents the average molecular weight of the produced mixture (relative to air) and is readily calculated from the producing-oil (condensate)/gas ratio, r_p; average surface-gas gravity $\bar{\gamma}_{\bar{g}}$; surface-condensate gravity, $\gamma_{\bar{o}}$; and surface-condensate molecular weight $M_{\bar{o}}$.

$$\gamma_w = \frac{\bar{\gamma}_{\bar{g}} + 4{,}580\, r_p \gamma_{\bar{o}}}{1 + 133{,}000\, r_p (\gamma/M)_{\bar{o}}}, \quad \text{(3.55)}$$

with r_p in STB/scf. Average surface-gas gravity is given by

$$\bar{\gamma}_{\bar{g}} = \frac{\sum_{i=1}^{N_{sp}} R_{pi}\gamma_{gi}}{\sum_{i=1}^{N_{sp}} R_{pi}}, \quad \text{(3.56)}$$

where R_{pi} = GOR of Separator Stage *i*. Standing[33] presents Eq. 3.55 graphically in **Fig. 3.9.**

When $M_{\bar{o}}$ is not available, Standing gives the following correlation.

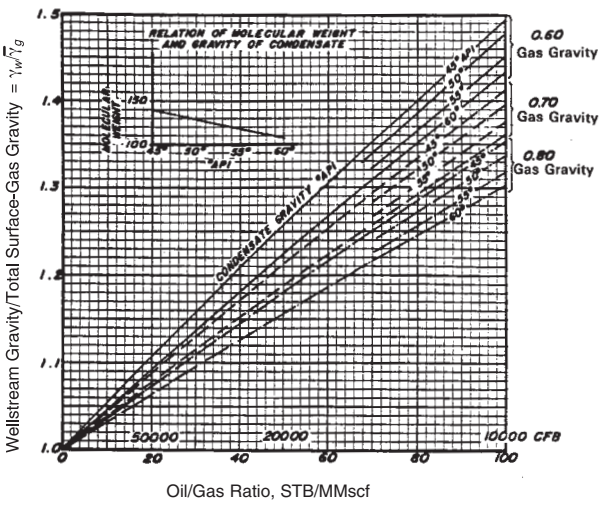

Fig. 3.9—Wellstream gravity relative to surface average gas gravity as a function of solution oil/gas ratio and surface gravities.

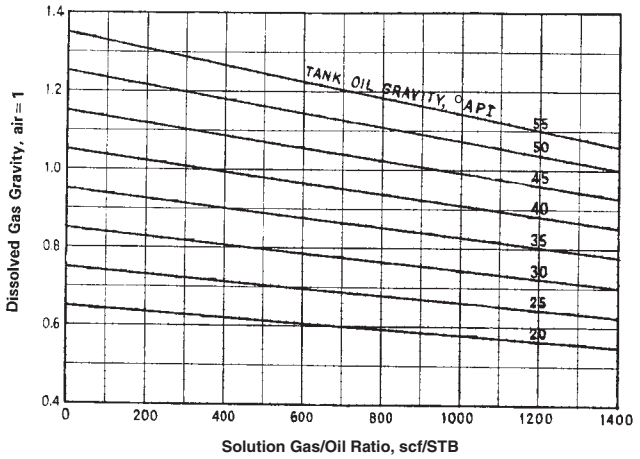

Fig. 3.10—Correlation for separator-oil dissolved gas gravity as a function of stock-tank-oil gravity and separator-oil GOR (from Ref. 41).

$$M_{\overline{o}} = 240 - 2.22\,\gamma_{\mathrm{API}}. \quad \ldots\ldots\ldots\ldots\ldots\ldots\ldots\ldots (3.57)$$

This relation should not be extrapolated outside the range $45 < \gamma_{\mathrm{API}} < 60$. Eilerts[34] gives a relation for $(\gamma/M)_{\overline{o}}$,

$$(\gamma/M)_{\overline{o}} = \left(1.892 \times 10^{-3}\right) + \left(7.35 \times 10^{-5}\right)\gamma_{\mathrm{API}} - \left(4.52 \times 10^{-8}\right)\gamma^2_{\mathrm{API}}, \quad \ldots\ldots\ldots\ldots\ldots (3.58)$$

which should be reliable for most condensates. When condensate molecular weight is not available, the recommended correlation for $M_{\overline{o}}$ is the Cragoe[35] correlation,

$$M_{\overline{o}} = \frac{6,084}{\gamma_{\mathrm{API}} - 5.9}, \quad \ldots\ldots\ldots\ldots\ldots\ldots\ldots\ldots (3.59)$$

which gives reasonable values for all surface condensates and stock-tank oils.

A typical problem that often arises in the engineering of gas-condensate reservoirs is that all the data required to calculate wellstream gas volumes and wellstream specific gravity are not available and must be estimated.[36-38] In practice, we often report only the first-stage-separator GOR (relative to stock-tank-oil volume) and gas specific gravity, R_{s1} and γ_{g1}, respectively; the stock-tank-oil gravity, $\gamma_{\overline{o}}$; and the primary-separator conditions, p_{sp1} and T_{sp1}.

To calculate γ_w from Eq. 3.55 we need total producing OGR, r_p, which equals the inverse of R_{s1} plus the additional gas that will be released from the first-stage separator oil, R_{s+},

$$r_p = \frac{1}{\left(R_{s1} + R_{s+}\right)}. \quad \ldots\ldots\ldots\ldots\ldots\ldots\ldots\ldots (3.60)$$

R_{s+} can be estimated from several correlations.[37,39] Whitson[38] proposes use of a bubblepoint pressure correlation (e.g., the Standing[40] correlation),

$$R_{s+} = A_1\gamma_{g+} \quad \ldots\ldots\ldots\ldots\ldots\ldots\ldots\ldots (3.61a)$$

$$\text{and } A_1 = \left[\left(\frac{p_{sp1}}{18.2} + 1.4\right)10^{\left(0.0125\gamma_{\mathrm{API}} - 0.00091T_{sp1}\right)}\right]^{1.205}, \quad \ldots\ldots\ldots\ldots\ldots (3.61b)$$

with p_{sp1} in psia, T_{sp1} in °F, and R_{s+} in scf/STB. γ_{g+} is the gas gravity of the additional solution gas released from the separator oil. The Katz[41] correlation (**Fig. 3.10**) can be used to estimate γ_{g+}, where a best-fit representation of his graphical correlation is

$$\gamma_{g+} = A_2 + A_3R_{s+}, \quad \ldots\ldots\ldots\ldots\ldots\ldots\ldots\ldots (3.62)$$

where $A_2 = 0.25 + 0.02\gamma_{\mathrm{API}}$ and $A_3 = -\left(3.57 \times 10^{-6}\right)\gamma_{\mathrm{API}}$.

Solving Eqs. 3.61 and 3.62 for R_{s+} gives

$$R_{s+} = \frac{A_1A_2}{\left(1 - A_1A_3\right)}. \quad \ldots\ldots\ldots\ldots\ldots\ldots\ldots\ldots (3.63)$$

Average surface separator gas gravity, $\overline{\gamma}_{\overline{g}}$, is given by

$$\overline{\gamma}_{\overline{g}} = \frac{\gamma_{g1}R_{s1} + \gamma_{g+}R_{s+}}{R_{s1} + R_{s+}}. \quad \ldots\ldots\ldots\ldots\ldots\ldots\ldots\ldots (3.64)$$

Although the Katz correlation is only approximate, the impact of a few percent error in γ_{g+} is not of practical consequence to the calculation of γ_w because R_{s+} is usually much less than R_{s1}.

3.3.5 Gas Viscosity. Viscosity of reservoir gases generally ranges from 0.01 to 0.03 cp at standard and reservoir conditions, reaching up to 0.1 cp for near-critical gas condensates. Estimation of gas viscosities at elevated pressure and temperature is typically a two-step procedure: (1) calculating mixture low-pressure viscosity μ_{gsc} at p_{sc} and T from Chapman-Enskog theory[3,6] and (2) correcting this value for the effect of pressure and temperature with a corresponding-states or dense-gas correlation. These correlations relate the actual viscosity μ_g at p and T to low-pressure viscosity by use of the ratio μ_g/μ_{gsc} or difference $(\mu_g - \mu_{gsc})$ as a function of pseudoreduced properties p_{pr} and T_{pr} or as a function of pseudoreduced density ρ_{pr}.

Gas viscosities are rarely measured because most laboratories do not have the required equipment; thus, the prediction of gas viscosity is particularly important. Gas viscosity of reservoir systems is often estimated from the graphical correlation $\mu_g/\mu_{gsc} = \mathrm{f}(T_r, p_r)$ proposed by Carr *et al.*[42] (**Fig. 3.11**). Dempsey[43] gives a polynomial approximation of the Carr *et al.* correlation. With these correlations, gas viscosities can be estimated with an accuracy of about ±3% for most applications. The Dempsey correlation is valid in the range $1.2 \leqq T_r \leqq 3$ and $1 \leqq p_r \leqq 20$.

The Lee-Gonzalez gas viscosity correlation (used by most PVT laboratories when reporting gas viscosities) is given by[44]

$$\mu_g = A_1 \times 10^{-4}\exp\left(A_2\rho_g^{A_3}\right), \quad \ldots\ldots\ldots\ldots\ldots (3.65a)$$

$$\text{where } A_1 = \frac{\left(9.379 + 0.01607M_g\right)T^{1.5}}{209.2 + 19.26M_g + T},$$

$$A_2 = 3.448 + \left(986.4/T\right) + 0.01009M_g,$$

$$\text{and } A_3 = 2.447 - 0.2224A_2, \quad \ldots\ldots\ldots\ldots\ldots (3.65b)$$

with μ_g in cp, ρ_g in g/cm^3, and T in °R. McCain[19] indicates the accuracy of this correlation is 2 to 4% for $\gamma_g < 1.0$, with errors up to 20% for rich gas condensates with $\gamma_g > 1.5$.

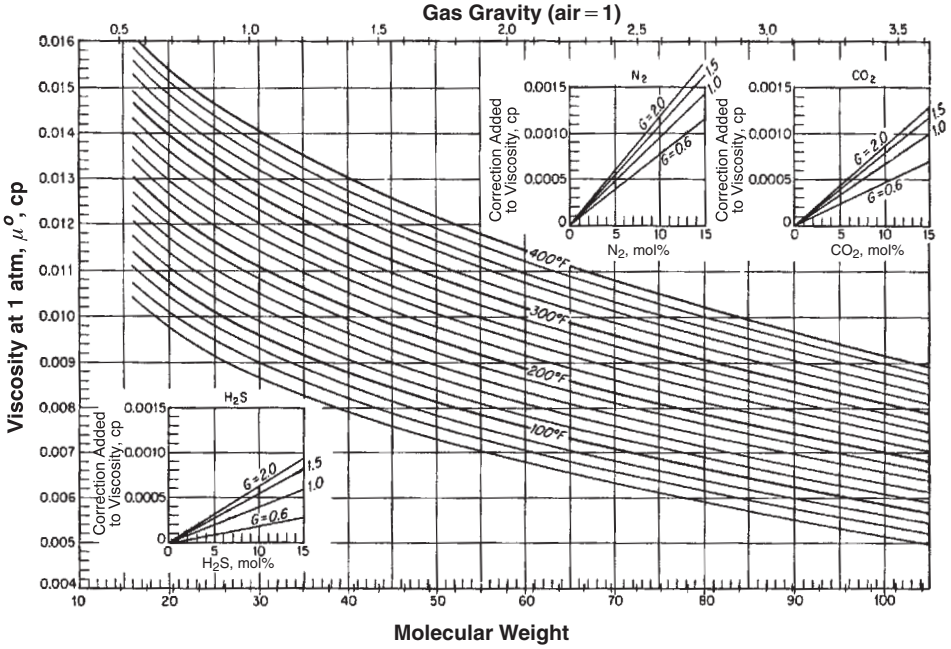

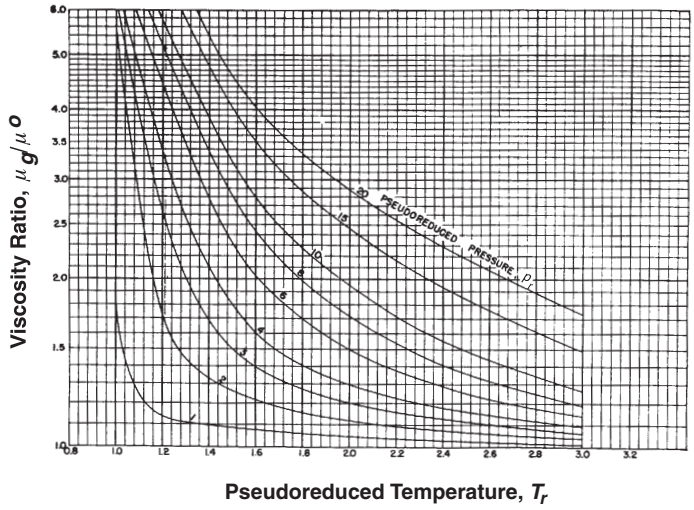

Fig. 3.11—Carr *et al.*[42] gas-viscosity correlation.

Lucas[45] proposes the following gas viscosity correlation, which is valid in the range $1 < T_r < 40$ and $0 < p_r < 100$ (**Fig. 3.12**)[6]:

$$\mu_g/\mu_{gsc} = 1 + \frac{A_1 p_{pr}^{1.3088}}{A_2 p_{pr}^{A_5} + \left(1 + A_3 p_{pr}^{A_4}\right)^{-1}}, \quad \ldots\ldots (3.66a)$$

where $A_1 = \dfrac{(1.245 \times 10^{-3}) \exp\left(5.1726 T_{pr}^{-0.3286}\right)}{T_{pr}}$,

$$A_2 = A_1\left(1.6553 T_{pr} - 1.2723\right),$$

$$A_3 = \frac{0.4489 \exp\left(3.0578 T_{pr}^{-37.7332}\right)}{T_{pr}},$$

$$A_4 = \frac{1.7368 \exp\left(2.2310 T_{pr}^{-7.6351}\right)}{T_{pr}},$$

and $A_5 = 0.9425 \exp\left(-0.1853 T_{pr}^{0.4489}\right)$, ... (3.66b)

where $\mu_{gsc}\xi = \left[0.807 T_{pr}^{0.618} - 0.357 \exp(-0.449 T_{pr}) + 0.340 \exp(-4.058 T_{pr}) + 0.018\right]$,

$$\xi = 9{,}490\left(\frac{T_{pc}}{M^3 p_{pc}^4}\right)^{1/6},$$

and $p_{pc} = RT_{pc}\dfrac{\sum_{i=1}^{N} y_i Z_{ci}}{\sum_{i=1}^{N} y_i v_{ci}}$, ... (3.67)

with ξ in cp^{-1}, T and T_c in °R, and p_c in psia. Special corrections should be applied to the Lucas correlation when polar compounds, such as H_2S and water, are present in a gas mixture. The effect of H_2S is always $<1\%$ and can be neglected, and appropriate corrections can be made to treat water if necessary.

Given its wide range of applicability, the Lucas method is recommended for general use. When compositions are not available, correlations for pseudocritical properties in terms of specific gravity can be used instead. Standing[2] gives equations for μ_{gsc} in terms of γ_g, temperature, and nonhydrocarbon content,

$$\mu_{gsc} = (\mu_{gsc})_{\text{uncorrected}} + \Delta\mu_{N_2} + \Delta\mu_{CO_2} + \Delta\mu_{H_2S}, \quad \ldots\ldots (3.68a)$$

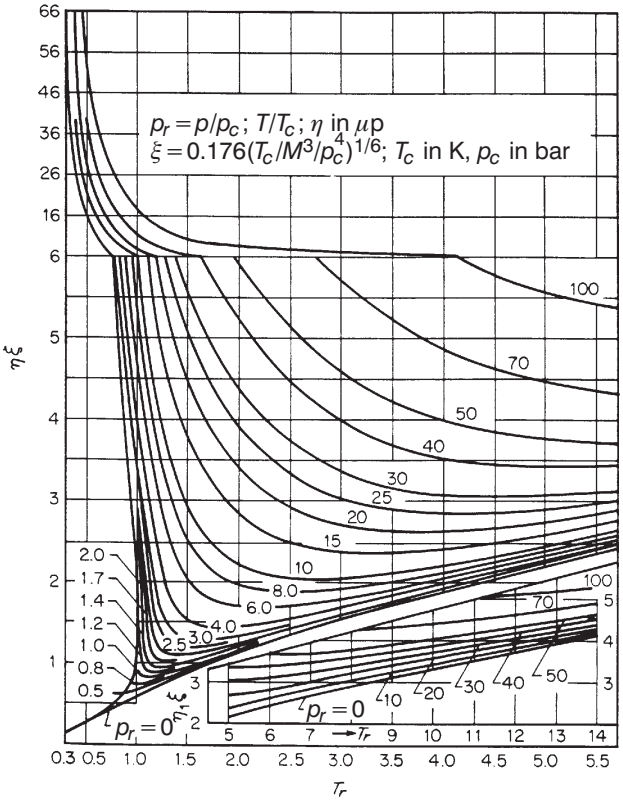

Fig. 3.12—Lucas[45] corresponding-states generalized viscosity correlation (Ref. 6); η = dynamic viscosity and μp = micropoise = 10^{-6} poise = 10^{-4} cp.

$$\text{where } (\mu_{gsc})_{\text{uncorrected}} = (8.188 \times 10^{-3}) + [(1.709 \times 10^{-5}) - (2.062 \times 10^{-6})\gamma_g]T - (6.15 \times 10^{-3}) \log \gamma_g,$$

$$\Delta\mu_{N_2} = y_{N_2}[(8.48 \times 10^{-3}) \log \gamma_g + (9.59 \times 10^{-3})],$$

$$\Delta\mu_{CO_2} = y_{CO_2}[(9.08 \times 10^{-3}) \log \gamma_g + (6.24 \times 10^{-3})],$$

$$\text{and } \Delta\mu_{H_2S} = y_{H_2S}[(8.49 \times 10^{-3}) \log \gamma_g + (3.73 \times 10^{-3})]. \quad \ldots\ldots\ldots\ldots\ldots (3.68b)$$

Reid *et al.*[6] review other gas viscosity correlations with accuracy similar to that of the Lucas correlation.

3.3.6 Dewpoint Pressure. The prediction of retrograde dewpoint pressure is not widely practiced. It is generally recognized that the complexity of retrograde phase behavior necessitates experimental determination of the dewpoint condition. Sage and Olds'[46] data are perhaps the most extensive tabular correlation of dewpoint pressures. Eilerts *et al.*[47,48] also present dewpoint pressures for several light-condensate systems.

Nemeth and Kennedy[49] have proposed a dewpoint correlation based on composition and C_{7+} properties.

$$\ln p_d = A_1\left[z_{C_2} + z_{CO_2} + z_{H_2S} + z_{C_6} + 2(z_{C_3} + z_{C_4}) + z_{C_5} + 0.4z_{C_1} + 0.2z_{N_2}\right] + A_2\gamma_{C_{7+}} + A_3\left[\frac{z_{C_1}}{\left(z_{C_{7+}} + 0.002\right)}\right] + A_4T + \left(A_5 z_{C_{7+}} M_{C_{7+}}\right) + A_6\left(z_{C_{7+}} M_{C_{7+}}\right)^2 + A_7\left(z_{C_{7+}} M_{C_{7+}}\right)^3 + A_8\left[\frac{M_{C_{7+}}}{\left(\gamma_{C_{7+}} + 0.0001\right)}\right] + A_9\left[\frac{M_{C_{7+}}}{\left(\gamma_{C_{7+}} + 0.0001\right)}\right]^2 + A_{10}\left[\frac{M_{C_{7+}}}{\left(\gamma_{C_{7+}} + 0.0001\right)}\right]^3 + A_{11}, \quad \ldots\ldots\ldots\ldots\ldots (3.69)$$

where $A_1 = -2.0623054$, $A_2 = 6.6259728$, $A_3 = -4.4670559 \times 10^{-3}$, $A_4 = 1.0448346 \times 10^{-4}$, $A_5 = 3.2673714 \times 10^{-2}$, $A_6 = -3.6453277 \times 10^{-3}$, $A_7 = 7.4299951 \times 10^{-5}$, $A_8 = -1.1381195 \times 10^{-1}$, $A_9 = 6.2476497 \times 10^{-4}$, $A_{10} = -1.0716866 \times 10^{-6}$, and $A_{11} = 1.0746622 \times 10^{1}$.

The range of properties used to develop this correlation includes dewpoints from 1,000 to 10,000 psia, temperatures from 40 to 320°F, and a wide range of reservoir compositions. The correlation usually can be expected to predict dewpoints with an accuracy of ± 10% for condensates that do not contain large amounts of nonhydrocarbons. This is acceptable in light of the fact that experimental dewpoint pressures are probably determined with an accuracy of only ± 5%. The correlation is generally used only for preliminary reservoir studies conducted before an experimental dewpoint is available.

Organick and Golding[50] and Kurata and Katz[51] present graphical correlations for dewpoint pressure.

3.3.7 Total FVF. Total FVF,[3,17,46] B_t, is defined as the volume of a two-phase, gas-oil mixture (or sometimes a single-phase mixture) at elevated pressure and temperature divided by the stock-tank-oil volume resulting when the two-phase mixture is brought to surface conditions,

$$B_t = \frac{V_o + V_g}{(V_o)_{sc}} = \frac{V_o + V_g}{V_{\bar{o}}}. \quad \ldots\ldots\ldots\ldots\ldots (3.70)$$

B_t is used for calculating the oil in place for gas-condensate reservoirs, where $V_o = 0$ in Eq. 3.70. Assuming 1 res bbl of hydrocarbon PV, the initial condensate in place is given by $N = 1/B_t$ (in STB) and the initial "dry" separator gas in place is $G = N/r_p$, where r_p = initial producing (solution) OGR.

For gas-condensate systems, Sage and Olds[46] give a tabulated correlation for B_t.

$$B_t = \frac{R_p T}{p} Z^*, \quad \ldots\ldots\ldots\ldots\ldots (3.71)$$

where R_p = producing GOR in scf/STB, B_t is in bbl/STB, T is in °R, and p is in psia. Z^* varies with pressure and temperature, where the tabulated correlation for Z^* is well represented by

$$Z^* = A_0 + A_1 p + A_2 p^{1.5} + A_3\frac{p}{T} + A_4\frac{p^{1.5}}{T}, \quad \ldots\ldots\ldots (3.72)$$

where $A_0 = 5.050 \times 10^{-3}$, $A_1 = -2.740 \times 10^{-6}$, $A_2 = 3.331 \times 10^{-8}$, $A_3 = 2.198 \times 10^{-3}$, and $A_4 = -2.675 \times 10^{-5}$ with p in psia and T in °R. Although the Sage and Olds data only cover the range $600 < p < 3{,}000$ psia and $100 < T < 250$°F, Eq. 3.72 gives acceptable results up to 10,000 psia and 350°F (when gas volume is much larger than oil volume).

When reservoir hydrocarbon volume consists only of gas, the following relations apply for total FVF.

$$B_t = B_{gd}R_p = B_{gw}\left(R_p + C_{\bar{o}g}\right), \quad \ldots\ldots\ldots\ldots\ldots (3.73a)$$

$$C_{\bar{o}g} = 133{,}000(\gamma_{\bar{o}}/M_{\bar{o}}), \quad \ldots\ldots\ldots\ldots\ldots (3.73b)$$

$$M_{\bar{o}} \approx 6{,}084/(\gamma_{API} - 5.9), \quad \ldots\ldots\ldots\ldots\ldots (3.73c)$$

$$\text{and } \gamma_{API} = 141.5/(131.5 + \gamma_{\bar{o}}), \quad \ldots\ldots\ldots\ldots\ldots (3.73d)$$

where B_{gd} = dry gas FVF in ft³/scf, B_{gw} = wet-gas FVF in ft³/scf (given by Eq. 3.38), $C_{\bar{o}g}$ = gas equivalent conversion factor in scf/STB (see Chap. 7), and R_p = producing GOR in scf/STB.

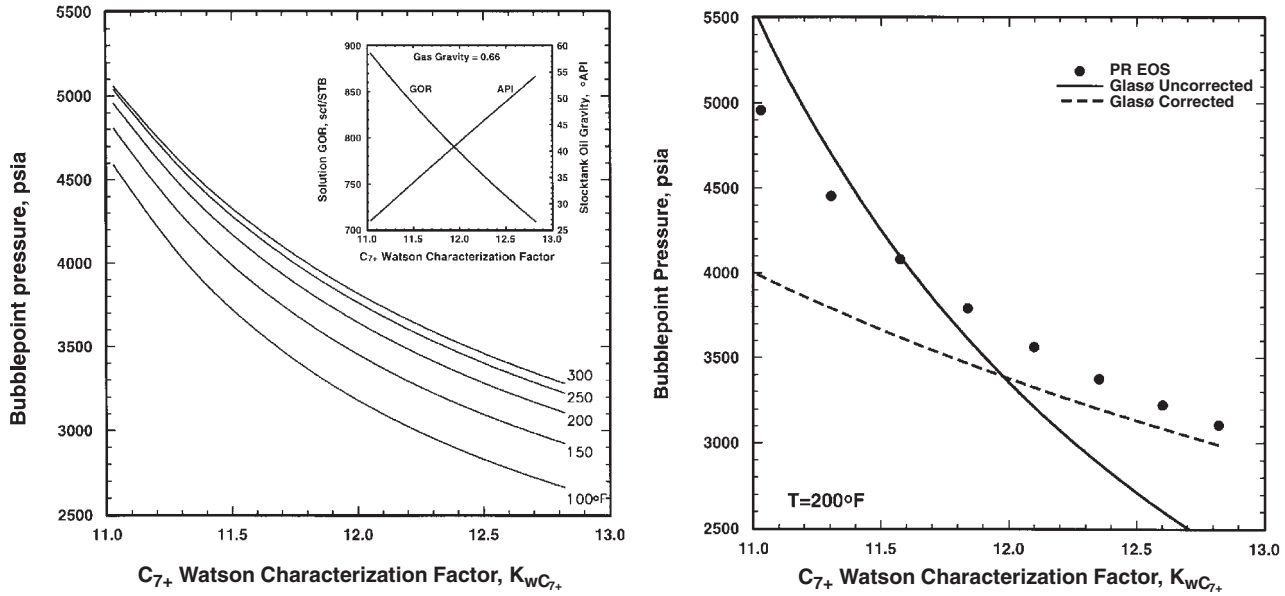

Fig. 3.13—Effect of paraffinicity, K_W, on bubblepoint pressure.

Standing[3] gives a graphical correlation for B_t using a correlation parameter A defined as

$$A = R_p \frac{T^{0.5}}{\gamma_g^{0.3}} \gamma_o^a, \quad \ldots\ldots\ldots\ldots\ldots\ldots\ldots\ldots\ldots (3.74)$$

where $a = 2.9 \times 10^{-0.00027 R_p}$. Standing's correlation is valid for both oil and gas-condensate systems and can be represented with

$$\log B_t = -5.262 - \frac{47.4}{-12.22 + \log A^*}, \quad \ldots\ldots\ldots (3.75a)$$

$$\text{where } \log A^* = \log A - \left(10.1 - \frac{96.8}{6.604 + \log p}\right) \quad \ldots (3.75b)$$

and A is given by Eq. 3.74. On the basis of data from North Sea oils, Glasø[52] gives a correlation for B_t using the Standing correlation parameter A (Eq. 3.74):

$$\log B_t = \left(8.0135 \times 10^{-2}\right) + 0.47257 \log A^* + 0.17351\left(\log A^*\right)^2, \quad \ldots\ldots\ldots\ldots\ldots\ldots (3.76)$$

where $A^* = A p^{-1.1089}$.

Either the Standing or the Glasø correlations for B_t can be used with approximately the same accuracy. However, neither correlation is consistent with the limiting conditions

$$B_t = B_o \quad \text{for} \quad V_g = 0 \quad \ldots\ldots\ldots\ldots\ldots\ldots\ldots\ldots (3.77a)$$

$$\text{and } B_t = B_{gd} R_p \quad \text{for} \quad V_o = 0. \quad \ldots\ldots\ldots\ldots\ldots\ldots (3.77b)$$

B_t correlations evaluated at a bubblepoint usually will underpredict the actual B_{ob} by ≈ 0.2.

3.4 Oil Mixtures

This section gives correlations for PVT properties of reservoir oils, including bubblepoint pressure and oil density, compressibility, FVF, and viscosity. With only a few exceptions, oil properties have been correlated in terms of surface-oil and -gas properties, including solution gas/oil ratio, oil gravity, average surface-gas gravity, and temperature. A few correlations are also given in terms of composition and component properties.

Reservoir oils typically contain dissolved gas consisting mainly of methane and ethane, some intermediates (C_3 through C_6), and lesser quantities of nonhydrocarbons. The amount of dissolved gas has an important effect on oil properties. At the bubblepoint a discontinuity in the system volumetric behavior is caused by gas coming out of solution, with the system compressibility changing dramatically.[8] An accurate method is needed to correlate the bubblepoint pressure, temperature, and solution gas/oil ratio.

Oil properties can be grouped into two categories: saturated and undersaturated properties. Saturated properties apply at pressures at or below the bubblepoint, and undersaturated properties apply at pressures greater than the bubblepoint. For oils with initial GOR's less than ≈ 500 scf/STB, assuming linear variation of undersaturated-oil properties with pressure is usually acceptable.

3.4.1 Bubblepoint Pressure. The correlation of bubblepoint pressure has received more attention than any other oil-property correlation. Standing[3,17,40] developed the first accurate bubblepoint correlation, which was based on California crude oils.

$$p_b = 18.2(A - 1.4), \quad \ldots\ldots\ldots\ldots\ldots\ldots\ldots (3.78)$$

where $A = \left(R_s/\gamma_g\right)^{0.83} 10^{\left(0.00091T - 0.0125\gamma_{API}\right)}$, with R_s in scf/STB, T in °F, and p_b in psia.

Lasater[53] used a somewhat different approach to correlate bubblepoint pressure, where mole fraction y_g of solution gas in the reservoir oil is used as the main correlating parameter[17]:

$$p_b = A \frac{T}{\gamma_g}, \quad \ldots\ldots\ldots\ldots\ldots\ldots\ldots\ldots (3.79)$$

with T in °R and p_b in psia. The function $A(y_g)$ is given graphically by Lasater, and his correlation can be accurately described by

$$A = 0.83918 \times 10^{1.17664 y_g} y_g^{0.57246}; \; y_g \leqq 0.6 \quad \ldots\ldots (3.80a)$$

$$\text{and } A = 0.83918 \times 10^{1.08000 y_g} y_g^{0.31109}; \; y_g > 0.6, \quad \ldots\ldots (3.80b)$$

$$\text{where } y_g = \left[1 + \frac{133{,}000\,(\gamma/M)_o}{R_s}\right]^{-1}, \quad \ldots\ldots\ldots\ldots (3.81)$$

with R_s in scf/STB. In this correlation, the gas mole fraction is dependent mainly on solution gas/oil ratio, but also on the properties of the stock-tank oil. The Cragoe[35] correlation given by Eq. 3.59 is recommended for estimating M_o when stock-tank-oil molecular weight is not known.

Standing's approach was used by Glasø[52] for North Sea oils, resulting in the correlation

$$\log p_b = 1.7669 + 1.7447 \log A - 0.30218(\log A)^2, \quad \ldots\ldots\ldots\ldots\ldots\ldots (3.82)$$

where $A = \left(R_s/\gamma_g\right)^{0.816} \left(T^{0.172}/\gamma_{API}^{0.989}\right)$ with p_b in psia, T in °F and R_s in scf/STB. Glasø's corrections for nonhydrocarbon content and stock-tank-oil paraffinicity are not widely used, primarily be-

cause the necessary data are not available. Sutton and Farshad[54] mention that the API correction for paraffinicity worsened bubblepoint predictions for gulf coast fluids. **Fig. 3.13** gives an explanation for this observation.

Fig. 3.13 shows the effect of paraffinicity (which is quantified by the Watson characterization factor, K_w) on bubblepoint pressure; the figure is based on calculations with a tuned EOS for an Asian oil (solid circles). The oil composition is constant in the example calculation. The 12 C_{7+} fractions are each split into a paraffinic pseudocomponent and an aromatic pseudocomponent (i.e., 24 C_{7+} pseudocomponents). The paraffinic fraction was varied, and bubblepoint calculations were made. The variation in paraffinicity is expressed in terms of the overall C_{7+} Watson characterization factor. Also shown in the figure are the variation in solution gas/oil ratio and the oil specific gravity with $K_{wC_{7+}}$.

The actual reservoir oil has a $K_{wC_{7+}} = 11.55$, where the EOS bubblepoint is close to the uncorrected Glasø bubblepoint prediction. When the correction for paraffinicity is applied, the correction gives a poorer bubblepoint prediction (even though the overall trend in bubblepoints is improved by the Glasø paraffinicity corrections).

A quantitatively similar correction to the Glasø correction (but easier to use) is based on the estimate for Whitson's[55,56] Watson characterization factor, K_w, and yields

$$(\gamma_o)_{\text{corrected}} = (\gamma_o)_{\text{measured}}(K_w/11.9)^{1.1824}. \quad \ldots\ldots\ldots\ldots (3.83)$$

The corrected specific gravity correlation is used in the Glasø bubblepoint correlation instead of the measured specific gravity. An estimate of K_w for the stock-tank oil must be available to use this correction.

Vazquez and Beggs[57] give the following correlations. For $\gamma_{\text{API}} \leqq 30$,

$$p_b = \left[27.64\left(\frac{R_s}{\gamma_{gc}}\right)10^{\left(\frac{-11.172\,\gamma_{\text{API}}}{T+460}\right)}\right]^{0.9143}, \quad \ldots\ldots\ldots\ldots (3.84)$$

and, for $\gamma_{\text{API}} > 30$,

$$p_b = \left[56.06\left(\frac{R_s}{\gamma_{gc}}\right)10^{\left(\frac{-10.393\gamma_{\text{API}}}{T+460}\right)}\right]^{0.8425}, \quad \ldots\ldots\ldots\ldots (3.85)$$

with p_b in psia, T in °F and R_s in scf/STB. These equations are based on a large number of data from commercial laboratories. Vazquez and Beggs correct for the effect of separator conditions using a modified gas specific gravity, γ_{gc}, which is correlated with first-stage-separator pressure and temperature, and stock-tank-oil gravity.

$$\gamma_{gc} = \gamma_g\left[1 + (0.5912 \times 10^{-4})\gamma_{\text{API}}T_{sp}\log\left(\frac{p_{sp}}{114.7}\right)\right], \quad \ldots\ldots\ldots\ldots (3.86)$$

with T_{sp} in °F and p_{sp} in psia.

Standing's correlation can be used to develop field- or reservoir-specific bubblepoint correlations. A linear relation is usually assumed between bubblepoint pressure and the Standing correlating coefficient. This is a standard approach used in the industry, and the Standing bubblepoint correlating parameter is well suited for developing field-specific correlations.

Sometimes the solution gas/oil ratio is needed at a given pressure, and this is readily calculated by solving the bubblepoint correlation for R_s. For the Standing correlation,

$$R_s = \gamma_g\left[\frac{(0.055p + 1.4)10^{0.0125\gamma_{\text{API}}}}{10^{0.00091T}}\right]^{1.205}; \quad \ldots\ldots\ldots (3.87)$$

similar relations can be derived for the other bubblepoint correlations.

In summary, significant differences in predicted bubblepoint pressures should not be expected for most reservoir oils with most of the previous correlations. The Lasater and Standing equations are recommended for general use and as a starting point for developing reservoir-specific correlations. Correlations developed for a specific region, such as Glasø's correlation for the North Sea, should probably be used in that region and, in the case of Glasø's correlation, may be extended to other regions by use of the paraffinicity correction.

3.4.2 Oil Density. Density of reservoir oil varies from 30 lbm/ft^3 for light volatile oils to 60 lbm/ft^3 for heavy crudes with little or no solution gas. Oil compressibility may range from 3×10^{-6} psi^{-1} for heavy crude oils to 50×10^{-6} psi^{-1} for light oils. The variation of oil compressibility with pressure is usually small, although for volatile oils the effect can be significant, particularly for material-balance and reservoir-simulation calculations of highly undersaturated volatile oils. Several methods have been used successfully to correlate oil volumetric properties, including extensions of ideal-solution mixing, EOS's, corresponding-states correlations, and empirical correlations.

Oil density based on black-oil properties is given by

$$\rho_o = \frac{62.4\gamma_o + 0.0136\gamma_g R_s}{B_o}, \quad \ldots\ldots\ldots\ldots (3.88)$$

with ρ_o in lbm/ft^3, B_o in bbl/STB, and R_s in scf/STB. Correlations can be used to estimate R_s and B_o from γ_o, γ_g, p, and T.

Standing-Katz Method. Standing[3,17] and Standing and Katz[58] give an accurate method for estimating oil densities that uses an extension of ideal-solution mixing.

$$\rho_o = \rho_{po} + \Delta\rho_p - \Delta\rho_T, \quad \ldots\ldots\ldots\ldots (3.89)$$

where ρ_{po} is the pseudoliquid density at standard conditions and the terms $\Delta\rho_T$ and $\Delta\rho_p$ give corrections for temperature and pressure, respectively. Pseudoliquid density is calculated with ideal-solution mixing and correlations for the apparent liquid densities of ethane

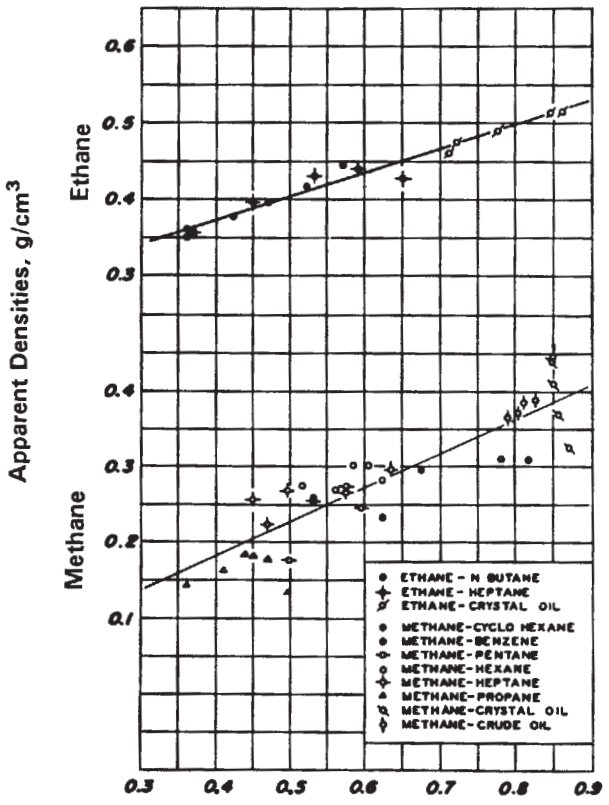

Fig. 3.14—Apparent liquid densities of methane and ethane (from Standing[33]).

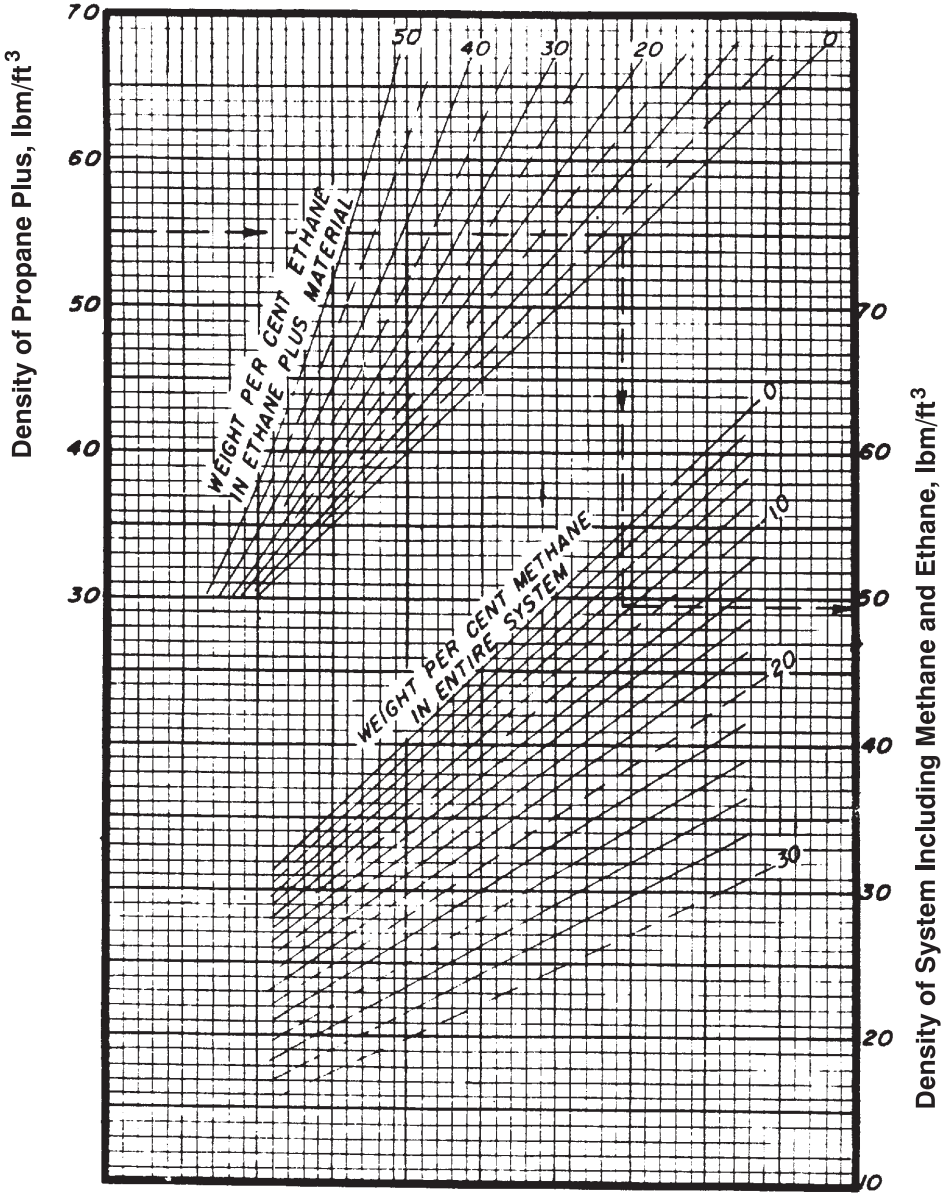

Fig. 3.15—Chart for calculating pseudoliquid density of reservoir oil (from Standing[33]).

and methane at standard conditions. Given oil composition x_i, ρ_{po} is calculated from

$$\rho_{po} = \frac{\sum_{i=1}^{N} x_i M_i}{\sum_{i=1}^{N} (x_i M_i / \rho_i)}, \quad \ldots\ldots\ldots\ldots\ldots\ldots\ldots\ldots (3.90)$$

where Standing and Katz show that apparent liquid densities ρ_i of C_2 and C_1 are functions of the densities ρ_{2+} and ρ_{po}, respectively (**Fig. 3.14**).

$$\rho_{C_2} = 15.3 + 0.3167\rho_{C_{2+}}$$

$$\rho_{C_1} = 0.312 + 0.45\rho_{po}, \quad \ldots\ldots\ldots\ldots\ldots\ldots\ldots\ldots (3.91)$$

$$\text{where } \rho_{C_{2+}} = \frac{\sum_{i=C_2}^{C_{7+}} x_i M_i}{\sum_{i=C_2}^{C_{7+}} (x_i M_i / \rho_i)}, \quad \ldots\ldots\ldots\ldots\ldots\ldots\ldots\ldots (3.92)$$

with ρ in lbm/ft^3. Application of these correlations results in an apparent trial-and-error calculation for ρ_{po}. Standing[33] presents a graphical correlation (**Fig. 3.15**) based on these relations, where ρ_{po} is found from $\rho_{C_{3+}}$ and weight fractions of C_2 and C_1 (w_{C_2} and w_{C_1}, respectively).

Figs. 3.16 and 3.17 show the pressure and temperature corrections, $\Delta\rho_p$ and $\Delta\rho_T$, graphically. $\Delta\rho_p$ is a function of ρ_{po}, and $\Delta\rho_T$ is a function of $(\rho_{po} + \Delta\rho_p)$. Madrazo[59] introduced modified curves for $\Delta\rho_p$ and $\Delta\rho_T$ that improve predictions at higher pressures and temperatures. Standing[3] gives best-fit equations for his original graphical correlations of $\Delta\rho_p$ and $\Delta\rho_T$ (Eqs. 3.98 and 3.99), which are not recommended at temperatures >240°F; instead, Madrazo's graphical correlation can be used. The correction factors can also be used to determine isothermal compressibility and oil FVF at undersaturated conditions.

The treatment of nonhydrocarbons in the Standing-Katz method has not received much attention, and the method is not recommended when concentrations of nonhydrocarbons exceed 10 mol%. Standing[3] suggests that an apparent liquid density of 29.9 lbm/ft^3 can be used for nitrogen but does not address how the nonhydrocarbons should be considered in the calculation procedure (i.e., as part of the C_{3+} material or following the calculation of ρ_{C_2} and ρ_{C_1}). Madrazo indicates that the volume contribution of nonhydrocar-

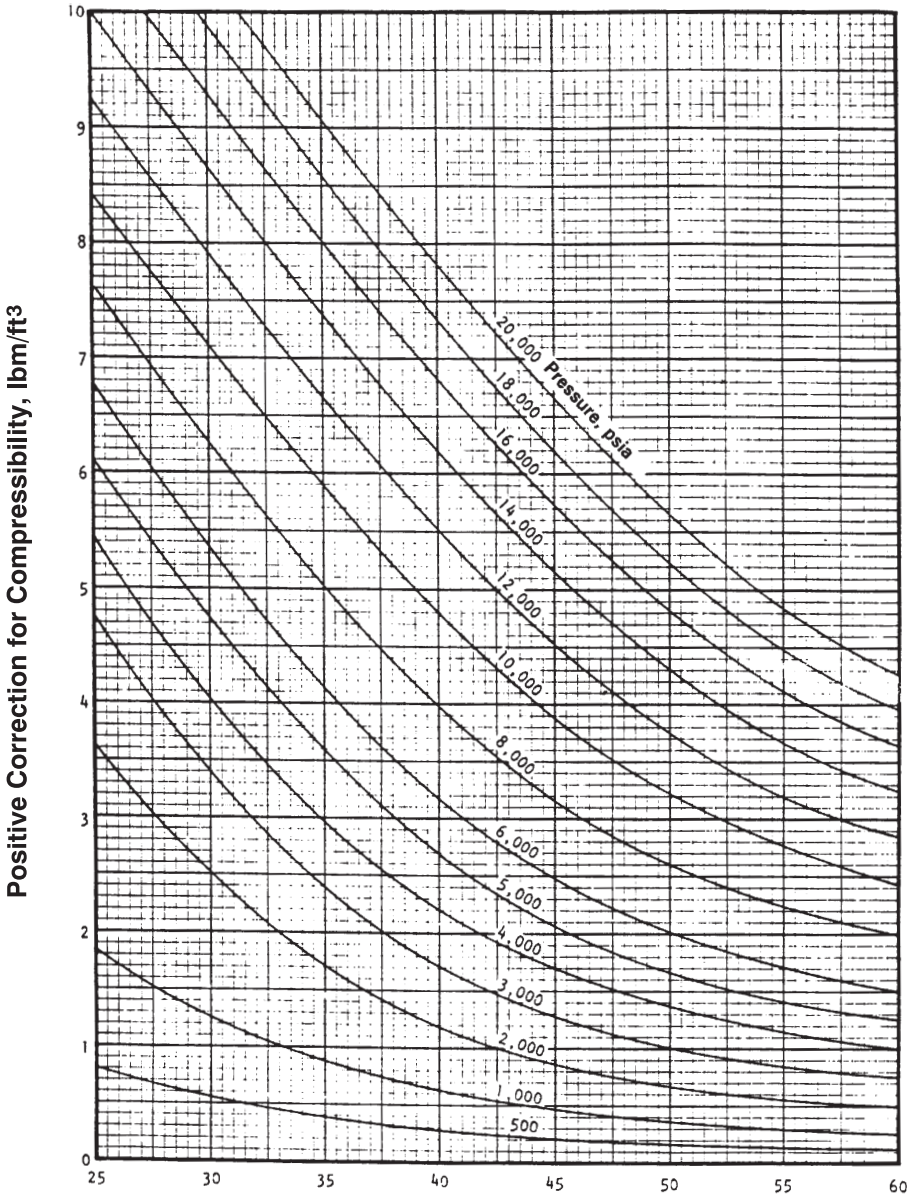

Fig. 3.16—Pressure correction to the pseudoliquid density at 14.7 psia and 60°F (from Ref. 59).

bons can be neglected completely if the total content is <6 mol%. Vogel and Yarborough[60] suggest that the weight fraction of nitrogen should be added to the weight fraction of ethane.

Using additive volumes and Eqs. 3.91 and 3.92, we can show that $\rho_{C_{2+}}$ and ρ_{po} can be calculated explicitly. Thus, the following is the most direct procedure for calculating ρ_o from the Standing-Katz method.

1. Calculate the mass of each component.

$$m_i = x_i M_i. \quad \ldots\ldots\ldots\ldots\ldots\ldots\ldots\ldots\ldots\ldots \quad (3.93)$$

2. Calculate $V_{C_{3+}}$.

$$V_{C_{3+}} = \sum_{i=C_3}^{C_{7+}} \frac{m_i}{\rho_i}, \quad \ldots\ldots\ldots\ldots\ldots\ldots\ldots\ldots \quad (3.94)$$

where ρ_i are component densities at standard conditions (Appendix A).

3. Calculate $\rho_{C_{2+}}$.

$$\rho_{C_{2+}} = \frac{-b + \sqrt{b^2 - 4ac}}{2a}, \quad \ldots\ldots\ldots\ldots\ldots\ldots \quad (3.95)$$

where $a = 0.3167 V_{C_{3+}}$, $b = m_{C_2} - 0.3167 m_{C_{2+}} + 15.3 V_{C_{3+}}$, and $c = -15.3 m_{C_{2+}}$.

4. Calculate $V_{C_{2+}}$.

$$V_{C_{2+}} = V_{C_{3+}} + \frac{m_{C_2}}{\rho_{C_2}}$$

$$= V_{C_{3+}} + \frac{m_{C_2}}{15.3 + 0.3167\rho_{C_{2+}}}. \quad \ldots\ldots\ldots\ldots \quad (3.96)$$

5. Calculate ρ_{po}.

$$\rho_{po} = \frac{-b + \sqrt{b^2 - 4ac}}{2a}, \quad \ldots\ldots\ldots\ldots\ldots\ldots \quad (3.97)$$

where $a = 0.45 V_{C_{2+}}$, $b = m_{C_1} - 0.45 m_{C_{1+}} + 0.312 V_{C_{2+}}$, and $c = -0.312 m_{C_{1+}}$.

6. Calculate the pressure effect on density.

$$\Delta\rho_p = 10^{-3}\left[0.167 + \left(16.181 \times 10^{-0.0425\rho_{po}}\right)\right] p$$

$$- 10^{-8}\left[0.299 + \left(263 \times 10^{-0.0603\rho_{po}}\right)\right] p^2. \quad \ldots\ldots \quad (3.98)$$

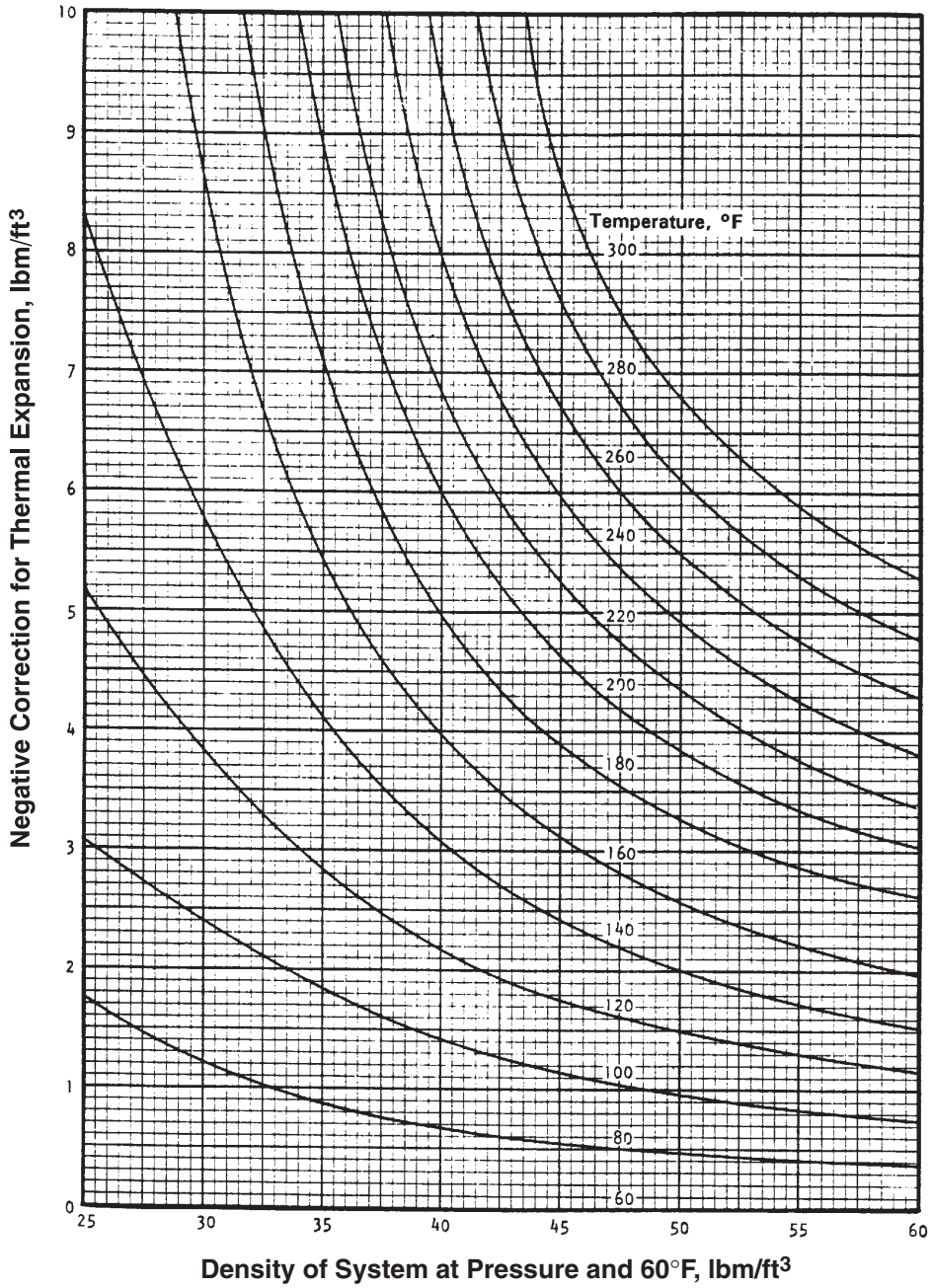

Fig. 3.17—Temperature correction to the pseudoliquid density at pressure and 60°F (from Ref. 59).

7. Calculate the temperature effect on density.

$$\Delta\rho_T = (T - 60)\left[0.0133 + 152.4(\rho_{po} + \Delta\rho_p)^{-2.45}\right] - (T - 60)^2\left\{(8.1 \times 10^{-6}) - \left[0.0622 \times 10^{-0.0764(\rho_{po}+\Delta\rho_p)}\right]\right\}. \quad \ldots\ldots\ldots\ldots \quad (3.99)$$

8. Calculate mixture density from Eq. 3.89.

In the absence of oil composition, Katz[41] suggests calculating the pseudoliquid density from stock-tank-oil gravity, γ_o, solution gas/oil ratio, R_s, and apparent liquid density of the surface gas, ρ_{ga}, taken from a graphical correlation (**Fig. 3.18**),

$$\rho_{po} = \frac{62.4\gamma_o + 0.0136\,R_s\gamma_g}{1 + 0.0136(R_s\gamma_g/\rho_{ga})}. \quad \ldots\ldots\ldots\ldots\ldots\ldots \quad (3.100)$$

Standing gives an equation for ρ_{ga}.

$$\rho_{ga} = 38.52 \times 10^{-0.00326\gamma_{API}} + (94.75 - 33.93 \log \gamma_{API}) \log \gamma_g, \quad \ldots\ldots\ldots\ldots \quad (3.101)$$

with ρ_{ga} in lbm/ft^3 and R_s in scf/STB.

Alani-Kennedy[61] Method. The Alani-Kennedy method for calculating oil density is a modification of the original van der Waals EOS, with constants a and b given as functions of temperature for normal paraffins C_1 to C_{10} and *iso*-butane (**Table 3.1**); two sets of coefficients are reported for methane (for temperatures from 70 to 300°F and from 301 to 460°F) and two sets for ethane (for temperatures from 100 to 249°F and from 250 to 460°F). Lohrenz *et al.*[62] give Alani-Kennedy temperature-dependent coefficients for nonhydrocarbons N_2, CO_2, and H_2S (Table 3.1). The Alani-Kennedy equations are summarized next. Eqs. 3.102b and 3.102c are in the original van der Waals EOS but are not used.

$$p = \frac{RT}{v - b} - \frac{a}{v^2}, \quad \ldots\ldots\ldots\ldots\ldots\ldots\ldots\ldots \quad (3.102a)$$

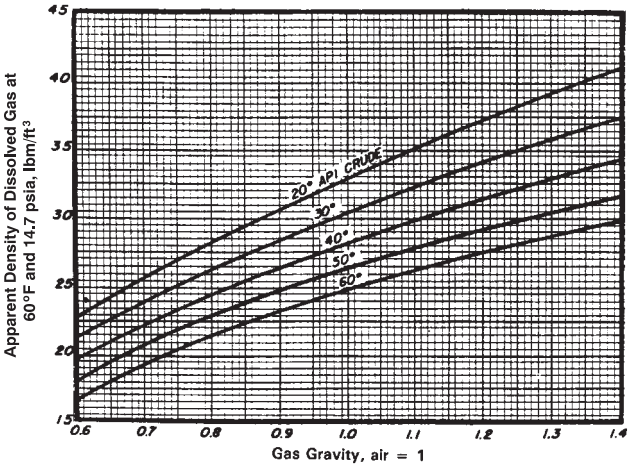

Fig. 3.18—Apparent pseudoliquid density of separator gas (from Standing,[33] after Katz[41]).

$$a_i = \frac{27}{64}\frac{R^2T_{ci}^2}{p_{ci}}, \quad \ldots\ldots\ldots\ldots\ldots\ldots\ldots\ldots\ldots\ldots \quad (3.102b)$$

$$b_i = \frac{1}{8}\frac{RT_{ci}}{p_{ci}}, \quad \ldots\ldots\ldots\ldots\ldots\ldots\ldots\ldots\ldots\ldots \quad (3.102c)$$

$$a = \sum_{i=1}^{N} x_i a_i, \quad \ldots\ldots\ldots\ldots\ldots\ldots\ldots\ldots\ldots\ldots \quad (3.102d)$$

$$b = \sum_{i=1}^{N} x_i b_i, \quad \ldots\ldots\ldots\ldots\ldots\ldots\ldots\ldots\ldots\ldots \quad (3.102e)$$

$$a_i = \frac{a_{1i}}{T} + \log a_{2i};\ i \neq C_{7+}, \quad \ldots\ldots\ldots\ldots\ldots \quad (3.102f)$$

and $$b_i = b_{1i}T + b_{2i};\ i \neq C_{7+}, \quad \ldots\ldots\ldots\ldots\ldots \quad (3.102g)$$

where $$\log a_{C_{7+}} = \left(3.8405985 \times 10^{-3}\right)M_{C_{7+}} - \left(9.5638281 \times 10^{-4}\right)\frac{M_{C_{7+}}}{\gamma_{C_{7+}}} + \frac{261.80818}{T} + \left(7.3104464 \times 10^{-6}\right)M_{C_{7+}}^2 + 10.753517 \quad \ldots\ldots\ldots\ldots\ldots\ldots \quad (3.103a)$$

and $$b_{C_{7+}} = \left(3.499274 \times 10^{-2}\right)M_{C_{7+}} - 7.2725403\gamma_{C_{7+}} + \left(2.232395 \times 10^{-4}\right)T - \left(1.6322572 \times 10^{-2}\right)\frac{M_{C_{7+}}}{\gamma_{C_{7+}}} + 6.2256545, \quad \ldots\ldots\ldots\ldots\ldots\ldots \quad (3.103b)$$

with ρ in lbm/ft^3, v in ft^3/lbm mol, T in °R, p in psia, and R = universal gas constant = 10.73.

Solution of the cubic equation for volume is presented in Chap. 4. Density is given by $\rho = M/v$, where M is the mixture molecular weight and v is the molar volume given by the solution to the cubic equation. The Alani-Kennedy method can also be used to estimate oil compressibilities.

Rackett,[63] Hankinson and Thomson,[64] and Hankinson *et al.*[65] give accurate correlations for pure-component saturated-liquid densities, and although these correlations can be extended to mixtures, they have not been tested extensively for reservoir systems. Cullick *et al.*[66] give a modified corresponding-states method for predicting density of reservoir fluids, The method has a better foundation and extrapolating capability than the methods discussed previously (particularly for systems with nonhydrocarbons); however, space does not allow presentation of the method in its entirety.

Either the Standing-Katz or Alani-Kennedy method should estimate the densities of most reservoir oils with an accuracy of ±2%. The Alani-Kennedy method is suggested for systems at temperatures >250°F and for systems containing appreciable amounts of nonhydrocarbons (>5 mol%). Cubic EOS's (e.g., Peng-Robinson or Soave-Redlich-Kwong) that use volume translation also estimate liquid densities with an accuracy of a few percent (e.g., the recommended characterization procedures in Chap. 5 or other proposed characterizations[67,68]).

TABLE 3.1—CONSTANTS FOR ALANI-KENNEDY[61] OIL DENSITY CORRELATION

Component	a_1	a_2	$b_1 \times 10^4$	b_2
N_2	4,300	2.293	4.49	0.3853
CO_2	8,166	126.0	0.1818	0.3872
H_2S	13,200	0.0	17.9	0.3945
C_1				
At 70 to 300°F	9,160.6413	61.893223	−3.3162472	0.50874303
At 300 to 460°F	147.47333	3,247.4533	−14.072637	1.8326695
C_2				
At 100 to 250°F	46,709.573	−404.48844	5.1520981	0.52239654
At 250 to 460°F	17,495.343	34.163551	2.8201736	0.62309877
C_3	20,247.757	190.24420	2.1586448	0.90832519
i-C_4	32,204.420	131.63171	3.3862284	1.1013834
n-C_4	33,016.212	146.15445	2.902157	1.1168144
i-C_5	37,046.234	299.62630	2.1954785	1.4364289
n-C_5	37,046.234	299.62630	2.1954785	1.4364289
n-C_6	52,093.006	254.56097	3.6961858	1.5929406
n-C_7	82,295.457	64.380112	5.2577968	1.7299902
n-C_8	89,185.432	149.39026	5.9897530	1.9310993
n-C_9	124,062.650	37.917238	6.7299934	2.1519973
n-C_{10}	146,643.830	26.524103	7.8561789	2.3329874

3.4.3 Undersaturated-Oil Compressibility. With measured data or an appropriate correlation for B_o or ρ_o, Eq. 3.14 readily defines the isothermal compressibility of an oil at pressures greater than the bubblepoint. "Instantaneous" undersaturated-oil compressibility, defined by Eq. 3.15 with the pressure derivative evaluated at a specific pressure, is used in reservoir simulation and well-test interpretation. Another definition of oil compressibility may be used in material-balance calculations (e.g., Craft and Hawkins[69])—the "cumulative" or "average" compressibility defines the cumulative volumetric change of oil from the initial reservoir pressure to current reservoir pressure.

$$\bar{c}_o(p) = \frac{V_{oi}\int_p^{p_i} c_o(p)\,\mathrm{d}p}{V_{oi}(p_i - p)}$$

$$= -\left(\frac{1}{V_{oi}}\right)\left[\frac{V_{oi} - V_o(p)}{p_i - p}\right]. \quad \ldots\ldots\ldots\ldots\ldots (3.104)$$

The cumulative compressibility is readily identified because it is multiplied by the cumulative reservoir pressure drop, $p_i - p_R$. Usually $\bar{c}_o$ is assumed constant; however, this assumption may not be justified for high-pressure volatile oils.

Oil compressibility is used to calculate the variation in undersaturated density and FVF with pressure.

$$\rho_o = \rho_{ob}\exp\left[c_o(p - p_b)\right]$$

$$\approx \rho_{ob}\left[1 - c_o(p_b - p)\right] \quad \ldots\ldots\ldots\ldots\ldots\ldots (3.105a)$$

and $B_o = B_{ob}\exp\left[c_o(p_b - p)\right]$

$$\approx B_{ob}\left[1 - c_o(p - p_b)\right], \quad \ldots\ldots\ldots\ldots\ldots (3.105b)$$

where consistent units must be used. These equations are derived from the definition of isothermal compressibility assuming that c_o is constant. When oil compressibility varies significantly with pressure, Eqs. 3.105a and 3.105b are not really valid. The approximations $\rho_o \approx \rho_{ob}[1 - c_o(p_b - p)]$ and $B_o \approx B_{ob}[1 - c_o(p - p_b)]$ are used in many applications, and to predict volumetric behavior correctly with these relations requires that c_o be defined by

$$c_o(p) = -\left(\frac{1}{V_{ob}}\right)\left[\frac{V_o(p) - V_{ob}}{p - p_b}\right]. \quad \ldots\ldots\ldots\ldots\ldots (3.106)$$

Strictly speaking, the compressibility of an oil mixture is defined only for pressures greater than the bubblepoint pressure. If an oil is at its bubblepoint, the compressibility can be determined and defined only for a positive change in pressure. A reduction in pressure from the bubblepoint results in gas coming out of solution and, subsequently, a change in the mass of the original system for which compressibility is to be determined. Implicit in the definition of compressibility is that the system mass remains constant.

Vazquez and Beggs[57] propose the following correlation for instantaneous undersaturated-oil compressibility.

$$c_o = A/p, \quad \ldots\ldots\ldots\ldots\ldots\ldots\ldots\ldots\ldots (3.107)$$

where
$A = 10^{-5}(5R_{sb} + 17.2T - 1,180\gamma_{gc} + 12.61\gamma_{\mathrm{API}} - 1,433)$, with c_o in psi^{-1}, R_{sb} in scf/STB, T in °F, and p in psia. With this correlation for oil compressibility, undersaturated-oil FVF can be calculated analytically from

$$B_o = B_{ob}(p_b/p)^A. \quad \ldots\ldots\ldots\ldots\ldots\ldots\ldots (3.108)$$

If measured pressure/volume data are available (see Sec. 6.4 in Chap. 6), these data can be used to determine A (e.g., by plotting V_o/V_{ob} vs. p/p_b on log-log paper). Constant A can then be used to compute compressibilities from the simple relation $c_o = A/p$.

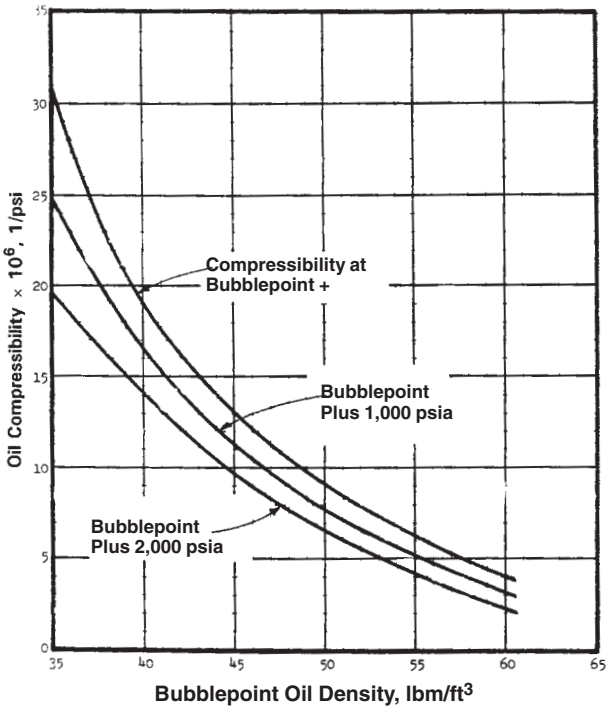

Fig. 3.19—Undersaturated-oil-compressibility correlation (from Standing[33]).

Constant A determined in this way is a useful correlating parameter, one that helps to identify erroneous undersaturated p-V_o data.

Standing[33] gives a graphical correlation for undersaturated c_o (**Fig. 3.19**) that can be represented by

$$c_o = 10^{-6}\exp\left[\frac{\rho_{ob} + 0.004347(p - p_b) - 79.1}{(7.141 \times 10^{-4})(p - p_b) - 12.938}\right], \quad \ldots\ldots\ldots\ldots\ldots (3.109)$$

with c_o in psi^{-1}, ρ_{ob} in $\mathrm{lbm/ft}^3$, and p in psia.

The Alani-Kennedy EOS can also be solved analytically for oil compressibility, and Trube[70] gives a corresponding-states method for determining oil compressibility with charts.

Any of the correlations mentioned here should yield reasonable estimates of c_o. However, we recommend that experimental data be used for volatile oils when c_o is greater than about $20 \times 10^{-6}\,\mathrm{psi}^{-1}$. A simple polynomial fit of the relative volume data, $V_{ro} = V_o/V_{ob}$, from a PVT report allows an accurate and explicit equation for undersaturated-oil compressibility.

$$V_{ro} = A_0 + A_1 p + A_2 p^2 \ldots\ldots\ldots\ldots\ldots\ldots (3.110a)$$

and $c_o = -\frac{1}{V_{ro}}\left(\frac{\partial V_{ro}}{\partial p}\right)_T$

$$= \frac{-\left(A_1 + 2A_2 p\right)}{A_0 + A_1 p + A_2 p^2}, \quad \ldots\ldots\ldots\ldots\ldots (3.110b)$$

where A_0, A_1, and A_2 are determined from experimental data. Alternatively, measured data can be fit by use of Eq. 3.108.

3.4.4 Bubblepoint-Oil FVF. Oil FVF ranges from 1 bbl/STB for oils containing little solution gas to about 2.5 bbl/STB for volatile oils. B_{ob} increases more or less linearly with the amount of gas in solution, a fact which explains why B_{ob} correlations are similar to bubblepoint pressure correlations. For example, Standing's[3,17,40] correlation for California crude oils is

$$B_{ob} = 0.9759 + \left(12 \times 10^{-5}\right)A^{1.2}, \quad \ldots\ldots\ldots\ldots\ldots (3.111)$$

where $A = R_s(\gamma_g/\gamma_o)^{0.5} + 1.25T$.

Glasø's[52] correlation for North Sea crude oils is

$$\log(B_{ob} - 1) = -6.585 + 2.9133 \log A - 0.2768(\log A)^2, \quad \ldots\ldots\ldots\ldots\ldots\ldots (3.112)$$

where $A = R_s(\gamma_g/\gamma_o)^{0.526} + 0.968T$.

The Vazquez and Beggs[57] correlation, based on data from commercial laboratories, is

$$B_{ob} = 1 + (4.677 \times 10^{-4})R_s + (0.1751 \times 10^{-4})(T - 60) \times \left(\frac{\gamma_{API}}{\gamma_{gc}}\right) - (1.8106 \times 10^{-8})R_s(T - 60)\left(\frac{\gamma_{API}}{\gamma_{gc}}\right) \quad \ldots\ldots\ldots\ldots\ldots\ldots (3.113a)$$

for $\gamma_{API} \leqq 30$ and

$$B_{ob} = 1 + (4.67 \times 10^{-4})R_s + (0.11 \times 10^{-4})(T - 60)\left(\frac{\gamma_{API}}{\gamma_{gc}}\right) - (0.1337 \times 10^{-8})R_s(T - 60)\left(\frac{\gamma_{API}}{\gamma_{gc}}\right) \quad \ldots\ldots\ldots (3.113b)$$

for $\gamma_{API} > 30$, where the effect of separator conditions is included by use of a corrected gas gravity γ_{gc} (Eq. 3.86).

The Standing and the Vazquez-Beggs correlations indicate that a plot of B_o vs. R_s should correlate almost linearly. This plot is useful for checking the consistency of reported PVT data from a differential liberation plot. Eq. 3.114,[71] which performs considerably better for Middle Eastern oils, also suggests a linear relationship between B_{ob} and R_s.

$$B_{ob} = 1.0 + (0.177342 \times 10^{-3})R_s + (0.220163 \times 10^{-3}) \times R_s(\gamma_g/\gamma_o) + (4.292580 \times 10^{-6})R_s(T - 60)(1 - \gamma_o) + (0.528707 \times 10^{-3})(T - 60). \quad \ldots\ldots\ldots\ldots\ldots (3.114)$$

All three B_{ob} correlations (Eqs. 3.113a, 3.113b, and 3.114) should give approximately the same accuracy. Sutton and Farshad's[54] comparative study of gulf coast oils indicates that Standing's correlation is slightly better for $B_{ob} < 1.4$ and that Glasø's correlation is best for $B_{ob} > 1.4$.

3.4.5 Saturated-Oil Compressibility. Perrine[8] introduces a definition for the compressibility of a saturated oil that includes the shrinkage effect of saturated-oil FVF, $\partial B_o/\partial p$, *and* the expansion effect of gas coming out of solution, $B_g(\partial R_s/\partial p)$,

$$c_o = -\frac{1}{B_o}\left(\frac{\partial B_o}{\partial p}\right)_T + \frac{1}{5.615}\frac{B_g}{B_o}\left(\frac{\partial R_s}{\partial p}\right)_T. \quad \ldots\ldots\ldots (3.115)$$

c_o is used in the definition of total system compressibility, c_t.

$$c_t = c_f + c_w S_w + c_o S_o + c_g S_g, \quad \ldots\ldots\ldots\ldots (3.116)$$

where c_f = rock compressibility. B_g has units ft³/scf. R_s is in scf/STB, and B_o in bbl/STB = saturated-oil FVF at the pressure of interest, at or below the original oil's bubblepoint pressure (where both gas and oil are present).

3.4.6 Oil Viscosity. Typical oil viscosities range from 0.1 cp for near-critical oils to > 100 cp for heavy crudes. Temperature, stock-tank-oil density, and dissolved gas are the key parameters determining oil viscosity, where viscosity decreases with decreasing stock-tank-oil density (increasing oil gravity), increasing temperature, and increasing solution gas.

Oil viscosity is one of the most difficult properties to estimate, and most methods offer an accuracy of only about 10 to 20%. Two approaches are used to estimate oil viscosity: empirical and corresponding-states correlations. The empirical methods correlate gas-saturated-oil viscosity in terms of dead-oil (residual or stock-tank-oil) viscosity and solution gas/oil ratio. Undersaturated-oil viscosity is related to bubblepoint viscosity and the ratio or difference in actual and bubblepoint pressures. Corresponding-states methods use reduced density or reduced pressure and temperature as correlating parameters.

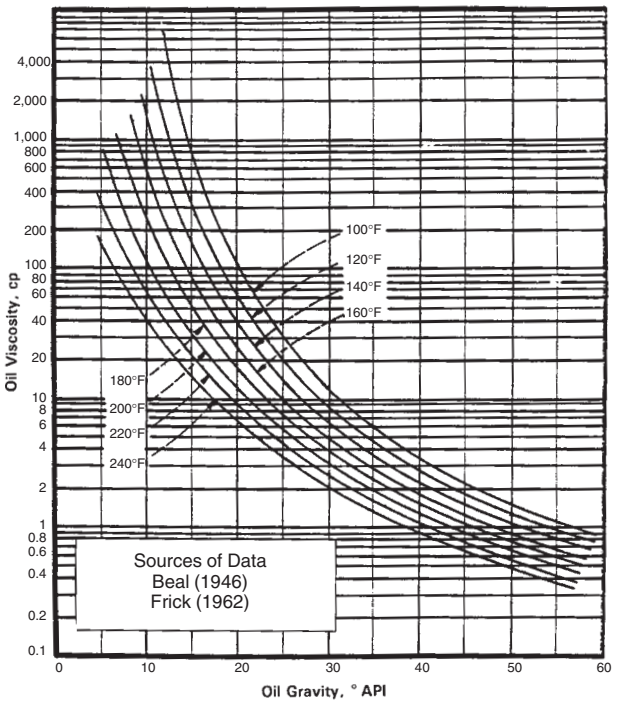

Fig. 3.20—Beal dead-oil (stock-tank-oil) viscosity correlation including data in Frick (from Standing[33]).

3.4.7 Dead-Oil (Residual- or Stock-Tank-Oil) Viscosity. Several correlations for dead-oil viscosity are given in terms of oil gravity and temperature. Standing,[3] for example, gives best-fit equations for the original Beal[72] graphical correlation,

$$\mu_{oD} = \left(0.32 + \frac{1.8 \times 10^7}{\gamma_{API}^{4.53}}\right)\left(\frac{360}{T + 200}\right)^A, \quad \ldots\ldots\ldots (3.117)$$

where $A = 10^{\left[0.43 + \left(8.33/\gamma_{API}\right)\right]}$.

A somewhat modified version of the original correlation is given in **Fig. 3.20** by Standing.[33] Beggs[18] and Beggs and Robinson[73] give the following equation for the original Beal correlation,

$$\mu_{oD} = -1 + 10^{\left[T^{-1.163}\exp\left(6.9824 - 0.04658\gamma_{API}\right)\right]}. \quad \ldots\ldots (3.118)$$

Bergman* claims that the temperature dependence of the Beggs and Robinson correlation is not valid at lower temperatures (< 70°F) and suggests the following correlation, based on viscosity data, for pure compounds and reservoir oils.

$$\ln \ln(\mu_{oD} + 1) = A_0 + A_1 \ln(T + 310), \quad \ldots\ldots\ldots (3.119)$$

where $A_0 = 22.33 - 0.194\gamma_{API} + 0.00033\gamma_{API}^2$ and $A_1 = -3.20 + 0.0185\gamma_{API}$.

Glasø[52] gives a relation (used in the paraffinicity correction of his bubblepoint pressure correlation) for oils with $K_w = 11.9$.

$$\mu_{oD} = (3.141 \times 10^{10})T^{-3.444}(\log \gamma_{API})^{[10.313(\log T) - 36.447]}. \quad \ldots\ldots\ldots\ldots\ldots (3.120)$$

Al-Khafaji *et al.*[74] give the correlation

$$\mu_{oD} = \frac{10^{4.9563 - 0.00488T}}{(\gamma_{API} + T/30 - 14.29)^{2.709}}, \quad \ldots\ldots\ldots (3.121)$$

with T in °F and μ_{oD} in cp for Eqs. 3.117 through 3.121.

*Personal communication with D.F. Bergman, Amoco Research, Tulsa, Oklahoma (1992).

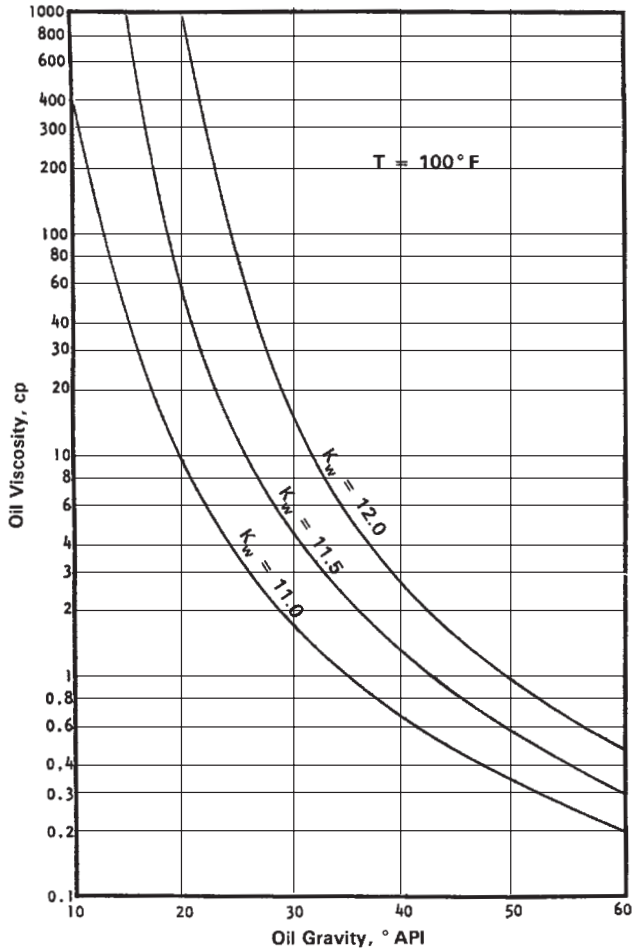

Fig. 3.21—Dead-oil (stock-tank-oil) viscosities at 100°F for varying paraffinicity (from Ref. 33).

Standing[75] gives a relation for dead-oil viscosity in terms of dead-oil density, temperature, and the Watson characterization factor.

$$\log(\mu_{oD}/\rho_o) = \frac{1}{A_3\left[K_w-(8.24/\gamma_o)\right] + 1.639A_2 - 1.059} - 2.17, \quad \ldots\ldots\ldots\ldots\ldots\ldots (3.122a)$$

where $A_1 = 1 + 8.69 \log\frac{T+460}{560}$, ... (3.122b)

$$A_2 = 1 + 0.554 \log\frac{T+460}{560}, \quad \ldots\ldots\ldots\ldots\ldots\ldots (3.122c)$$

$$A_3 = -0.1285\frac{(2.87A_1 - 1)\gamma_o}{2.87A_1 - \gamma_o}, \quad \ldots\ldots\ldots\ldots\ldots\ldots (3.122d)$$

and $\rho_o = \frac{\gamma_o}{1 + 0.000321(T-60)10^{0.00462\gamma_{API}}}$, ... (3.122e)

with μ in cp, T in °F, and ρ in g/cm^3 for Eqs. 3.117 through 3.122. Eqs. 3.122a through 3.122e represent a best fit of the nomograph for viscosity in terms of temperature, gravity, and characterization factor. Eq. 3.122e (at standard pressure and temperature) is a best fit of thermal expansion data for crude oils.

Dead-oil viscosity is one of the most unreliable properties to predict with correlations primarily because of the large effect that oil type (paraffinicity, aromaticity, and asphaltene content) has on viscosity. For example, the oil viscosity of a crude oil with $K_w = 12$ may be 3 to 100 times the viscosity of a less paraffinic crude oil having the same gravity and $K_w = 11$. For this reason the Standing correlation based on the Watson characterization factor is recommended when K_w is known. Using an incorrectly estimated K_w, however, may lead to a potentially large error in dead-oil viscosity.

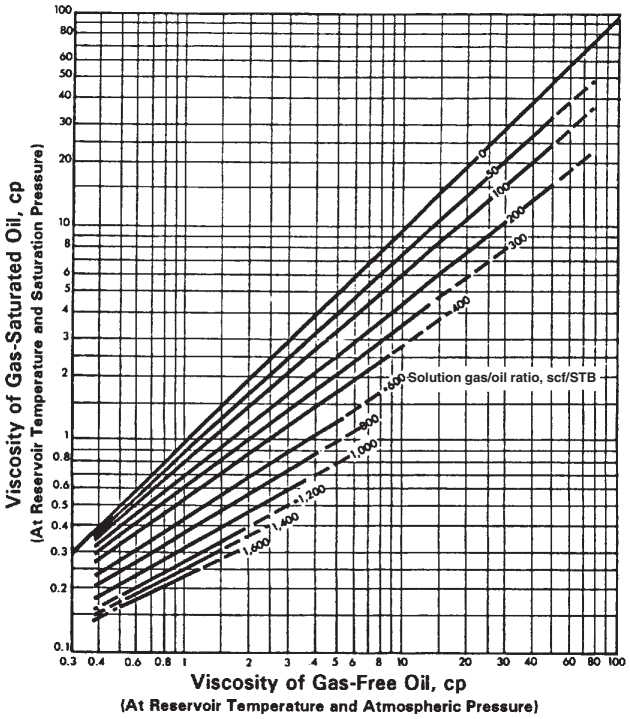

Fig. 3.22—Live-oil (saturated) viscosity as a function of dead-oil viscosity and solution gas/oil ratio (from Standing,[33] after Beal[72] correlation).

Fig. 3.21 shows dead-oil viscosities calculated at 100°F for a range of paraffinicities expressed in terms of K_w, together with the Bergman* and Glasø[48] correlations.

3.4.8 Bubblepoint-Oil Viscosity. The original approach by Chew and Connally[76] for correlating saturated-oil viscosity in terms of dead-oil viscosity and solution gas/oil ratio is still widely used.

$$\mu_{ob} = A_1(\mu_{oD})^{A_2}. \quad \ldots\ldots\ldots\ldots\ldots\ldots (3.123)$$

Fig. 3.22 shows the variation in μ_{ob} with μ_{oD} as a function of R_s. The functional relations for A_1 and A_2 reported by various authors differ somewhat, but most are best-fit equations of Chew and Connally's tabulated results.

***Beggs and Robinson.*[73]**

$$A_1 = 10.715(R_s + 100)^{-0.515} \quad \ldots\ldots\ldots\ldots\ldots\ldots (3.124a)$$

and $A_2 = 5.44(R_s + 150)^{-0.338}$. ..... (3.124b)

Bergman.*

$$\ln A_1 = 4.768 - 0.8359 \ln(R_s + 300) \quad \ldots\ldots\ldots\ldots\ldots\ldots (3.125a)$$

and $A_2 = 0.555 + \frac{133.5}{R_s + 300}$. ..... (3.125b)

***Standing.*[3]**

$$A_1 = 10^{-\left(7.4\times10^{-4}\right)R_s + \left(2.2\times10^{-7}\right)R_s^2} \quad \ldots\ldots\ldots\ldots\ldots\ldots (3.126a)$$

and $A_2 = \frac{0.68}{10^{\left(8.62\times10^{-5}\right)R_s}} + \frac{0.25}{10^{\left(1.1\times10^{-3}\right)R_s}} + \frac{0.062}{10^{\left(3.74\times10^{-3}\right)R_s}}$. ..... (3.126b)

***Aziz et al.*[77]**

$$A_1 = 0.20 + \left(0.80 \times 10^{-0.00081R_s}\right) \quad \ldots\ldots\ldots\ldots\ldots\ldots (3.127a)$$

and $A_2 = 0.43 + \left(0.57 \times 10^{-0.00072R_s}\right)$. ..... (3.127b)

*Personal communication with D.F. Bergman, Amoco Research, Tulsa, Oklahoma (1992).

Al-Khafaji *et al.*[74] extend the Chew-Connally[76] correlation to higher GOR's (up to 2,000 scf/STB).

$$A_1 = 0.247 + 0.2824A_0 + 0.5657A_0^2 - 0.4065A_0^3 + 0.0631A_0^4 \quad \ldots\ldots\ldots\ldots\ldots\ldots (3.128a)$$

and $$A_2 = 0.894 + 0.0546A_0 + 0.07667A_0^2 - 0.0736A_0^3 + 0.01008A_0^4, \quad \ldots\ldots\ldots\ldots\ldots (3.128b)$$

where $A_0 = \log(R_s)$ and $R_s = 0.1$ yields $A_1 = A_2 = 1$. R_s is given in scf/STB for Eqs. 3.124 through 3.128. Chew and Connally indicate that their correlation is based primarily on data with GOR's of $<1{,}000$ scf/STB and that the scatter in A_1 at higher GOR's is probably the result of insufficient data. Eqs. 3.128a and 3.128b are based on additional data at higher GOR's. Eqs. 3.127a and 3.128b appear to be the most well behaved.

An interesting observation by Abu-Khamsin and Al-Marhoun[78] is that saturated-oil viscosity, μ_{ob}, correlates very well with saturated-oil density, ρ_{ob}.

$$\ln \mu_{ob} = -2.652294 + 8.484462\rho_{ob}^4, \quad \ldots\ldots\ldots (3.129)$$

with ρ_{ob} in g/cm^3. This behavior is expected from the Lohrenz *et al.*[62] correlation discussed later. Although Abu-Khamsin and Al-Marhoun do not comment on the applicability of Eq. 3.129 to undersaturated oils, it would seem reasonable that their correlation should apply to both saturated and undersaturated oils. In fact, the correlation even appears to predict accurately dead-oil viscosities, μ_{oD}, except at low temperatures for heavy crudes. Simon and Graue give graphical correlations for the viscosity of saturated CO_2/oil systems (see Chap. 8).[79]

3.4.9 Undersaturated-Oil Viscosities. Beal[72] gives the variation of undersaturated-oil viscosity with pressure graphically where it has been curve fit by Standing.[2]

$$\frac{\mu_o - \mu_{ob}}{0.001(p - p_b)} = 0.024\mu_{ob}^{1.6} + 0.038\mu_{ob}^{0.56}. \quad \ldots\ldots\ldots (3.130)$$

The Vazquez and Beggs[57] correlation is

$$\mu_o = \mu_{ob}(p/p_b)^A, \quad \ldots\ldots\ldots\ldots\ldots\ldots\ldots (3.131)$$

where $A = 2.6\,p^{1.187}\exp\left[-11.513 - (8.98 \times 10^{-5})p\right]$.

A more recent correlation by Abdul-Majeed *et al.*[80] is

$$\mu_o = \mu_{ob} + 10^{\left[A - 5.2106 + 1.11\log(p - p_b)\right]}, \quad \ldots\ldots\ldots (3.132a)$$

where $A = 1.9311 - 0.89941(\ln R_s) - 0.001194\gamma_{API}^2 + 0.0092545\gamma_{API}(\ln R_s)$. $\ldots\ldots\ldots\ldots\ldots (3.132b)$

Eq. 3.132 is based on the observation that a plot of $\log(\mu_o - \mu_{ob})$ vs. $\log(p - p_b)$ plots as a straight line with slope of ≈ 1.11. Because this observation appears to be fairly general, it can be used to check reported undersaturated-oil viscosities and to develop field-specific correlations.

Sutton and Farshad[54] and Khan *et al.*[81] present results that indicate that the Standing equation gives good results and that the Vazquez-Beggs correlation tends to overpredict viscosities somewhat. Abdul-Majeed *et al.*[80] indicate that both the Standing and Vazquez-Beggs correlations overpredict viscosities of North African and Middle Eastern oils (253 data), and that their own correlation performed best for these data and for the data used by Vazquez and Beggs.

3.4.10 Compositional Correlation. In compositional reservoir simulation of miscible-gas-injection processes and the depletion of near-critical reservoir fluids, the oil and gas compositions may be very similar. A single viscosity relation consistent for both phases is therefore desired. Several corresponding-states viscosity correlations can be used for both oil and high-pressure gas mixtures; the Lohrenz *et al.*[62] correlation has become a standard in compositional reservoir simulation. Lohrenz *et al.* use the Jossi *et al.*[82] correlation for dense-gas mixtures ($\rho_{pr} > 0.1$),[6]

$$\left[(\mu - \mu^o)\xi_T + 10^{-4}\right]^{1/4} = 0.10230 + 0.023364\rho_{pr} + 0.058533\rho_{pr}^2 - 0.040758\rho_{pr}^3 + 0.0093324\rho_{pr}^4, \quad \ldots\ldots\ldots\ldots\ldots (3.133a)$$

where $$\xi_T = 5.35\left(\frac{T_{pc}}{M^3 p_{pc}^4}\right)^{1/6}, \quad \ldots\ldots\ldots\ldots (3.133b)$$

$$\rho_{pr} = \frac{\rho}{\rho_{pc}} = \frac{\rho}{M}v_{pc}, \quad \ldots\ldots\ldots\ldots\ldots\ldots (3.133c)$$

and $$\mu^o = \frac{\sum_{i=1}^{N} z_i\mu_i\sqrt{M_i}}{\sum_{i=1}^{N} z_i\sqrt{M_i}}. \quad \ldots\ldots\ldots\ldots\ldots\ldots (3.133d)$$

Pseudocritical properties T_{pc}, p_{pc}, and v_{pc} are calculated with Kay's mixing rule.

Component viscosities, μ_i, can be calculated from the Lucas[45] low-pressure correlation Eq. 3.67 or from the Stiel and Thodos[83] correlation (as suggested by Lohrenz *et al.*[62]).

$$\mu_i\xi_{Ti} = (34 \times 10^{-5})T_{ri}^{0.94} \quad \ldots\ldots\ldots\ldots\ldots\ldots (3.134a)$$

for $T_{ri} \leqq 1.5$, and

$$\mu_i\xi_{Ti} = (17.78 \times 10^{-5})(4.58T_{ri} - 1.67)^{5/8} \quad \ldots\ldots (3.134b)$$

for $T_{ri} > 1.5$, where $\xi_{Ti} = 5.35\left(T_{ci}M_i^3/p_{ci}^4\right)^{1/6}$.

Lohrenz *et al.*[62] give a special relation for $v_{cC_{7+}}$ of the C_{7+} fraction.

$$v_{cC_{7+}} = 21.573 + 0.015122M_{C_{7+}} - 27.656\gamma_{C_{7+}} + 0.070615M_{C_{7+}}\gamma_{C_{7+}}, \quad \ldots\ldots\ldots\ldots\ldots (3.135)$$

with μ in cp, ξ in cp^{-1}, ρ in lbm/ft^3, v in ft^3/lbm mol, T in °R, p in psia, and M in lbm/lbm mol. The Lohrenz *et al.* method is very sensitive to mixture density and to the critical volumes of heavy components. Adjustment of the critical volumes of heavy (and sometimes light) components to match experimental oil viscosities is usually necessary.

3.5 IFT and Diffusion Coefficients

3.5.1 IFT. Weinaug and Katz[84] propose an extension of the Macleod[85] relationship for multicomponent mixtures.

$$\sigma_{go}^{1/4} = \sum_{i=1}^{N} P_i\left(x_i\frac{\rho_o}{M_o} - y_i\frac{\rho_g}{M_g}\right), \quad \ldots\ldots\ldots\ldots\ldots (3.136)$$

with σ in dynes/cm (mN/m) and ρ in g/cm^3. P_i is the parachor of Component i, which can be calculated by group contributions, as shown in **Table 3.2**. For *n*-alkanes, the parachors can be expressed by

$$P_i = 25.2 + 2.86M_i. \quad \ldots\ldots\ldots\ldots\ldots\ldots (3.137)$$

Several authors propose parachors for pure hydrocarbons that deviate from the group-contribution values. For example, $P_{C_1} = 77$ is often cited for methane instead of the group-contribution value of $P_{C_1} = 71$. Likewise, $P_{N_2} = 41$ is often used for nitrogen instead of the group-contribution value of $P_{N_2} = 35$. **Fig. 3.23** plots parachors vs. molecular weight for pure components and petroleum fractions.

TABLE 3.2—PARACHORS FOR PURE COMPONENTS AND COMPOUND GROUPS

Pure Component	
C_1	71
C_2	111
C_3	151
C_4 (also *i*-C_4)	191
C_5 (also *i*-C_5)	231
C_6	271
C_7	311
C_8	351
C_9	391
C_{10}	431
N_2	35
CO_2	49
H_2S	80
Group	
C	9.0
H	15.5
CH_3	55.5
CH_2 [in $(CH_2)_n$]	40.0
N	17.5
O	20.0
S	49.1

Example: For methane, CH_4. $P_{C1}=P_C+4(P_H)=9+4(15.5)=71$.

Nokay[86] gives a simple relation for parachors of pure hydrocarbons (paraffins, olefins, naphthenes, and aromatics) with a normal boiling point between 400 and 1,400°R and specific gravity <1,

$$\log P_i = -4.20895 + 2.29319 \log\left(\frac{T_{bi}}{\gamma_i^{0.5937}}\right), \quad \ldots\ldots (3.138)$$

with T_b in °R.

Katz and Saltman[87] and Katz *et al.*[88] give parachor data for C_{7+} fractions measured by Standing and Katz,[58,89] which are approximately correlated by

$$P_i = 35 + 2.40M_i. \quad \ldots\ldots\ldots\ldots (3.139)$$

The API recommended procedure for estimating petroleum fraction IFT's is based on an unpublished correlation.[27] The graphical correlation can be expressed by

$$\sigma_i = \frac{602(1 - T_{ri})^{1.194}}{K_{wi}}, \quad \ldots\ldots\ldots\ldots (3.140)$$

where $K_w = T_b^{1/3}/\gamma$, with T_b in °R. The parachor can be estimated with the Macleod relation,

$$P_i = \sigma_i^{1/4}\left(\frac{M_i}{\rho_{sLi}}\right), \quad \ldots\ldots\ldots\ldots (3.141)$$

where $\rho_{sL} \gg \rho_{sv}$ is assumed. The saturated-liquid density can be estimated, for example, with the Rackett[63] equation.

$$\rho_{sLi} = \frac{M_i p_{ci}}{RT_{ci}} Z_{Ri}^{-\left[1+\left(1-T_{ri}\right)^{2/7}\right]}, \quad \ldots\ldots\ldots\ldots (3.142)$$

where $Z_{Ri} \approx Z_{ci} \approx 0.291 - 0.08\omega_i$ $\ldots\ldots\ldots\ldots (3.143)$

and R = universal gas constant. The parachors predicted from Eqs. 3.140 through 3.143 are practically constant for a given petroleum fraction (i.e., the temperature effect cancels out).

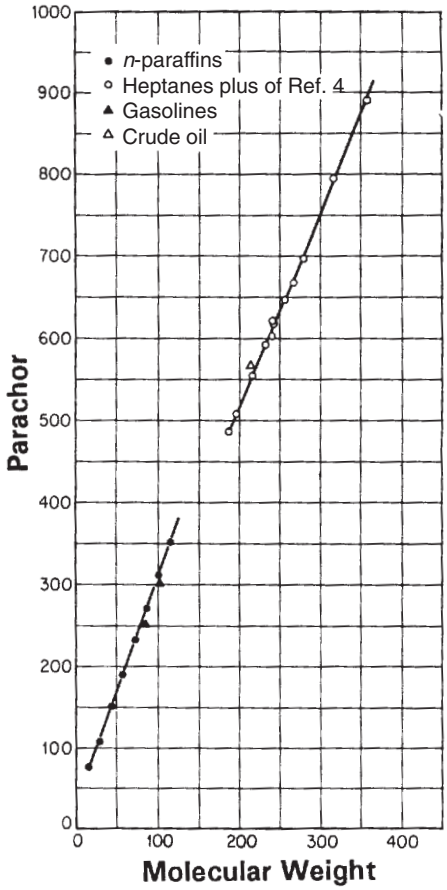

Fig. 3.23—Hydrocarbon parachors.

Firoozabadi *et al.*[90] give an equation that can be used to approximate the parachor of pure hydrocarbons from C_1 through C_6 and for C_{7+} fractions,

$$P_i = 11.4 + 3.23M_i - 0.0022M_i^2. \quad \ldots\ldots\ldots\ldots (3.144)$$

They also discuss the qualitative effect of asphaltenes on IFT and suggest that the parachor of asphaltic substances generally will not follow the relations of lighter C_{7+} fractions.

Ramey[91] gives a method for estimating gas/oil IFT with black-oil PVT properties. We extend the method here to include the effect of solution oil/gas ratio, r_s. Considering stock-tank oil and separator gas as the "components" ($\overline{o}$ and $\overline{g}$) making up reservoir oil and gas, respectively, the Weinaug-Katz[84] relation can be written

$$\sigma_{go}^{1/4} = P_{\overline{o}}\left[x_{\overline{o}}\left(\frac{\rho_o}{M_o}\right) - y_{\overline{o}}\left(\frac{\rho_g}{M_o}\right)\right] + P_{\overline{g}}\left[x_{\overline{g}}\left(\frac{\rho_o}{M_o}\right) - y_{\overline{g}}\left(\frac{\rho_g}{M_g}\right)\right], \quad \ldots\ldots\ldots\ldots (3.145a)$$

where $x_{\overline{o}} = \dfrac{1}{1 + (7.52 \times 10^{-6})R_s(M_{\overline{o}}/\gamma_{\overline{o}})}$, $\ldots\ldots\ldots$ (3.145b)

$$x_{\overline{g}} = 1 - x_{\overline{o}}, \quad \ldots\ldots\ldots\ldots (3.145c)$$

$$y_{\overline{o}} = \frac{1}{1 + (7.52 \times 10^{-6})(M_{\overline{o}}/\gamma_{\overline{o}})r_s}, \quad \ldots\ldots\ldots\ldots (3.145d)$$

$$y_{\overline{g}} = 1 - y_{\overline{o}}, \quad \ldots\ldots\ldots\ldots (3.145e)$$

$$\rho_o = \frac{62.4\gamma_{\overline{o}} + 0.0136\gamma_{\overline{g}}R_s}{62.4B_o}, \quad \ldots\ldots\ldots\ldots (3.145f)$$

$$\rho_g = 0.0932\left(pM_g/ZT\right), \quad \ldots\ldots\ldots\ldots (3.145g)$$

$$M_o = x_{\overline{o}}M_{\overline{o}} + x_{\overline{g}}M_{\overline{g}}, \quad \ldots\ldots\ldots\ldots (3.145h)$$

$$M_g = y_{\bar{o}} M_{\bar{o}} + y_{\bar{g}} M_{\bar{g}}, \quad \ldots\ldots\ldots\ldots\ldots\ldots\ldots\ldots \text{(3.145i)}$$

$$M_{\bar{o}} = 6,084/\gamma_{\text{API}} - 5.9\,, \quad \ldots\ldots\ldots\ldots\ldots\ldots\ldots\ldots \text{(3.145j)}$$

$$M_{\bar{g}} = 28.97\gamma_{\bar{g}}, \quad \ldots\ldots\ldots\ldots\ldots\ldots\ldots\ldots\ldots\ldots \text{(3.145k)}$$

$$P_{\bar{o}} = (2.376 + 0.0102\gamma_{\text{API}})/M_{\bar{o}}\,, \quad \ldots\ldots\ldots\ldots\ldots \text{(3.145l)}$$

$$\text{and } P_{\bar{g}} = 25.2 + 2.86M_{\bar{g}}, \quad \ldots\ldots\ldots\ldots\ldots\ldots\ldots \text{(3.145m)}$$

with ρ in g/cm^3, R_s in scf/STB, B_o in bbl/STB, T in °R, and p in psia and where $x_{\bar{o}}$ and $x_{\bar{g}}$ = mole fractions of the surface-oil and -gas components, respectively, in the oil phase, and $y_{\bar{o}}$ and $y_{\bar{g}}$ = mole fractions of the surface-oil and -gas components, respectively, in the gas phase. In the traditional black-oil approach $r_s = 0$, simplifying the relations to those originally suggested by Ramey.[91]

Eq. 3.145 is useful in black-oil reservoir simulation and when compositional data are not available. The black-oil approach generally is not recommended for predicting gas/oil IFT's unless the surface-oil parachor has been fit to experimental IFT data (or to IFT's calculated with compositions and densities from an EOS characterization by use of Eq. 3.136).

3.5.2 Diffusion Coefficients. Molecular diffusion in multicomponent mixtures is a complex problem. The standard engineering approach uses an effective diffusion coefficient for Component i in a mixture, D_{im}, where D_{im} can be calculated in one of two ways: (1) from binary diffusion coefficients and mixture composition or (2) from Component i properties and mixture viscosity. The first approach uses the Wilke[92] formula to calculate D_{im}.

$$D_{im} = \frac{1 - y_i}{\sum_{\substack{j=1 \\ j \neq i}}^{N} y_j / D_{ij}}, \quad \ldots\ldots\ldots\ldots\ldots\ldots\ldots \text{(3.146)}$$

where y_i = mixture mole fraction and $D_{ij} = D_{ji}$ is the binary diffusivity at the pressure and temperature of the mixture.

Sigmund[93] correlates the effect of pressure and temperature on diffusion coefficients using a corresponding-states approach with reduced density.

$$\frac{\rho_M D_{ij}}{\rho_M^o D_{ij}^o} = 0.99589 + 0.096016\rho_{pr} - 0.22035\rho_{pr}^2 + 0.032874\rho_{pr}^3, \quad \ldots\ldots\ldots\ldots\ldots\ldots \text{(3.147)}$$

where D_{ij} = diffusion coefficient at pressure and temperature, ρ_{pr} = pseudoreduced density = $\rho_M/\rho_{Mpc} = (\rho/M)v_{pc}$, ρ_M = mixture molar density, $\rho_M^o D_{ij}^o$ = low-pressure density-diffusivity product, and v_{pc} = pseudocritical molar volume calculated with Kay's[5] mixing rule. Note that the ratio $\rho_M D_{ij}/\rho^o D_{ij}^o$ is the same for all binary pairs in a mixture because ρ_{pr} is a function of only mixture density and composition.

da Silva and Belery[12] note that the Sigmund correlation does not work well for liquid systems and propose the following extrapolation for $\rho_{pr} > 3$.

$$\frac{\rho_M D_{ij}}{\rho_M^o D_{ij}^o} = 0.18839\exp(3 - \rho_{pr}), \quad \ldots\ldots\ldots\ldots\ldots\ldots \text{(3.148)}$$

which avoids negative D_{ij} for oils at $\rho_{pr} > 3.7$ as estimated by the Sigmund correlation.

Low-pressure binary gas diffusion coefficients,[6] D_{ij}^o, can be estimated from

$$D_{ij}^o = 0.001883\frac{T^{3/2}\left[(1/M_i) + (1/M_j)\right]^{0.5}}{p^o \sigma_{ij}^2 \Omega_{ij}}, \quad \ldots\ldots\ldots \text{(3.149a)}$$

$$\text{where } \Omega_{ij} = \frac{1.06036}{T_{ij}^{0.1561}} + \frac{0.193}{\exp(0.47635T_{ij})} + \frac{1.03587}{\exp(1.52996T_{ij})} + \frac{1.76474}{\exp(3.89411T_{ij})}, \quad \ldots\ldots\ldots\ldots\ldots\ldots \text{(3.149b)}$$

$$T_{ij} = \frac{T}{(\epsilon/k)_{ij}}, \quad \ldots\ldots\ldots\ldots\ldots\ldots\ldots\ldots\ldots \text{(3.149c)}$$

$$(\epsilon/k)_{ij} = \left[(\epsilon/k)_i(\epsilon/k)_j\right]^{1/2}, \quad \ldots\ldots\ldots\ldots\ldots\ldots \text{(3.149d)}$$

$$(\epsilon/k)_i = 65.3T_{ci}Z_{ci}^{18/5}, \quad \ldots\ldots\ldots\ldots\ldots\ldots\ldots\ldots \text{(3.149e)}$$

$$\sigma_{ij} = 0.5(\sigma_i + \sigma_j), \quad \ldots\ldots\ldots\ldots\ldots\ldots\ldots\ldots\ldots \text{(3.149f)}$$

$$\text{and } \sigma_i = 0.1866\frac{v_{ci}^{1/3}}{Z_{ci}^{6/5}}, \quad \ldots\ldots\ldots\ldots\ldots\ldots\ldots \text{(3.149g)}$$

with the diffusion coefficient, D_{ij}^o, in cm^2/s; molecular weight, M, in kg/kmol; temperature, T, in K, pressure; p, in bar; Lennard Jones 12-6 potential parameter, σ, in Å; Lennard-Jones 12-6 potential parameter, ε/k, in K; and critical volume, v_c, in m^3/kmol and where Z_c = critical compressibility factor and i and j = diffusing and concentrated species, respectively.

To obtain the low-pressure density-diffusivity product, we use the ideal-gas law, $\rho_M^o = p^o/RT$, to get

$$D_{ij}^o \rho_M^o = (2.2648 \times 10^{-5})\frac{T^{1/2}\left[(1/M_i) + (1/M_j)\right]^{1/2}}{\sigma_{ij}^2 \Omega_{ij}}, \quad \ldots\ldots\ldots\ldots\ldots\ldots \text{(3.150)}$$

where ρ and ρ_M have units g mol/cm^3.

The accuracy of the Sigmund correlation for liquids is not known, but the extension proposed by da Silva and Belery (Eq. 148) for large reduced densities does avoid negative diffusivities calculated by the Sigmund equation.[94] Renner[95] proposes a generalized correlation for effective diffusion coefficients of light hydrocarbons and CO_2 in reservoir liquids that can be used as an alternative to the Sigmund-type correlation.

$$D_{im} = 10^{-9}\mu_o^{-0.4562} M_i^{-0.6898} \rho_{Mi}^{1.706} p^{-1.831} T^{4.524}, \quad \ldots\ldots\ldots\ldots\ldots\ldots \text{(3.151)}$$

with D in cm^2/s and where μ_o = oil viscosity in cp, M_i = molecular weight, ρ_{Mi} = molar density of Component i at p and T in g mol/cm^3, p = pressure in psia, and T = temperature in K. This correlation is based on 141 experimental data with the following property ranges: $0.2 < \mu_o < 134$ cp; $16 < M_i < 44$; $0.04 < \rho_{Mi} < 7$ kmol/m^3; $14.7 < p < 2{,}560$ psia; and $273 < T < 333$ K, where $i = CO_2$, C_1, C_2, and C_3.

Renner also gives a correlation for diffusivity of CO_2 in water/brine systems.

$$D_{CO_2-w} = (6.392 \times 10^3)\mu_{CO_2}^{6.911}\mu_w^{-0.1584}, \quad \ldots\ldots\ldots \text{(3.152)}$$

with D in cm^2/s and μ in cp.

3.6 *K*-Value Correlations

This section covers the estimation of equilibrium K values by correlations and the calculation of two-phase equilibrium when K values are known. The K value is defined as the ratio of equilibrium gas composition y_i to the equilibrium liquid composition x_i,

$$K_i \equiv y_i/x_i\,. \quad \ldots\ldots\ldots\ldots\ldots\ldots\ldots\ldots\ldots\ldots \text{(3.153)}$$

K_i is a function of pressure, temperature, and overall composition. K values can be estimated with empirical correlations or by satisfying the equal-fugacity constraint with an EOS (see Chap. 4).

Although the increasing use of EOS's has tended to lessen interest in empirical K-value correlations, empirical methods are still useful for such engineering calculations as (1) multistage surface separation, (2) compositional reservoir material balance, and (3) checking the consistency of separator-oil and gas compositions.

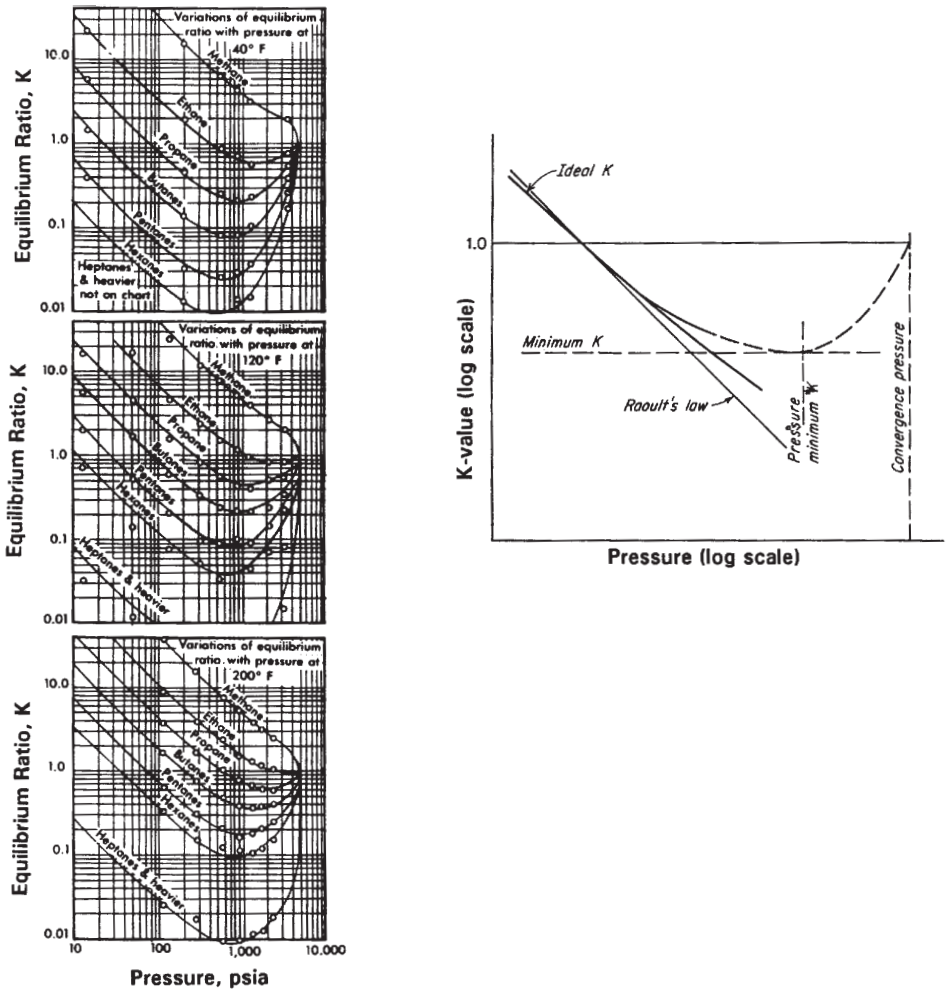

Fig. 3.24—General behavior of a *K* value vs. pressure plot on log-log scale.

Several methods for correlating K values have appeared in the past 50 years. Most rely on two limiting conditions for describing the pressure dependence of K values. First, at low pressures, Raoult's and Dalton's laws[3] can be used to show that

$$K_i \approx p_{vi}(T)/p, \quad \ldots\ldots\ldots\ldots\ldots\ldots\ldots\ldots \quad (3.154)$$

where p_v = component vapor pressure at the system temperature. The limitations of this equation are that temperature must be less than the component critical temperature (because vapor pressure is not defined at supercritical temperatures) and that the component behaves as an ideal gas. Also, the equation implies that the K value is independent of overall composition. In fact, the pressure dependence of low-pressure K values is closely approximated by Eq. 3.154.

The second observation is that, at high pressures, the K values of all components in a mixture tend to converge to unity at the same pressure. This pressure is called the convergence pressure[96] and, for binaries, represents the actual mixture critical pressure. For multicomponent mixtures, the convergence pressure is a nonphysical condition unless the system temperature equals the mixture critical temperature.[97,98] This is because a mixture becomes single phase at the bubblepoint or dewpoint pressure before reaching the convergence pressure.

The log-log plot of K_i vs. pressure in **Fig. 3.24** shows how the ideal-gas and convergence-pressure conditions define the K-value behavior at limiting conditions. For light components (where $T > T_{ci}$), K values decrease monotonically toward the convergence pressure. For heavier components (where $T < T_{ci}$), K values initially decrease as a function of pressure at low pressures, passing through unity when system pressure equals the vapor pressure of a particular component, reaching a minimum, and finally increasing toward unity at the convergence pressure.

For reservoir fluids, the pressure where K values reach a minimum is usually $>1{,}000$ psia (**Fig. 3.25**), implying that K values are more or less independent of convergence pressure (i.e., composition) at pressures $<1{,}000$ psia. This observation has been used to develop general "low-pressure" K-value correlations for surface-separator calculations.

3.6.1 Hoffman *et al.* Method. Hoffman *et al.*[99] propose a method for correlating K values that has received widespread application.

$$K_i = \frac{10^{(A_0 + A_1 F_i)}}{p}$$

$$\text{or } \log K_i p = A_0 + A_1 F_i, \quad \ldots\ldots\ldots\ldots\ldots\ldots \quad (3.155)$$

$$\text{where } F_i = \frac{1/T_{bi} - 1/T}{1/T_{bi} - 1/T_{ci}} \log(p_{ci}/p_{sc}); \quad \ldots\ldots\ldots\ldots \quad (3.156)$$

T_c = critical temperature; p_c = pressure; T_b = normal boiling point; p_{sc} = pressure at standard conditions; and A_1 and A_0 = slope and intercept, respectively, of the plot $\log(K_i p)$ vs. F_i.

Hoffman *et al.* show that measured K values for a reservoir gas condensate correlate well with the proposed equation. They found that trend of $\log(K_i p)$ vs. F_i is linear for components C_1 through C_6 at all pressures, while the function turns downward for heavier components at low pressures. Interestingly, the trend becomes more linear for all components at higher pressures.

As **Fig. 3.26** shows, Slope A_1 and Intercept A_0 vary with pressure. For low pressures, $K_i \approx p_v/p$. With the Clapeyron vapor pressure relation,[5] $\log(p_v) = a - b/T$ results in $A_0 = \log(p_{sc})$ and $A_1 = 1$. These limiting values of A_0 and A_1 are close to the values found when $A_0(p)$ and $A_1(p)$ are extrapolated to $p = p_{sc}$. Because

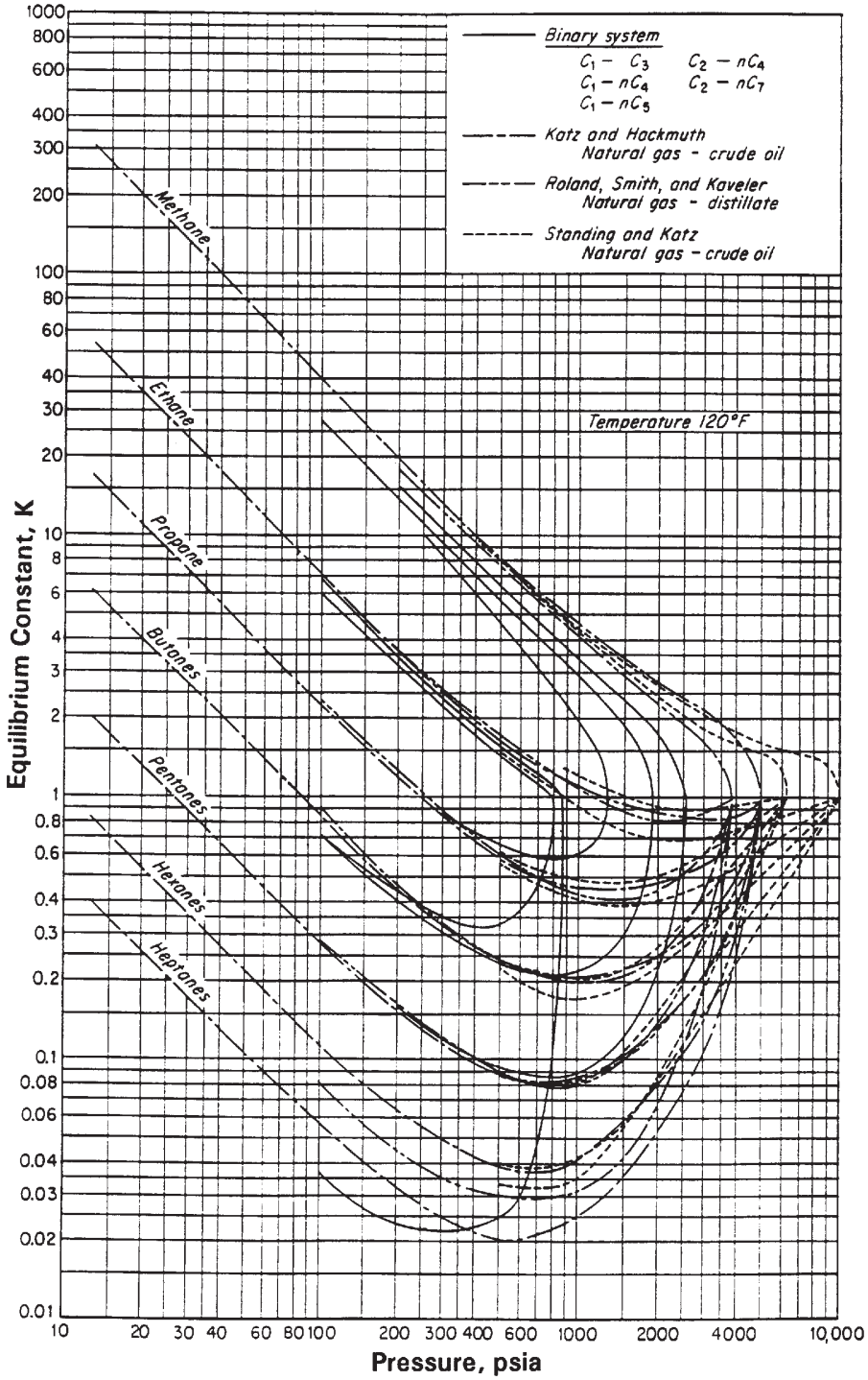

Fig. 3.25—*K* values at 120°F for binary- and reservoir-fluid systems with convergence pressures ranging from 800 to 10,000 psia (from Standing[3]).

K values tend toward unity as pressure approaches the convergence pressure, p_K, it is necessary that $A_0 = \log(p_K)$ and $A_1 \to 0$. Several authors have noted that plots of $\log(K_i p)$ vs. F_i tend to converge at a common point. Brinkman and Sicking[101] suggest that this "pivot" point represents the convergence pressure where $K_i = 1$ and $p = p_K$. The value of F_i at the pivot point, F_K, is easily shown to equal $\log(p_K/p_{sc})$.

It is interesting to note that the well-known Wilson[102,103] equation,

$$K_i = \frac{\exp 5.37(1 + \omega_i)\left(1 - T_{ri}^{-1}\right)}{p_{ri}}, \quad \ldots\ldots\ldots\ldots\ldots (3.157)$$

is identical to the Hoffman *et al.*[99] relation for $A_0 = \log(p_{sc})$ and $A_1 = 1$ when the Edmister[104] correlation for acentric factor equation,

$$\omega_i = \frac{3}{7}\frac{T_{bi}/T_{ci}}{1 - T_{bi}/T_{ci}}\log(p_{ci}/p_{sc}) - 1, \quad \ldots\ldots\ldots\ldots (3.158)$$

is used in the Wilson equation. Note that $5.37 = (7/3)\ln(10)$.

Whitson and Torp[100] suggest a generalized form of the Hoffman *et al.*[99] equation in terms of convergence pressure and acentric factor.

$$K_i = \left(\frac{p_{ci}}{p_K}\right)^{A_1 - 1}\frac{\exp\left[5.37\,A_1\,(1 + \omega_i)\left(1 - T_{ri}^{-1}\right)\right]}{p_{ri}}, \quad \ldots\ldots\ldots\ldots\ldots (3.159)$$

where A_1 = a function of pressure, with $A_1 = 1$ at $p = p_{sc}$ and $A_1 = 0$ at $p = p_K$. The key characteristics of K values vs. pressure

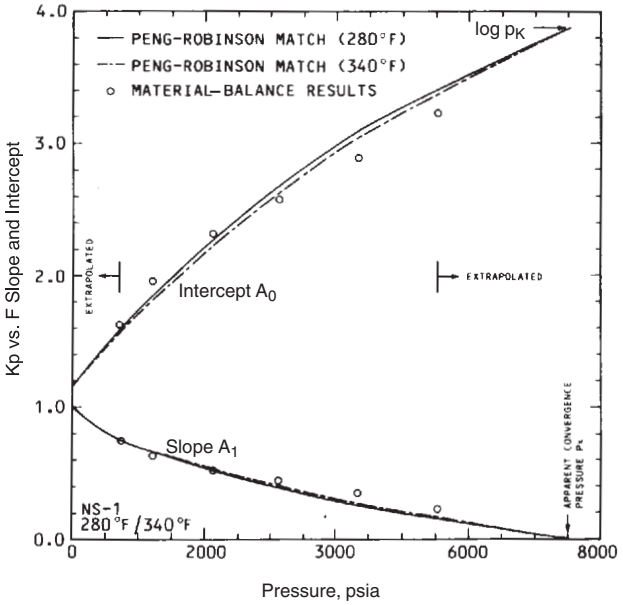

Fig. 3.26—Pressure dependence of slope, A_1, and intercept, A_0, in Hoffman *et al. Kp-F* relationship (Eq. 3.155) for a North Sea gas condesate NS-1 (from Whitson and Torp[100]).

and temperature are correctly predicted by Eq. 3.159, where the following pressure dependence for A_1 is suggested.

$$A_1 = 1 - (p/p_K)^{A_2}, \quad \ldots\ldots\ldots\ldots\ldots\ldots\ldots\ldots (3.160)$$

where A_2 ranges from 0.5 to 0.8 and pressures p and p_K are given in psig. Canfield[105] also suggests a simple K-value correlation based on convergence pressure.

3.6.2 Standing Low-Pressure *K* Values. Standing[106] uses the Hoffman *et al.*[99] method to generate a low-pressure K-value equation for surface-separator calculations ($p_{sp} < 1{,}000$ psia and $T_{sp} < 200$°F). Standing fits A_1 and A_0 in Eq. 3.155 as a function of pressure using K-value data from an Oklahoma City crude oil. He treats the C_{7+} by correlating the behavior of $K_{C_{7+}}$ as a function of "effective" carbon number $n_{C_{7+}}$. The Standing equations are

$$K_i = \frac{1}{p_{sp}} 10^{\left(A_0 + A_1 F_i\right)}, \quad \ldots\ldots\ldots\ldots\ldots\ldots\ldots\ldots (3.161a)$$

$$F_i = b_i\left(1/T_{bi} - 1/T\right), \quad \ldots\ldots\ldots\ldots\ldots\ldots\ldots\ldots (3.161b)$$

$$b_i = \log\left(p_{ci}/p_{sc}\right)/\left(1/T_{bi} - 1/T_{ci}\right), \quad \ldots\ldots\ldots\ldots\ldots\ldots (3.161c)$$

$$A_0(p) = 1.2 + \left(4.5 \times 10^{-4}\right)p + \left(15 \times 10^{-8}\right)p^2, \quad \ldots\ldots\ldots\ldots\ldots\ldots (3.161d)$$

$$A_1(p) = 0.890 - \left(1.7 \times 10^{-4}\right)p - \left(3.5 \times 10^{-8}\right)p^2, \quad \ldots\ldots\ldots\ldots\ldots\ldots (3.161e)$$

$$n_{C_{7+}} = 7.3 + 0.0075T + 0.0016p, \quad \ldots\ldots\ldots\ldots\ldots\ldots (3.161f)$$

$$b_{C_{7+}} = 1{,}013 + 324n_{C_{7+}} - 4.256n^2_{C_{7+}}, \quad \ldots\ldots\ldots\ldots (3.161g)$$

and $$T_{bC_{7+}} = 301 + 59.85n_{C_{7+}} - 0.971n^2_{C_{7+}}, \quad \ldots\ldots\ldots\ldots (3.161h)$$

with T in °R except when calculating $n_{C_{7+}}$ (for $n_{C_{7+}}$, T is in °F) and p in psia. Standing suggests modified values of b_i and T_{bi} for nonhydrocarbons, methane, and ethane (**Table 3.3**). Glasø and Whitson[107] show that these equations are accurate for separator flash calculations of crude oils with GOR's ranging from 300 to 1,500 scf/STB and oil gravity ranging from 26 to 48°API. Experience shows, however, that significant errors in calculated GOR may result for lean gas condensates, probably because of inaccurate C_1 and C_{7+} K values. The Hoffman *et al.* method with Standing's low-pressure correlations are particularly useful for checking the consistency of separator-gas and -oil compositions.

TABLE 3.3—VALUES OF *b* AND T_b FOR USE IN STANDING LOW-PRESSURE *K*-VALUE CORRELATION

Component, i	b_i (cycle-°R)	Tb_i °R
N_2	470	109
CO_2	652	194
H_2S	1,136	331
C_1	300	94
C_2	1,145	303
C_3	1,799	416
i-C_4	2,037	471
n-C_4	2,153	491
i-C_5	2,368	542
n-C_5	2,480	557
C_6 (lumped)	2,738	610
n-C_6	2,780	616
n-C_7	3,068	669
n-C_8	3,335	718
n-C_9	3,590	763
n-C_{10}	3,828	805

For C_{7+} fractions, see Eqs. 3.161f through 3.161h

3.6.3 Galimberti-Campbell Method. Galimberti and Campbell[108,109] suggested another useful approach for correlating K values where

$$\log K_i = A_0 + A_1 T^2_{ci} \quad \ldots\ldots\ldots\ldots\ldots\ldots\ldots\ldots (3.162)$$

is shown to correlate K values for several simple mixtures containing hydrocarbons C_1 through C_{10} at pressures up to 3,000 psia and temperatures from -60 to 300°F.

Whitson developed a low-pressure K-value correlation, based on data from Roland,[110] at pressures $<1{,}000$ psia and temperatures from 40 to 200°F, for separator calculations of gas condensates.

$$A_0 = 4.276 - \left(7.6 \times 10^{-4}\right)T + \left[-1.18 + \left(5.675 \times 10^{-4}\right)T\right]\log p, \quad \ldots\ldots\ldots (3.163a)$$

$$A_1 = 10^{-6}\left\{\left(-4.9563 + 0.00955T\right) + \left[\left(1.9094 \times 10^{-3}\right) - \left(1.235 \times 10^{-5}\right)T + \left(3.34 \times 10^{-8}\right)T^2\right]p\right\}, \quad \ldots (3.163b)$$

$$T_{c_{C1}} = 343 - 0.04p, \quad \ldots\ldots\ldots\ldots\ldots\ldots\ldots\ldots (3.163c)$$

and $$T_{cC7+} = 1{,}052.5 - 0.5125T + 0.00375T^2, \quad \ldots\ldots (3.163d)$$

with p in psia, T in °F, and T_c in °R.

3.6.4 Nonhydrocarbon *K* Values. Lohrenz *et al.*[111] reported nonhydrocarbon K values as a function of pressure, temperature, and convergence pressure.

$$\ln K_{H_2S} = \left(1 - \frac{p}{p_K}\right)^{0.8}\left[6.3992127 + \frac{1{,}399.2204}{T} - 0.76885112\ln p - \frac{18.215052\ln p}{T} - \frac{1{,}112{,}446.2}{T^2}\right], \quad \ldots\ldots\ldots\ldots\ldots\ldots (3.164a)$$

$$\ln K_{N_2} = \left(1 - \frac{p}{p_K}\right)^{0.4}\left(11.294748 - \frac{1,184.2409}{T} - 0.90459907 \ln p\right), \quad \ldots\ldots\ldots\ldots\ldots\ldots \quad (3.164b)$$

$$\ln K_{CO_2} = \left(1 - \frac{p}{p_K}\right)^{0.6}\left(7.0201913 - \frac{152.7291}{T} - 1.8896974 \times \ln p + \frac{1,719.2956 \ln p}{T} - \frac{644,740.69 \ln p}{T^2}\right), \quad \ldots\ldots\ldots\ldots\ldots\ldots \quad (3.164c)$$

with p in psia and T in °R. For low-pressure K-value estimation, the first term in Eq. 3.164 simplifies to unity (assuming that $1 - p/p_K \approx 1$) and the K values become functions of pressure and temperature only. However, these equations do not give the correct low-pressure value of $\partial(\ln K_i)/\partial(\ln p) = -1$

3.6.5 Convergence-Pressure Estimation. For correlation purposes, convergence pressure is used as a variable to define the composition dependence of K values. Convergence pressure is a function of overall composition and temperature. Whitson and Michelsen[112] show that convergence pressure is a thermodynamic phenomenon, with the characteristics of a true mixture critical point, that can be predicted with EOS's.

Rzasa *et al.*[113] give an empirical correlation for convergence pressure as a function of temperature and the product $(M\gamma)_{C_{7+}}$. Standing[2] suggests that convergence pressure of reservoir fluids varies almost linearly with C_{7+} molecular weight.

Convergence pressure can also be calculated with a trial-and-error procedure suggested by Rowe.[97,98,114] This procedure involves the use of several empirical correlations for estimating mixture critical pressure and temperature, pseudocomponent critical properties, and the K values of methane and octane. The Galimberti and Campbell[108,109] K-value method is used to estimate K values of other components by interpolation and extrapolation of the C_1 and C_8 K values. This approach to convergence pressure is necessary if the K values are used for processes that approach critical conditions or where K values change significantly because of overall composition effects. The method cannot, of course, be more accurate than the correlations it uses and therefore is expected to yield only qualitatively correct results.

For reservoir calculations where convergence pressure can be assumed constant (e.g., pressure depletion), a more direct approach to determining convergence pressure is suggested. With a K-value correlation of the form $K_i = K(p_K, p, T)$ as in Eq. 3.159, the convergence pressure can be estimated from a single experimental saturation pressure. For a bubblepoint and a dewpoint, Eqs. 3.165 and 3.166, respectively, must be satisfied.

$$F(p_K) = 1 - \sum_{i=1}^{N} z_i K_i(p_K, p_b, T) = 0 \quad \ldots\ldots\ldots\ldots \quad (3.165)$$

$$\text{and } F(p_K) = 1 - \sum_{i=1}^{N} \frac{z_i}{K_i\left(p_K, p_d, T\right)} = 0, \quad \ldots\ldots\ldots\ldots \quad (3.166)$$

where z_i, p_b, or p_d and T are specified and p_K is determined.

The two-phase flash calculation, with K values given, is discussed in Chap. 4 in the Phase-Split Calculation section.

References

1. *The SI Metric System of Units and SPE Metric Standard,* SPE, Richardson, Texas (June 1982).
2. van der Waals, J.D.: "Continuity of the Gaseous and Liquid State of Matter," PhD dissertation, U. of Leiden (1873).
3. Standing, M.B.: *Volumetric and Phase Behavior of Oil Field Hydrocarbon Systems*, SPE, Richardson, Texas (1981).
4. Standing, M.B. and Katz, D.L.: "Density of Natural Gases," *Trans.*, AIME (1942) **146,** 140.
5. Kay, W.B.: "Density of Hydrocarbon Gases and Vapors at High Temperature and Pressure," *Ind. Eng. Chem.* (1936) No. 28, 1014.
6. Reid, R.C., Prausnitz, J.M., and Polling, B.E.: *The Properties of Gases and Liquids*, fourth edition, McGraw-Hill Book Co. Inc., New York City (1987) 388–485.
7. Sutton, R.P.: "Compressibility Factors for High-Molecular Weight Reservoir Gases," paper SPE 14265 presented at the 1985 SPE Annual Technical Conference and Exhibition, Las Vegas, Nevada, 22–25 September.
8. Ramey, H.J. Jr.: "Rapid Methods for Estimating Reservoir Compressibilities," *JPT* (April 1964) 447; *Trans.*, AIME, **231.**
9. Fetkovich, M.J., Reese, D.E., and Whitson, C.H.: "Application of a General Material Balance for High-Pressure Gas Reservoirs," *SPE Journal* (March 1998) 3.
10. Fick, A.: *Am. Phys.*, Leipzig (1855) **170,** 59.
11. Coats, K.H.: "Implicit Compositional Simulation of Single-Porosity and Dual-Porosity Reservoirs," paper SPE 18427 presented at the 1989 SPE Symposium on Reservoir Simulation, Houston, 6–8 February.
12. da Silva, F.V. and Belery, P.: "Molecular Diffusion in Naturally Fractured Reservoirs—A Decisive Recovery Mechanism," paper SPE 19672 presented at the 1987 SPE Annual Technical Conference and Exhibition, San Antonio, Texas, 8–11 October.
13. Amyx, J.W., Bass, D.M. Jr., and Whiting, R.L.: *Petroleum Reservoir Engineering*, McGraw-Hill Book Co. Inc., New York City (1960).
14. Christoffersen, K. and Whitson, C.H.: "Gas/Oil Capillary Pressure of Chalk at Elevated Pressures," *SPEFE* (September 1995) 153.
15. Delclaud, J., Rochon, J., and Nectoux, A.: "Investigation of Gas/Oil Relative Permeabilities: High-Permeability Oil Reservoir Application," paper SPE 16966 presented at the 1987 SPE Annual Technical Conference and Exhibition, Dallas, 27–30 September.
16. Katz, D.L. *et al.*: *Handbook of Natural Gas Engineering*, McGraw-Hill Book Co. Inc., New York City (1959) 69–93.
17. Standing, M.B.: *Oil-System Correlations*, P.P. Handbook (ed.), McGraw-Hill Book Co. Inc., New York City (1962).
18. Beggs, H.D.: "Oil System Correlations," *Petroleum Engineering Handbook*, SPE, Richardson, TX (1987) Chap. 22.
19. McCain, W.D. Jr.: "Reservoir-Fluid Property Correlations—State of the Art," *SPERE* (May 1991) 266.
20. Whitson, C.H. and Torp, S.B.: "Evaluating Constant Volume Depletion Data," *JPT* (March 1983) 610; *Trans.*, AIME, **275.**
21. Hall, K.R. and Yarborough, L.: "A New EOS for *Z*-factor Calculations," *Oil & Gas J.* (18 June 1973) 82.
22. Yarborough, L. and Hall, K.R.: "How to Solve EOS for *Z*-factors," *Oil & Gas J.* (18 February 1974) 86.
23. Takacs, G.: "Comparisons Made for Computer *Z*-factor Calculations," *Oil & Gas J.* (20 December 1976) 64.
24. Dranchuk, P.M. and Abou-Kassem, J.H.: "Calculation of *Z*-Factors for Natural Gases Using Equations of State," *J. Cdn. Pet. Tech.* (July–September 1975) **14,** No. 3, 34.
25. Brill, J.P. and Beggs, H.D.: "Two-Phase Flow in Pipes," paper presented at the U. Tulsa INTERCOMP Course, The Hague (1974).
26. Lee, B.I. and Kesler, M.G.: "A Generalized Thermodynamic Correlation Based on Three-Parameter Corresponding States," *AIChE J.* (1975) **21,** 510.
27. *API Technical Data Book—Petroleum Refining*, third edition, API, New York City (1977).
28. Starling, K.E., Mannan, M., and Savidge, J.L.: "Equation Predicts Supercompressibility for Wet, Sour Gases," *Oil & Gas J.* (2 January 1989) 31.
29. Ely, J.F. and Hanley, H.J.M.: *Ind. Eng. Chem. Fund.* (1983) **22,** 90.
30. Wichert, E. and Aziz, K.: "Compressibility Factor of Sour Natural Gases," *Cdn. J. Chem. Eng.* (1971) **49,** 267.
31. Wichert, E. and Aziz, K.: "Calculate *Z*'s for Sour Gases," *Hydro. Proc.* (May 1972) **51,** 119.
32. Matthews, T.A., Roland, C.H., and Katz, D.L.: "High Pressure Gas Measurement," *Petroleum Refiner* (1942) **21,** No. 6, 58.
33. Standing, M.B.: *Petroleum Engineering Data Book*, Norwegian Inst. of Technology, Trondheim, Norway (1974).
34. Eilerts, C.K.: "Gas Condensate Reservoir Engineering, 1. The Reserve Fluid, Its Composition and Phase Behavior," *Oil & Gas J.* (1 February 1947).
35. Cragoe, C.S.: "Thermodynamic Properties of Petroleum Products," U.S. Dept. of Commerce, Washington, DC (1929) 97.
36. Gold, D.K., McCain, W.D. Jr., and Jennings, J.W.: "An Improved Method for the Determination of the Reservoir Gas Gravity for Retrograde Gases," paper SPE 17310 presented at the 1988 SPE Permian Basin Oil and Gas Recovery Conference, Midland, Texas, 10–11 March.

37. Gold, D.K., McCain, W.D. Jr., and Jennings, J.W.: "An Improved Method for the Determination of the Reservoir Gas Gravity for Retrograde Gases," *JPT* (July 1989) 41, 747; *Trans.*, AIME, **287.**
38. Whitson, C.H.: "Discussion of An Improved Method for the Determination of the Reservoir-Gas Specific-Gravity for Retrograde Gases," *JPT* (November 1989) 1216.
39. Leshikar, A.G.: "How to Estimate Equivalent Gas Volume of Stock Tank Condensate," *World Oil* (January 1961) 108.
40. Standing, M.B.: "A Pressure-Volume-Temperature Correlation for Mixtures of California Oils and Gases," *Drill. & Prod. Prac.* (1947) 275.
41. Katz, D.L.: "Prediction of the Shrinkage of Crude Oils," *Drill. & Prod. Prac.* (1942) 137.
42. Carr, N.L., Kobayashi, R., and Burrows, D.B.: "Viscosity of Hydrocarbon Gases Under Pressure," *Trans.*, AIME (1954) **201,** 264.
43. Dempsey, J.R.: "Computer Routine Treats Gas Viscosity as a Variable," *Oil & Gas J.* (16 August 1965) 141.
44. Lee, A.L., Gonzalez, M.H., and Eakin, B.E.: "The Viscosity of Natural Gases," *JPT* (August 1966) 997; *Trans.*, AIME, **237.**
45. Lucas, K.: *Chem. Ing. Tech.* (1981) **53,** 959.
46. Sage, B.H. and Olds, R.H.: "Volumetric Behavior of Oil and Gas from Several San Joaquin Valley Fields," *Trans.*, AIME (1947) **170,** 156.
47. Eilerts, C.K.: *Phase Relations of Gas Condensate Fluids,* Monograph 10, U.S. Bureau of Mines, American Gas Assn., New York City (1957) **1 and 2.**
48. Eilerts, C.K. *et al.*: "Phase Relations of a Gas-Condensate Fluid at Low Tempertures, Including the Critical State," *Pet. Eng.* (February 1948) **19,** 154.
49. Nemeth, L.K. and Kennedy, H.T.: "A Correlation of Dewpoint Pressure With Fluid Composition and Temperature," *SPEJ* (June 1967) 99; *Trans.*, AIME, **240.**
50. Organick, E.I. and Golding, B.H.: "Prediction of Saturation Pressures for Condensate-Gas and Volatile-Oil Mixtures," *Trans.*, AIME (1952) **195,** 135.
51. Kurata, F. and Katz, D.L.: "Critical Properties of Volatile Hydrocarbon Mixtures," *Trans.*, AIChE (1942) **38,** 995.
52. Glasø, O.: "Generalized Pressure/Volume/Temperature Correlations," *JPT* (November 1980) 785.
53. Lasater, J.A.: "Bubblepoint Pressure Correlation," *Trans.*, AIME (1958) **213,** 379.
54. Sutton, R.P. and Farshad, F.F.: "Evaluation of Empirically Derived PVT Properties for Gulf of Mexico Crude Oils," *SPERE* (February 1990) 79.
55. Whitson, C.H.: "Characterizing Hydrocarbon Plus Fractions," paper SPE 12233 presented at the 1980 SPE European Offshore Petroleum Conference, London, 21–24 October.
56. Whitson, C.H.: "Characterizing Hydrocarbon Plus Fractions," *SPEJ* (August 1983) 683; *Trans.*, AIME, **275.**
57. Vazquez, M. and Beggs, H.D.: "Correlations for Fluid Physical Property Prediction," *JPT* (June 1980) 968.
58. Standing, M.B. and Katz, D.L.: "Density of Crude Oils Saturated With Natural Gas," *Trans.*, AIME (1942) **146,** 159.
59. Madrazo, A.: "Liquid-Density Correlation of Hydrocarbon Systems," *Trans.*, AIME (1960) **219,** 386.
60. Vogel, J.L. and Yarborough, L.: "The Effect of Nitrogen on the Phase Behavior and Physical Properties of Reservoir Fluids," paper SPE 8815 presented at the 1980 SPE Annual Technical Conference and Exhibition, Tulsa, Oklahoma, 20–23 April.
61. Alani, G.H. and Kennedy, H.T.: "Volumes of Liquid Hydrocarbons at High Temperatures and Pressures," *Trans.*, AIME (1960) **219,** 288.
62. Lohrenz, J., Bray, B.G., and Clark, C.R.: "Calculating Viscosities of Reservoir Fluids From Their Compositions," *JPT* (October 1964) 1171; *Trans.*, AIME, **231.**
63. Rackett, H.G.: "EOS for Saturated Liquids," *J. Chem. Eng. Data* (1970) **15,** No. 4, 514.
64. Hankinson, R.W. and Thomson, G.H.: "A New Correlation for Saturated Densities of Liquids and Their Mixtures," *AIChE J.* (1979) **25,** No. 4, 653.
65. Hankinson, R.W. *et al.*: "Volume Correction Factors for Lubricating Oils," *Oil & Gas J.* (28 September 1981) 297.
66. Cullick, A.S., Pebdani, F.N., and Griewank, A.K.: "Modified Corresponding States Method for Predicting Densities of Petroleum Reservoir Fluids," paper presented at the 1988 AIChE Spring Natl. Meeting, New Orleans, 7–10 March.
67. Chien, M.C.H. and Monroy, M.R.: "Two New Density Correlations," paper SPE 15676 presented at the 1976 SPE Annual Technical Conference and Exhibition, New Orleans, 5–8 October.
68. Ahmed, T.: *Hydrocarbon Phase Behavior*, first edition, Gulf Publishing Co., Houston (1989) 7.
69. Craft, B.C. and Hawkins, M.: *Applied Petroleum Reservoir Engineering*, first edition, Prentice-Hall, Englewood Cliffs, New Jersey (1959) 126–29.
70. Trube, A.S.: "Compressibility of Undersaturated Hydrocarbon Reservoir Fluids," *Trans.*, AIME (1957) **210,** 241.
71. Al-Marhoun, M.A.: "New Correlations for FVFs of Oil and Gas Mixtures," PhD dissertation, King Fahd U. of Petroleum & Minerals (1990).
72. Beal, C.: "The Viscosity of Air, Water, Natural Gas, Crude Oil and Its Associated Gases at Oilfield Temperatures and Pressures," *Trans.*, AIME (1946) **165,** 94.
73. Beggs, H.D. and Robinson, J.R.: "Estimating the Viscosity of Crude Oil Systems," *JPT* (September 1975) 1140.
74. Al-Khafaji, A.H., Abdul-Majeed, G.H., and Hassoon, S.F.: "Viscosity Correlation for Dead, Live, and Undersaturated Crude Oils," *J. Pet. Res.* (1987) **6,** No. 2, 1.
75. Standing, M.B.: "UOP Characterization Factor," TI program listing, available from C.H. Whitson, Norwegian Inst. of Science and Technology, NTNU, curtis@ipt.ntnu.no.
76. Chew, J.N. and Connally, C.A.: "A Viscosity Correlation for Gas-Saturated Crude Oils," *Trans.*, AIME (1959) **216,** 23.
77. Aziz, K., Govier, G.W., and Fogarasi, M.: "Pressure Drop in Wells Producing Oil and Gas," *J. Cdn. Pet. Tech.* (July–September 1972) 38.
78. Abu-Khamsin, S.A. and Al-Marhoun, M.A.: "Development of a New Correlation for Bubblepoint Oil Viscosity," *Arabian J. Sci. & Eng.* (April 1991) **16,** No. 2A, 99.
79. Simon, R., Rosman, A., and Zana, E.: "Phase-Behavior Properties of CO_2-Reservoir Oil Systems," *SPEJ* (February 1978) 20.
80. Abdul-Majeed, G.H., Kattan, R.R., and Salman, N.H.: "New Correlation for Estimating the Viscosity of Undersaturated Crude Oils," *J. Cdn. Pet. Tech.* (May–June 1990) **29,** No. 3, 80.
81. Khan, S.A. *et al.*: "Viscosity Correlations for Saudi Arabian Crude Oils," paper SPE 15720 presented at the 1987 SPE Middle East Oil Technical Conference and Exhibition, Manama, Bahrain, 8–10 March.
82. Jossi, J.A., Stiel, L.I., and Thodos, G.: "The Viscosity of Pure Substances in the Dense Gaseous and Liquid Phases," *AIChE J.* (1962) **8,** 59.
83. Stiel, L.I. and Thodos, G.: "The Viscosity of Nonpolar Gases at Normal Pressures," *AIChE J.* (1961) **7,** 611.
84. Weinaug, C.F. and Katz, D.L.: "Surface Tensions of Methane-Propane Mixtures," *Ind. & Eng. Chem.* (1943) **35,** 239.
85. Macleod, D.B.: "On a Relation Between Surface Tension and Density," *Trans.*, Faraday Soc. (1923) **19,** 38.
86. Nokay, R.: "Estimate Petrochemical Properties," *Chem. Eng.* (23 February 1959) 147.
87. Katz, D.L. and Saltman, W.: "Surface Tension of Hydrocarbons," *Ind. & Eng. Chem.* (January 1939) **31,** 91.
88. Katz, D.L., Monroe, R.R., and Trainer, R.P.: "Surface Tension of Crude Oils Containing Dissolved Gases," *Pet. Tech.* (September 1943).
89. Standing, M.B. and Katz, D.L.: "Vapor-Liquid Equilibria of Natural Gas-Crude Oil Systems," *Trans.*, AIME (1944) **155,** 232.
90. Firoozabadi, A. *et al.*: "Surface Tension of Reservoir Crude-Oil/Gas Systems Recognizing the Asphalt in the Heavy Fraction," *SPERE* (February 1988) 265.
91. Ramey, H.J. Jr.: "Correlations of Surface and Interfacial Tensions of Reservoir Fluids," paper SPE 4429 available from SPE, Richardson, Texas (1973).
92. Wilke, C.R.: "A Viscosity Equation for Gas Mixtures," *J. Chem. Phy.* (1950) **18,** 517.
93. Sigmund, P.M.: "Prediction of Molecular Diffusion at Reservoir Conditions. Part I—Measurement and Prediction of Binary Dense Gas Diffusion Coefficients," *J. Cdn. Pet. Tech.* (April–June 1976) 48.
94. Christoffersen, K.: "High-Pressure Experiments with Application to Naturally Fractured Chalk Reservoirs. 1. Constant Volume Diffusion. 2. Gas-Oil Capillary Pressure," Dr.Ing. dissertation, U. Trondheim, Trondheim, Norway (1992).
95. Renner, T.A.: "Measurement and Correlation of Diffusion Coefficients for CO_2 and Rich-Gas Applications," *SPERE* (May 1988) 517; *Trans.*, AIME, **285.**
96. Hadden, S.T.: "Convergence Pressure in Hydrocarbon Vapor-Liquid Equilibra," *Chem. Eng. Prog.* (1953) **49,** No. 7, 53.
97. Rowe, A.M. Jr.: "Applications of a New Convergence Pressure Concept to the Enriched Gas Drive Process," PhD dissertation, U. of Texas, Austin, Texas (1964).
98. Rowe, A.M. Jr.: "The Critical Composition Method—A New Convergence Pressure Method," *SPEJ* (March 1967) 54; *Trans.*, AIME, **240.**
99. Hoffmann, A.E., Crump, J.S., and Hocott, C.R.: "Equilibrium Constants for a Gas-Condensate System," *Trans.*, AIME (1953) **198,** 1.

100. Whitson, C.H. and Torp, S.B.: "Evaluating Constant Volume Depletion Data," *JPT* (March 1983) ; *Trans.*, AIME, **275.**
101. Brinkman, F.H. and Sicking, J.N.: "Equilibrium Ratios for Reservoir Studies," *Trans.*, AIME (1960) **219,** 313.
102. Wilson, G.M.: "Calculation of Enthalpy Data From a Modified Redlich-Kwong EOS," *Advances in Cryogenic Eng.* (1966) **11,** 392.
103. Wilson, G.M.: "A Modified Redlich-Kwong EOS, Application to General Physical Data Calculations," paper 15c presented at the 1969 AIChE Natl. Meeting, Cleveland, Ohio.
104. Edmister, W.C.: "Applied Hydrocarbon Thermodynamics, Part 4: Compressibility Factors and Equations of State," *Pet. Ref.* (April 1958) **37,** 173.
105. Canfield, F.B.: "Estimate *K*-Values with the Computer," *Hydro. Proc.* (April 1971) 137.
106. Standing, M.B.: "A Set of Equations for Computing Equilibrium Ratios of a Crude Oil/Natural Gas System at Pressures Below 1,000 psia," *JPT* (September 1979) 1193.
107. Glasø, O. and Whitson, C.H.: "The Accuracy of PVT Parameters Calculated From Computer Flash Separation at Pressures Less Than 1,000 psia," *JPT* (August 1980) 1811.
108. Galimberti, M. and Campbell, J.M.: "Dependence of Equilibrium Vaporization Ratios (*K*-Values) on Critical Temperature," *Proc.*, 48th NGPA Annual Convention (1969) 68.
109. Galimberti, M. and Campbell, J.M.: "New Method Helps Correlate *K* Values for Behavior of Paraffin Hydrocarbons," *Oil & Gas J.* (November 1969) 64.
110. Roland, C.H.: "Vapor Liquid Equilibrium for Natural Gas-Crude Oil Mixtures," *Ind. & Eng. Chem.* (1945) **37,** 930.
111. Lohrenz, J., Clark, G.C., and Francis, R.J.: "A Compositional Material Balance for Combination Drive Reservoirs With Gas and Water Injection," *JPT* (November 1963) 1233; *Trans.*, AIME, **228.**
112. Whitson, C.H. and Michelsen, M.L.: "The Negative Flash," *Fluid Phase Equilibria* (1989) **53,** 51.
113. Rzasa, M.J., Glass, E.D., and Opfell, J.B.: "Prediction of Critical Properties and Equilibrium Vaporization Constants for Complex Hydrocarbon Systems," *Chem. Eng. Prog.* (1952) **2,** 28.
114. Rowe, A.M. Jr.: "Internally Consistent Correlations for Predicting Phase Compositions for Use in Reservoir Composition Simulators," paper SPE 7475 presented at the 1978 SPE Annual Technical Conference and Exhibition, Houston, 1–3 October.

SI Metric Conversion Factors

Å	$\times 1.0$*	$E-01$	= nm
°API	$141.5/(131.5 + °API)$		= g/cm^3
bar	$\times 1.0$*	$E+05$	= Pa
bbl	$\times 1.589\ 873$	$E-01$	= m^3
Btu/lbm mol	$\times 2.236$	$E+03$	= J/mol
cp	$\times 1.0$*	$E-03$	= Pa·s
cSt	$\times 1.0$*	$E-06$	= m^2/s
dyne/cm	$\times 1.0$*	$E+00$	= mN/m
ft	$\times 3.048$*	$E-01$	= m
ft^2	$\times 9.290\ 304$*	$E-02$	= m^2
ft^3	$\times 2.831\ 685$	$E-02$	= m^3
ft^3/lbm mol	$\times 6.242\ 796$	$E-02$	= m^3/kmol
°F	$(°F-32)/1.8$		= °C
°F	$(°F+459.67)/1.8$		= K
in.^{2}	$\times 6.451\ 6$*	$E+00$	= cm^2
lbm	$\times 4.535\ 924$	$E-01$	= kg
lbm mol	$\times 4.535\ 924$	$E-01$	= kmol
psi	$\times 6.894\ 757$	$E+00$	= kPa
psi^{-1}	$\times 1.450\ 377$	$E-01$	= kPa^{-1}
°R	$\times 5/9$		= K

*Conversion factor is exact.